UNIVERSITY OF WEST BOHEMIA
FACULTY OF APPLIED SCIENCES
DEPARTMENT OF MATHEMATICS

MASTER'S THESIS

QUALITATIVE ANALYSIS OF NONLINEAR EQUATIONS OF REACTION-DIFFUSION TYPE WITH INTEGRO-DIFFERENTIAL OPERATORS OF FRACTIONAL ORDER

PILSEN, 2023 TOMÁŠ LESNIAK

Nahradit listem zadání.

Prohlášení

Prohlašuji, že jsem tuto diplomovou práci vypracoval samostatně a výhradně s použitím odborné literatury a pramenů, jejichž úplný seznam je její součástí.

V Plzni, dne 27. července 2023

. . . . . .
vlastnoruční podpis

Poděkování

Rád bych poděkoval svému vedoucímu práce prof. Ing. Petru Girgovi, Ph.D., za vedení, za přínosné podněty a návrhy, cenné rady a hlavně za veškerý čas, který mi věnoval při vedení této práce.

Abstrakt

Pomocí numerických simulací studujeme reakčně-difuzní problémy s difuzí popsanou frakcionálním laplaciánem. Frakcionální laplacián se objevuje např. v matematických modelech populační dynamiky, kde je pohyb jedinců způsoben tzv. Levyho skoky, nikoliv Brownovým pohybem. Uvažované problémy zahrnují nelineární reakční členy závislé na parametrech. Naším cílem je pochopit závislost řešení na těchto parametrech. Pro stacionární problémy provádíme numerické simulace a konstruujeme bifurkační diagramy pomocí algoritmů automatického sledování větví řešení (tzv. "branch following"). Pro řešení úloh používáme metodu konečných diferencí, kterou jsme implementovali v prostředí Matlab. Problémy studujeme v jedné nebo dvou prostorových dimenzích. V případě dvou rozměrů nám naše implementace konečných diferencí umožňuje studovat tyto problémy na poměrně obecných oblastech. Studujeme také evoluční problémy, pro které používáme implicitní Eulerovu metodu kombinovanou s konečnými diferencemi. K řešení nelineárních evolučních úloh používáme metodu monotónních iterací.

Klíčová slova: frakcionální laplacián, frakcionální diferenciální rovnice, stacionární úlohy, evoluční úlohy, numerické simulace, metoda konečných diferencí

Abstract

We use numerical simulations to study reaction-diffusion problems with diffusion driven by fractional Laplacian. Fractional Laplacian appears, e.g., in mathematical models of population dynamics where the dispersion of individuals is due to the so called Levy flights rather than due to Brownian motion. Problems under consideration involve nonlinear reaction terms depending on parameters. Our aim is to understand the dependence of solutions on these parameters. For stationary problems, we perform numerical simulations and construct bifurcation diagrams using some simple algorithms of branch following. To handle the problems numerically, we use method of finite differences which we implemented in Matlab. We study problems in one or two spatial dimensions. In the case of two dimensions, our implementation of finite differences allows us to study these problems on quite general domains. We also study evolution problems. Here we use implicit Euler method combined with finite differences. In order to solve nonlinear evolution problems we use method of monotone iterations.

Keywords: fractional Laplace operator, fractional differential equations, stationary problems, evolutionary problems, numerical simulations, method of finite differences

Contents

List of Symbols

Notation of number sets

$\mathbb{N}$	The set of all natural numbers, i.e., $\{1, 2, 3, \ldots\}$.
$\mathbb{R}^d$	The $d-$dimensional space of real numbers, i.e., $\underbrace{\mathbb{R} \times \mathbb{R} \times \ldots \times \mathbb{R}}_{d-\text{times}}$.
$\mathbf{x}$	Element of the $d-$dimensional space of real numbers, i.e., $\mathbf{x} = (x_1, x_2, \ldots, x_d)$. For $d = 2$, we frequently use more convenient notation $\mathbf{x} = (x, y)$.
0	With subtle abuse of notation, we use 0 to denote number zero and also to denote origin of the $d-$dimensional space $\mathbb{R}^d$.
$\mathbb{C}$	The set of all complex numbers.

Notation of general sets

Ω	A subset of $\mathbb{R}^d$, that is open, bounded and connected $\Omega \subset \mathbb{R}^d$.
$\overline{\Omega}$	Closure of Ω.
$\partial\Omega$	Boundary of Ω.
$B_r(\mathbf{x}_0)$	A ball of a radius r centered at $\mathbf{x}_0 \in \mathbb{R}^d$.
$\partial B_r(\mathbf{x}_0)$	A boundary of a ball $B_r(\mathbf{x}_0)$.
$\lvert\mathbf{x}\rvert$	The Eucleidian norm of a vector $\mathbf{x} \in \mathbb{R}^d$.

Notation of multivariate calculus

$u(\mathbf{x})$	Value of a function u at a point $\mathbf{x} \in \mathbb{R}^d$.
$u(x, y)$	Value of a function u at a point $(x, y) = \mathbf{x} \in \mathbb{R}^2$.
$u(t, x)$	Value of a function u at a point (t, x) in the time-space cylinder $[T_0, T] \times [L, R]$.
$u(t, x, y)$	Value of a function u at a point (t, x, y) in the time-space cylinder $[T_0, T] \times \Omega$.
$(-\Delta)^{\alpha/2} u$	Fractional Laplacian of u of an order $\alpha/2$, for definition see (1.1) on page 2 .
Δu	Ordinary Laplacian of u.

$(\nabla^2 u)_{i,j}$ Second difference centered at the point (x_i, y_j).

$u^{(n)}$ nth derivative of the function u, where derivatives of order one, two and three are denoted as u', u'', u''', respectively.

$\frac{\partial u}{\partial x_i}$ Partial derivative of the function u with respect to x_i, for $i = 1, \ldots, d$.

Notation of special functions

$[s]_+$ Non-negative part of $s \in \mathbb{R}$, i.e., $[s]_+ := \max\{0, s\}$.

$\Gamma(z)$ The Gamma function of $z \in \mathbb{C}$, i.e., $\Gamma(z) := \int_0^{+\infty} t^{z-1} e^{-t} \mathrm{d}t$ for $\mathrm{Re}\,(z) > 0$.

$B(z_1, z_2)$ The Beta function of $z_1, z_2 \in \mathbb{C}$, i.e., $B(z_1, z_2) := \int_0^1 t^{z_1-1}(1-t)^{z_2-1} \mathrm{d}t$ for $\mathrm{Re}\,(z_1), \mathrm{Re}\,(z_2) > 0$.

$\chi_{[a,b]}(x)$ Indicator function, i.e., $\chi_{[a,b]}(x) := \begin{cases} 1 & \text{if } x \in [a,b], \\ 0 & \text{otherwise.} \end{cases}$

${}_2F_1(a, b; c; z)$ The generalized hypergeometric function, i.e.,

$$ {}_2F_1(a, b; c; z) := \frac{\Gamma(c)}{\Gamma(a)\Gamma(b)} \sum_{s=0}^{\infty} \frac{\Gamma(a+s)\Gamma(b+s)}{\Gamma(c+s)s!} z^s $$

on the disk $|z| < 1$ in the complex domain, and by analytic continuation elsewhere, see `https://dlmf.nist.gov/15.2` for its definition with further details in the Digital Library of Mathematical Functions by the National Institute of Standards and Technology. Note that $F(a, b; c; z)$ does not exist when $c = 0, -1, -2, \ldots$.

Notation of spaces of functions

$C(\Omega)$, $C(\overline{\Omega})$ The space of continuous functions defined on Ω, $\overline{\Omega}$, respectively.

$C^k(\Omega)$ The set of functions $u \in C(\Omega)$ such that their partial derivatives up to the order k belongs to $C(\Omega)$.

$C^{0,\eta}(\overline{\Omega})$ The space of Hölder continuous functions on $\overline{\Omega}$. More specifically, let $\eta \in (0, 1)$, $\Omega \subset \mathbb{R}^d$ be open, connected, and bounded. Then we define

$$ C^{0,\eta}(\overline{\Omega}) := \left\{ u \in C(\overline{\Omega}) \colon [u]_\eta := \sup_{\mathbf{x},\mathbf{y} \in \overline{\Omega}, \mathbf{x} \neq \mathbf{y}} \frac{|u(\mathbf{x}) - u(\mathbf{y})|}{|\mathbf{x} - \mathbf{y}|^\eta} < +\infty \right\}. $$

Endowed with the norm

$$ \|u\|_{C^{0,\eta}(\overline{\Omega})} := \|u\|_{C(\overline{\Omega})} + [u]_\eta, $$

this space is Banach space.

$C^{0,\eta}_{\mathrm{loc}}(\Omega)$ The space of locally Hölder continuous functions on Ω, i.e.,

$$C^{0,\eta}_{\mathrm{loc}}(\Omega) := \left\{ u \in C(\Omega) \colon u|_{\overline{\Omega'}} \in C^{0,\eta}(\overline{\Omega'}) \text{ for any open and connected } \Omega' \text{ such that } \overline{\Omega'} \subset \Omega \right\}.$$

$L^p(\Omega)$ The space of Lebesgue integrable functions with the exponent p, for $1 \leq p < +\infty$.

$L^p_{\mathrm{loc}}(\Omega)$ The space of locally integrable functions, i.e.,

$$L^p_{\mathrm{loc}}(\Omega) := \{ u \colon \Omega \to \mathbb{R}, \text{measurable} \colon\ u|_K \in L^p(K)\ \forall K \subset \Omega,\ K \text{ compact} \},$$

where $1 \leq p < +\infty$.

$L^p(\Omega, w)$ The weighted Lesbegue space, i.e.,

$$L^p(\Omega, w) := \{ u \colon \Omega \to \mathbb{R}, \text{measurable} \colon\ \int_\Omega |u|^p w \, \mathrm{d}\mathbf{x} < +\infty \},$$

where $1 \leq p < +\infty$ and $w \colon \Omega \to R$ is nonnegative measurable function.

Notation related to vectors and matrices

$[\mathbf{A}]_{i,j}$ Element $A_{i,j}$ of the matrix $\mathbf{A} \in \mathbb{R}^{N \times N}$, for $i, j = 1, \ldots, N$, where $N \in \mathbb{N}$.

$[\mathbf{b}]_j$ j-th component of vector $\mathbf{b} \in \mathbb{R}^N$, for $j = 1, \ldots, N$, where $N \in \mathbb{N}$.

$[\mathbf{F}(\mathbf{u})]_j$ j-th component of the function $\mathbf{F} \colon \mathbb{R}^N \to \mathbb{R}^N$, for $j = 1, \ldots, N$, where $N \in \mathbb{N}$.

Introduction 1

The history of fractional calculus [28, pp. 1-36] can be traced back to 17^{th} century, when a question arose whether the meaning of usual derivative

$$u^{(n)} = \frac{d^n x}{dx^n}, \quad n \in \mathbb{N},$$

can be extended for any number n irrational, fractional or complex. It was L'Hospital who asked Leibnitz about the possibility of n being a fraction, with an answer given in 1695, that it would lead to a paradox. Moreover, Lebnitz prophetically added that one day 'this paradox' will be considerably useful. In 1819, there is a first mention of a derivative of an arbitrary order in the text by the French mathematician S. F. Lacroix, where Lacroix obtained a formula for derivative of an order $\frac{1}{2}$. Also, mathematicians as Euler and Fourier discussed the derivatives of arbitrary order but without any applications or examples. First applications of fractional calculus belongs to Niels Henrik Abel, who used the fractional calculus in the solution of an integral equation related to formulation of the tautochrome problem in 1823. It was the Abel's solution which probably motivated Liouville to attempt to provide a logical definition of a fractional derivative, which lead to his publications in 1832 and then several more through 1855. Between the year 1835 and 1850 there was a controversy related to the names mentioned before, that is Lacroix and Louiville. The controversy concerned the definition of a fractional derivative, where part of the mathematicians preferred the Lacroix's definition and part of the mathematicians preferred the Louiville's definition. Moving forward in time to 1938, M. Riesz introduced nowadays so called Riesz potential $\mathcal{I}_\alpha$, defined by

$$\mathcal{I}_\alpha u(\mathbf{x}) = \frac{\Gamma\left(\frac{d-\alpha}{2}\right)}{2^\alpha \pi^{d/2} \Gamma\left(\frac{\alpha}{2}\right)} \int_{\mathbb{R}^d} \frac{u(\mathbf{y})}{|\mathbf{y}-\mathbf{x}|^{d-\alpha}} \, \mathrm{d}y,$$

where $\alpha \in (0, d)$ and $d \in \mathbb{N}$ is the dimension. It can be shown that under certain assumptions (see [16, Th. 2.4]) the inverse of the Riesz operator $\mathcal{I}_\alpha$ is the fractional Laplace operator $-(-\Delta)^{\alpha/2}$. This was historically the first motivation to introduce the operator $-(-\Delta)^{\alpha/2}$ (see [27]).

The fractional Laplacian $(-\Delta)^{\alpha/2}$, for $\alpha \in (0, 2)$, appears both in pure and applied mathematics. The usage of the fractional order Laplacian ranges from models for fractional diffusion [8, 12, 34], through topics related to biology[2, 15, 17, 33]. To demonstrate that the fractional Laplacian is not an abstract construct, we refer the reader to [8], where the author

discusses the fact that the processes described by the fractional Laplacian can be directly observed, for example in the shape of a smokestack plume. One can observe, that the shape of the smokestack plume has rather conical shape than a shape of a paraboloid, which would correspond to diffusion driven by the ordinary Laplacian. We can go even farther back in time, where Richardson[26] in 1926 describes a phenomena where the diffusivity of particles in the atmosphere does not behave accordingly to the Brownian motion. Richardson then develops a model describing this behavior. Nevertheless, his model was able to describe the behavior just for spherical cloud of a particles. Based on Richardson's observation and models, Monin[24] in 1955 developed an integro-differential equation which models turbulent dispersal in two and three dimension. The operator appearing in Monin's equation turns out to be the fractional Laplacian. After Monin published his article[24], there was a rapid development in applications related to the fractional Laplacian.

In the monograph[25], which is a monograph we will use as a main source in following chapters, the author provides a physical motivation for the fractional Laplacian of a function of one variable. As a motivation, motions of random walkers on a one-dimensional grid of equidistant points are studied. These walkers have a 50% chance of moving to its direct neighboring node on the right and 50% chance of moving to its direct neighboring node on the left. If we would study how the system evolves in time, we would obtain an equation where an approximation of the ordinary Laplacian appears. If we would consider instead of random walkers so called random jumpers, which can jump to more distant locations than to its direct neighboring grid points with a probability described by so called heavy-tailed probability distributions, we would obtain an equation where an approximation of the Fractional Laplacian appears. For thorough discussion of these models, we refer the reader to [25, Chapter 1].

There are multiple ways of defining the fractional Laplacian operator, such as Fourier definition, distributional definition, Bochner's definition, Balakrishnan's definition, singular integral definition, Dynkin's definition, quadratic form definition, semigroup definition, definition as an inverse of Riesz potential or a definition through harmonic extension. All of the mentioned definitions are listed and discussed in [18]. Moreover, the article[18] also provides the equivalence criteria between the pairs of definitions of the fractional Laplacian. For our purposes, we will be using the singular integral definition of the fractional Laplacian $(-\Delta)^{\alpha/2}$. The fractional Laplacian at point $x \in \mathbb{R}^d$, where $d \in \mathbb{N}$ denotes the spatial dimension, is then defined for sufficiently smooth function by the following formula

$$(-\Delta)^{\alpha/2} u(\mathbf{x}) := c_{d,\alpha} \int_{\mathbb{R}^d} \text{p.v.} \frac{u(\mathbf{x}) - u(\mathbf{y})}{|\mathbf{x} - \mathbf{y}|^{d+\alpha}} \mathrm{d}\mathbf{y}, \tag{1.1}$$

where

$$c_{d,\alpha} := \frac{\frac{\alpha}{2} 2^{\alpha} \Gamma\left(\frac{d+\alpha}{2}\right)}{\pi^{\frac{d}{2}} \Gamma(1 - \frac{\alpha}{2})},$$

where $\alpha \in (0, 2)$. The abbreviation p.v. in (1.1) stands for the Cauchy principal value of the singular integral, defined as

$$\int_{\mathbb{R}^d} \text{p.v.} \frac{u(\mathbf{x}) - u(\mathbf{y})}{|\mathbf{x} - \mathbf{y}|^{d+\alpha}} \mathrm{d}\mathbf{y} := \lim_{\epsilon \to 0^+} \int_{\mathbb{R}^d \setminus B_\epsilon(x)} \frac{u(\mathbf{x}) - u(\mathbf{y})}{|\mathbf{x} - \mathbf{y}|^{d+\alpha}} \mathrm{d}\mathbf{y}.$$

To specify for which functions u the integral in (1.1) is well defined, is quite complicated in general. Thus, we will present a useful proposition from [30], which states sufficient conditions

on u for the integral in (1.1) to be well defined. Before we state the proposition, we define following weighted Lebesgue space

$$L^1\left(\mathbb{R}^d; \frac{1}{1+|\mathbf{x}|^{d+\alpha}}\right) := \left\{ v \in L^1_{\text{loc}}\left(\mathbb{R}^d\right) : \int_{\mathbb{R}^d} \frac{|v(\mathbf{x})|}{1+|\mathbf{x}|^{d+\alpha}} \mathrm{d}\mathbf{x} < \infty \right\}.$$

PROPOSITION 1.1. [30, Proposition 2.4] Let $u \in L^1\left(\mathbb{R}^d; \frac{1}{1+|\mathbf{x}|^{d+\alpha}}\right)$ be a function and $\Omega \subset \mathbb{R}^d$ be an open set such that, for some $\varepsilon > 0$,

(i) $u\big|_\Omega \in C^{0,\alpha+\varepsilon}_{\text{loc}}(\Omega)$ for any $\alpha < 1$, or

(ii) $u\big|_\Omega \in C^{1,\alpha+\varepsilon-1}_{\text{loc}}(\Omega)$ for $\alpha \geqslant 1$.

Then $(-\Delta)^{\alpha/2}u$ is a continuous function on Ω and its values are given by (1.1).

REMARK 1.2. Let us note that if $u\big|_\Omega \in C^2(\Omega)$ then (i) and (ii) are satisfied for any $\alpha \in (0,2)$.

In the following example, we will present a function u which satisfies the assumptions of the Proposition 1.1.

Example 1.3. Consider the following function $u\colon \mathbb{R}^d \to \mathbb{R}$ defined as

$$u(\mathbf{x}) = \frac{\Gamma\left(\frac{d}{2}\right)}{2^\alpha \Gamma\left(\frac{d+\alpha}{2}\right)\Gamma\left(1+\frac{\alpha}{2}\right)} \left[1-|\mathbf{x}|^2\right]_+^{\alpha/2}.$$

The function u belongs to $L^1\left(\mathbb{R}^d; \frac{1}{1+|\mathbf{x}|^{d+\alpha}}\right)$ since it is continuous on $\overline{B_1(0)}$ and zero outside $B_1(0)$ because of the term $\left[1-|\mathbf{x}|^2\right]_+$. By a straightforward calculation it can be proved that $u\big|_{B_1(0)} \in C^2(B_1(0))$. Hence u satisfies assumptions of Proposition 1.1 for $\Omega = B_1(0)$ and any $\alpha \in (0,2)$. Thus, $(-\Delta)^\alpha u$ is well defined in $B_1(0)$ and its values are given by (1.1) in $B_1(0)$. It is known by [4, Eq. (5.4.)], [13, pp. 89] that the function u is the solution of the following problem

$$\begin{cases} (-\Delta)^{\alpha/2}u = 1 \text{ in } B_1(0), \\ \qquad\quad u = 0 \text{ in } \mathbb{R}^d \backslash B_1(0). \end{cases}$$

Let us note that by a straightforward calculation it can be easily verified that $u\big|_{B_1(0)} \in C^3(B_1(0))$, indeed. This fact is later used in testing of our numerical linear solvers for stationary problems, which require the solution to be of class $C^3(\Omega)$ on the domain under consideration Ω, see Example 2.2 on page 23.

Example 1.4. Let $d \geq 1$, $\alpha \in (0,2)$ and $\mathbf{x} = (x_1, x_2, \ldots, x_d)$. Consider function $u\colon \mathbb{R}^d \to \mathbb{R}$ defined by

$$u(\mathbf{x}) = x_d \left[1-|\mathbf{x}|^2\right]_+^2.$$

The function u belongs to $L^1\left(\mathbb{R}^d; \frac{1}{1+|\mathbf{x}|^{d+\alpha}}\right)$ since it is continuous on $\overline{B_1(0)}$ and zero outside $B_1(0)$ because of the term $\left[1-|\mathbf{x}|^2\right]_+$. By straightforward calculation it can be proved that $u\big|_{B_1(0)} \in C^2(B_1(0))$. Furthermore, let $p > -1$. Following Dyda[10], we define

$$\Phi^{(d)}_{p,\alpha}(\mathbf{x}) = \frac{\mathcal{A}_{d,-\alpha} B(-\frac{\alpha}{2}, p+1)\pi^{d/2}}{\Gamma\left(\frac{d}{2}\right)} \, {}_2F_1\left(\frac{\alpha+d}{2}, -p+\frac{\alpha}{2}; \frac{d}{2}; \mathbf{x}\right),$$

where

$$\mathcal{A}_{d,-\alpha} = \frac{2^{\alpha}\Gamma\left(\frac{\alpha+d}{2}\right)}{\pi^{d/2}|\Gamma\left(-\frac{\alpha}{2}\right)|}.$$

Then by [10, Th. 1], the function u solves

$$\begin{cases} (-\Delta)^{\alpha/2}u = f(\mathbf{x}) \text{ in } B_1(0), \\ \qquad\quad u = 0 \text{ in } \mathbb{R}^d \setminus B_1(0), \end{cases}$$

with right-hand side of the following form

$$f(\mathbf{x}) = -x_d\, \Phi_{2,\alpha}^{(d+2)}(|\mathbf{x}|^2),$$

for $|\mathbf{x}| < 1$.

The main scope of our work is to implement numerical methods for problems involving fractional Laplacian in one and two dimensions, respectively. We will focus on stationary and evolutionary problems with zero Dirichlet boundary condition. More precisely, the stationary problems will be of the following type

$$\begin{cases} (-\Delta)^{\alpha/2}u(\mathbf{x}) = \lambda f(\mathbf{x}, u) \text{ in } \Omega, \\ \qquad\quad u(\mathbf{x}) = 0 \text{ in } \mathbb{R}^d \backslash \Omega, \end{cases} \tag{1.2}$$

where $d = 1$ or 2, $\alpha \in (0,2)$, $\lambda \in \mathbb{R}$ is parameter, and $\Omega \subset \mathbb{R}^d$ is a bounded, open and connected set (which reduces to a bounded open interval for one-dimensional case). Let us note that the theoretical study of existence and uniqueness of such problems is very difficult task and requires to deal with various concepts of generalized solutions such as weak, energy, or viscosity solutions that are better suited for the use of functional analytic tools, see e.g. [1, 5, 19, 23]. These theories are far beyond of the knowledge provided by basic courses of mathematical and functional analysis. So we will limit ourselves only to numerical studies of problem (1.2) for several selected examples of functions $f\colon \Omega \times \mathbb{R} \times \mathbb{R} \to \mathbb{R}$.

Concerning evolutionary problem, we study

$$\begin{cases} \dfrac{\partial u(t,\mathbf{x})}{\partial t} + (-\Delta)^{\alpha/2}u(t,\mathbf{x}) = f(t,\mathbf{x},u) & \text{in } (T_0,T)\times\Omega, \\ u(t,\mathbf{x}) = 0 & \text{in } (T_0,T)\times(\mathbb{R}\setminus\Omega), \\ u(T_0,\mathbf{x}) = u_{init}(\mathbf{x}) & \text{in } \Omega, \end{cases} \tag{1.3}$$

where $-\infty < T_0 < T < +\infty$ and d, α, Ω are as above. Here a formulation suitable for functional analytic methods is even much more complicated, see e.g. [3, 19]. Thus we will again limit ourselves only to numerical studies of problem (1.3) for several selected examples of functions $f\colon (T_0,T)\times\Omega\times\mathbb{R}\to\mathbb{R}$. Since we use method of monotone iterations to treat nonlinear evolutionary problems, our examples must satisfy structural assumption that $s_1 \le s_2$ implies $f(t,\mathbf{x},s_1) \le f(t,\mathbf{x},s_1)$ for any $t \in (T_0,T)$ and any $\mathbf{x} \in \Omega$, cf. [3, 19, 29]. The initial function $u_{init}(\mathbf{x})$ is assumed to be $L^2(\Omega)$ in the theoretical literature, see e.g. [19], which is satisfied in our examples.

Let us also note that our discretization schemes of fractional Laplacian require sufficient smoothness in spatial variables of solutions, e.g. $C^3(\Omega)$ for the one-dimensional case, but such

smoothness is not known a priori in practical situations. Thus, we cannot provide information about the convergence of solutions of our discretized problems to the solutions of original problems as the discretization step tends to zero. Despite this fact, we still believe that our library of Matlab written functions for performing numerical simulations and creating bifurcation diagrams for discretized problems can provide reasonably good insight into the problems involving fractional Laplacian, if used with caution. *This library of functions is the main output* of the work on this master's thesis and it is enclosed in the attached files.

This thesis is organized as follows. In the second chapter of the text, we will consider one dimensional case. We will start with the discretization of the fractional operator $(-\Delta)^{\alpha/2}$. After that, stationary and evolutionary problems, respectively, will be studied. Both for the stationary and evolutionary problems, we will consider right-hand side independent of the solution u at first and develop so called linear solver. Only then we will move on to the problems with a right-hand side involving u. Third chapter of the text focuses on the two dimensional case. The structure of the third chapter mimics the structure described for one dimension case with focus shifted to implementation details specific for domains with the shape more complicated than just a square. For each of the aforementioned case, we will include examples to demonstrate the results obtain by our solvers. Several of the examples will concerned right-hand sided for which the exact solution is known, more specifically we will be testing our solver on the problems presented in Example 1.3 and Example 1.4. Moreover, we will also consider right-hand sides for which the solutions are not known, furthermore the smoothness of the solutions are not know. In these cases, we will provide just numerical simulations.

Numerical study of Fractional Laplacian in bounded interval

2

In this chapter, we will focus on the numerical study of the fractional Laplacian in bounded interval, that is one dimensional case will be studied. The main source we are using throughout this chapter is the monograph [25, Chapt. 1 and Chapt. 2]. We are taking over the process of discretizing the operator with our contribution of filling in the missing steps in the derivation of the disretization schemes. Moreover, during the derivation of the disretization schemes we are also discussing the errors which are introduced during certain approximations. We are mostly using the notation which is used in the book, although there are a few cases for which we are introducing a little bit different notation for better readability of the text.

In the first section of this chapter, we are focusing on the discretization of the fractional Laplacian. The whole process is divided into multiple steps, where each step has its own subsection. At the end of the first section we will arrive at a matrix which will correspond to the discretized fractional Laplacian. Throughout this chapter, the matrix corresponding to the discretized fractional Laplacian will be in the core of every method we will implement. Also, pseudocode for the assembly of the matrix will be included at the end of the first section. Lastly, we will include an example in which the behavior of the matrix will be described.

In the following section we will study stationary version of the problem, that is the following problem

$$\begin{cases} (-\Delta)^{\alpha/2} u(x) = \lambda f(x,u) \text{ in } \Omega, \\ u(x) = 0 \text{ in } \mathbb{R}\backslash\Omega, \end{cases}$$

where $\alpha \in (0,2)$, $\lambda \in \mathbb{R}$, $\Omega = (L,R)$ for $-\infty < L < R < +\infty$. Firstly, we will focus on a problem with right-hand side independent of u, that is

$$\begin{cases} (-\Delta)^{\alpha/2} u(x) = f(x) \text{ in } \Omega, \\ u(x) = 0 \text{ in } \mathbb{R}\backslash\Omega. \end{cases}$$

After that, we will focus on the original problem, where u can occur as an argument of the right-hand side. To solve the nonlinear problem with the right-hand side dependent on u, Newton's method will be used. Also, because of the problem being dependent on parameter $\lambda \in \mathbb{R}$,

simple continuation algorithm will be used. With the help of this algorithm, we will solve the problem for different values of parameter λ in a given range $[\lambda_{min}, \lambda_{max}]$. Moreover, we will plot the bifurcation diagram, that is the dependence of the norm of the solution on the value of the parameter λ.

Last section is devoted to the evolutionary version of the problem, that is

$$\begin{cases} \dfrac{\partial u(t,x)}{\partial t} + (-\Delta)^{\alpha/2} u(t,x) = f(t,x,u) & \text{in } (T_0,T)\times\Omega, \\ u(t,x) = 0 & \text{in } (T_0,T)\times(\mathbb{R}\setminus\Omega), \\ u(T_0,x) = u_{init}(x) & \text{in } \Omega, \end{cases} \tag{2.1}$$

where $\alpha \in (0,2)$, $\Omega = (L,R)$ for $-\infty < L < R < +\infty$, $T_0 < T$. As in the case of the stationary case, we will start with a linear problem. That is a problem with right-hand side independent of u, specifically

$$\begin{cases} \dfrac{\partial u(t,x)}{\partial t} + (-\Delta)^{\alpha/2} u(t,x) = f(t,x) & \text{in } (T_0,T)\times\Omega, \\ u(t,x) = 0 & \text{in } (T_0,T)\times(\mathbb{R}\setminus\Omega), \\ u(T_0,x) = u_{init}(x) & \text{in } \Omega. \end{cases}$$

For this problem, implicit Euler method is used. After that, study of the nonlinear evolutionary problem (2.1) follows. In that case, we are using method of monotone iterations.

For every of the above described cases, we will include several examples, on which the behavior of the solutions can be observed. Also, each example will be solved for different values of the fractional order α, so the difference of the solutions can be seen.

2.1 Discretization matrix for fractional Laplacian

As mentioned above, the foundation for all of the solvers that were implemented, is to construct matrix corresponding to the fractional Laplace operator. As a starting point, assume the problem with right-hand side independent of solution itself

$$\begin{cases} (-\Delta)^{\alpha/2} u(x) = f(x) \text{ in } \Omega := (L,R), \\ u(x) = 0 \text{ in } \mathbb{R}\setminus\Omega, \end{cases} \tag{2.2}$$

where $\alpha \in (0,2)$, $-\infty < L < R < +\infty$. For the case $d = 1$, we obtain from the definition (1.1) of the fractional Laplacian operator

$$(-\Delta)^{\alpha/2} u(x) := c_{1,\alpha} \int_{-\infty}^{+\infty} \text{p.v.} \, \frac{u(x+v) - u(x)}{|v|^{1+\alpha}} \, \mathrm{d}v,$$

where

$$c_{1,\alpha} = \alpha \frac{2^{\alpha-1}}{\sqrt{\pi}} \frac{\Gamma\left(\frac{1+\alpha}{2}\right)}{\Gamma\left(\frac{2-\alpha}{2}\right)}.$$

Now, let u be a given sufficiently smooth function (to be specified later). For the development of the discretization scheme of the fractional Laplacian $(-\Delta)^{\alpha/2} u$, we introduce special notation for the integral on the right-hand side in the definition above

$$J(x) := \int_{-\infty}^{+\infty} \text{p.v.} \, \frac{u(x+v) - u(x)}{|v|^{1+\alpha}} \, \mathrm{d}v.$$

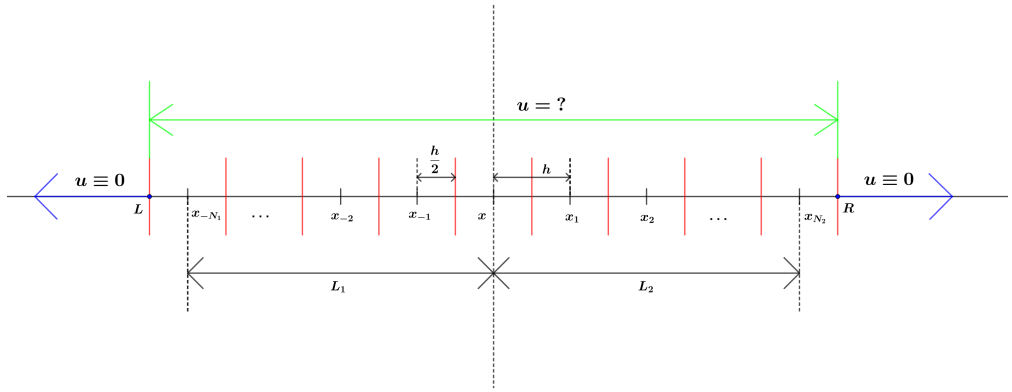

Figure 2.1: Division of the integration domain $(-\infty, +\infty)$ into three parts.

To evaluate value of $J(x)$ for a specific $x \in \mathbb{R}$, integration over $(-\infty, +\infty)$ is needed. Further, let us assume that our domain $\Omega = (L, R)$ contains $N \in \mathbb{N}$ equidistant nodes

$$L + h/2 =: x_{-N_1} < x_{-N_1+1} < \ldots < x_{-1} < x_0 := x < x_1 < \ldots < x_{N_2-1} < x_{N_2} := R - h/2,$$

where $x_{j+1} - x_j = h := \frac{R-L}{N}$, $N := N_1 + N_2 + 1$. We also define L_1, L_2 as

$$L_1 := x - x_{-N_1}\,, \quad L_2 := x_{N_2} - x\,.$$

For each node x_i, $i = -N_1, \ldots, -1, 0, 1, \ldots, N_2$, ith row of the desired matrix is constructed.

In order to construct a matrix which would correspond to discretized form of the operator, it is convenient to split up the integration domain into three parts

$$\begin{aligned} J(x) &= \int_{-\infty}^{\infty} \text{p.v.}\, \frac{u(x+v) - u(x)}{|v|^{1+\alpha}}\, \mathrm{d}v \\ &= \int_{-\infty}^{-L_1 - h/2} \frac{u(x+v) - u(x)}{|v|^{1+\alpha}}\, \mathrm{d}v + \int_{-L_1-h/2}^{L_2+h/2} \text{p.v.}\, \frac{u(x+v) - u(x)}{|v|^{1+\alpha}}\, \mathrm{d}v \\ &+ \int_{L_2+h/2}^{+\infty} \frac{u(x+v) - u(x)}{|v|^{1+\alpha}}\, \mathrm{d}v. \end{aligned} \tag{2.3}$$

The function $J(x)$ can be also rewritten[1] as

$$J(x) = J_1(x) + J_3(x) + J_2(x),$$

[1]The notation $J_1(x), J_3(x), J_2(x)$ is done in such a way, that the integrals $J_1(x), J_2(x)$ correspond to the notation in [25, pp. 54, 55].

where

$$J_1(x) = \int_{-\infty}^{-L_1-h/2} \frac{u(x+v)-u(x)}{|v|^{1+\alpha}}\,\mathrm{d}v,$$
$$J_2(x) = \int_{L_2+h/2}^{+\infty} \frac{u(x+v)-u(x)}{|v|^{1+\alpha}}\,\mathrm{d}v,$$
$$J_3(x) = \int_{-L_1-h/2}^{L_2+h/2} \text{p.v.}\ \frac{u(x+v)-u(x)}{|v|^{1+\alpha}}\,\mathrm{d}v.$$

This division of the original integral into these three parts is done in such a way that the term $J_3(x)$ represents the integral over the domain $\Omega = (L, R)$, in which our problem is being solved. Remaining two terms $J_1(x)$, $J_2(x)$ are over the complement of Ω. To have a better understanding of the division of $J(x)$ into the sum of $J_1(x)$, $J_2(x)$, $J_3(x)$ take a look at Figure 2.1. This is especially convenient for us, because with the help of the zero Dirichlet boundary condition in (2.2), $u(x+v) = 0$ and the terms $J_1(x)$, $J_2(x)$ get simplified as follows

$$J_1(x) = -u(x) \int_{-\infty}^{-L_1-h/2} \frac{1}{|v|^{1+\alpha}}\,\mathrm{d}v,$$
$$J_2(x) = -u(x) \int_{L_2+h/2}^{+\infty} \frac{1}{|v|^{1+\alpha}}\,\mathrm{d}v,$$

and can be easily calculated, as we will see later in this text. As of next, each of the three integrals of (2.3) will be taken care of separately in the following sections of this chapter.

2.1.1 Calculation of $J_3(x)$

Firstly, let us deal with the term

$$J_3(x) = \int_{-L_1-h/2}^{L_2+h/2} \text{p.v.}\ \frac{u(x+v)-u(x)}{|v|^{1+\alpha}}\,\mathrm{d}v,$$

where L_1, L_2, $h > 0$. To be able to calculate this integral effectively, let us split the integral into three more parts as follows

$$\begin{aligned}\int_{-L_1-h/2}^{L_2+h/2} \text{p.v.}\ \frac{u(x+v)-u(x)}{|v|^{1+\alpha}}\,\mathrm{d}v = &\int_{-L_1-h/2}^{-h/2} \frac{u(x+v)-u(x)}{|v|^{1+\alpha}}\,\mathrm{d}v \\ &+ \int_{-h/2}^{h/2} \text{p.v.}\ \frac{u(x+v)-u(x)}{|v|^{1+\alpha}}\,\mathrm{d}v \\ &+ \int_{h/2}^{L_2+h/2} \frac{u(x+v)-u(x)}{|v|^{1+\alpha}}\,\mathrm{d}v.\end{aligned} \tag{2.4}$$

Next, we will treat each of these integrals separately.

Beginning with the second integral

$$\int_{-h/2}^{h/2} \text{p.v.}\ \frac{u(x+v)-u(x)}{|v|^{1+\alpha}}\,\mathrm{d}v, \tag{2.5}$$

where, as mentioned before, $h > 0$. For increasing number of nodes $N \in \mathbb{N}$, spatial step h goes to zero. For that reason, assume $\rho > 0$ together with integral

$$\int_{-\rho}^{\rho} \text{p.v.}\ \frac{u(x+v)-u(x)}{|v|^{1+\alpha}}\,\mathrm{d}v. \tag{2.6}$$

We can see, that this integral is equal to the integral in (2.5) with $\rho = h/2$. Further, we will split the integral in (2.6) into two integrals

$$\begin{aligned}\int_{-\rho}^{\rho} \text{p.v.}\ \frac{u(x+v)-u(x)}{|v|^{1+\alpha}}\,\mathrm{d}v &= \int_{-\rho}^{\rho} \text{p.v.}\ \frac{u(x+v)-u(x)-u'(x)v+u'(x)v}{|v|^{1+\alpha}}\,\mathrm{d}v \\ &= \int_{-\rho}^{\rho} \text{p.v.}\ \frac{u(x+v)-u(x)-u'(x)v}{|v|^{1+\alpha}}\,\mathrm{d}v + u'(x)\int_{-\rho}^{\rho} \text{p.v.}\ \frac{v}{|v|^{1+\alpha}}\,\mathrm{d}v.\end{aligned} \tag{2.7}$$

Each of these two integrals will be evaluated separately.

We will start with the first one, for which we claim that

$$\int_{-\rho}^{\rho} \text{p.v.}\ \frac{u(x+v)-u(x)-u'(x)v}{|v|^{1+\alpha}}\,\mathrm{d}v \approx u''(x)\frac{\rho^{2-\alpha}}{2-\alpha}, \tag{2.8}$$

or more precisely

$$\lim_{\rho\to 0}\left|\frac{2-\alpha}{\rho^{2-\alpha}}\int_{-\rho}^{\rho} \text{p.v.}\ \frac{u(x+v)-u(x)-u'(x)v}{|v|^{1+\alpha}}\,\mathrm{d}v - u''(x)\right| = 0.$$

Using Taylor formula centered at x with remainder in the integral form, we obtain

$$\begin{aligned}u(x+v) &= u(x)+u'(x)v+\frac{1}{2}u''(x)v^2+\frac{1}{2}\int_x^{x+v} u'''(t)(x+v-t)^2\,\mathrm{d}t \left|\begin{array}{ll} t=x+vs & \mathrm{d}t = v\,\mathrm{d}s \\ L=0, & H=1\end{array}\right| \\ &= u(x)+u'(x)v+\frac{1}{2}u''(x)v^2+\frac{1}{2}v^3\int_0^1 (1-s)^2u'''(x+vs)\,\mathrm{d}s.\end{aligned}$$

Substituting into the left side of (2.8), we have

$$\begin{aligned}\int_{-\rho}^{\rho} \text{p.v.}\ \frac{u(x+v)-u(x)-u'(x)v}{|v|^{1+\alpha}}\,\mathrm{d}v &= \int_{-\rho}^{\rho} \text{p.v.}\ \frac{\frac{1}{2}v^2\left(u''(x)+v\int_0^1(1-s)^2u'''(x+vs)\,\mathrm{d}s\right)}{|v|^{1+\alpha}}\,\mathrm{d}v \\ &= \int_{-\rho}^{\rho} \text{p.v.}\ \frac{1}{2}\left(u''(x)+v\int_0^1(1-s)^2u'''(x+vs)\,\mathrm{d}s\right)|v|^{1-\alpha}\,\mathrm{d}v \\ &= \frac{1}{2}\int_{-\rho}^{\rho}\left(u''(x)+v\int_0^1(1-s)^2u'''(x+vs)\,\mathrm{d}s\right)|v|^{1-\alpha}\,\mathrm{d}v \\ &= \frac{1}{2}\int_{-\rho}^{\rho}u''(x)|v|^{1-\alpha}\,\mathrm{d}v \\ &\quad+\frac{1}{2}\int_{-\rho}^{\rho}v\int_0^1(1-s)^2u'''(x+vs)\,\mathrm{d}s\,|v|^{1-\alpha}\,\mathrm{d}v,\end{aligned}$$

where we have removed symbol p.v., since $1-\alpha \in (-1,1)$ and the integral exists as the usual Lebesgue integral. By a simple calculation, we have

$$\frac{1}{2}\int_{-\rho}^{\rho}u''(x)|v|^{1-\alpha}\,\mathrm{d}v = \frac{u''(x)}{2}\int_{-\rho}^{\rho}|v|^{1-\alpha}\,\mathrm{d}v = u''(x)\int_0^{\rho}v^{1-\alpha}\,\mathrm{d}v = u''(x)\frac{\rho^{2-\alpha}}{2-\alpha}.$$

It remains to prove that

$$\lim_{\rho\to 0}\frac{2-\alpha}{\rho^{2-\alpha}}\frac{1}{2}\int_{-\rho}^{\rho}v\int_0^1(1-s)^2u'''(x+vs)\,\mathrm{d}s|v|^{1-\alpha}\,\mathrm{d}v = 0. \tag{2.9}$$

Assume, that the third derivative of u satisfies the following assumption

$$u''' \in L^p[x-1, x+1] \text{ where } p > 1.$$

For $0 < \rho < 1$[2], we will prove that

$$\begin{aligned}\left|\int_{-\rho}^{\rho} v \int_0^1 (1-s)^2 u'''(x+vs)\,\mathrm{d}s\,|v|^{1-\alpha}\,\mathrm{d}v\right| &\le \left|\int_{-\rho}^{0} v \int_0^1 (1-s)^2 u'''(x+vs)\,\mathrm{d}s\,|v|^{1-\alpha}\,\mathrm{d}v\right| \\ &\quad + \left|\int_0^{\rho} v \int_0^1 (1-s)^2 u'''(x+vs)\,\mathrm{d}s\,|v|^{1-\alpha}\,\mathrm{d}v\right| \\ &\le 2\|u'''\|_{L^p([x-1,x+1])}\frac{\rho^{2-\alpha+1/p'}}{2-\alpha+1/p'}.\end{aligned} \tag{2.10}$$

Using this estimate, we obtain

$$\begin{aligned}0 &\le \lim_{\rho\to 0}\left|\frac{2-\alpha}{\rho^{2-\alpha}}\frac{1}{2}\int_{-\rho}^{\rho} v\int_0^1 (1-s)^2 u'''(x+vs)\,\mathrm{d}s|v|^{1-\alpha}\,\mathrm{d}v\right| \\ &\le \lim_{\rho\to 0}\left|\frac{2-\alpha}{\rho^{2-\alpha}}\right|\frac{1}{2}\left(2\|u'''\|_{L^p([x-1,x+1])}\frac{\rho^{2-\alpha+1/p'}}{2-\alpha+1/p'}\right) = 0,\end{aligned}$$

which implies (2.9). Now, it remains to prove (2.10). Indeed, we have

$$\begin{aligned}\left|\int_0^{\rho} v\int_0^1 (1-s)^2 u'''(x+vs)\,\mathrm{d}s\,v^{1-\alpha}\,\mathrm{d}v\right| &= \left|\int_0^{\rho}\int_0^1 (1-s)^2 u'''(x+vs)\,v\,v^{1-\alpha}\,\mathrm{d}s\,\mathrm{d}v\right| \\ &\le \int_0^{\rho}\int_0^1 \left|(1-s)^2 u'''(x+vs)\,v\,v^{1-\alpha}\right|\,\mathrm{d}s\,\mathrm{d}v \\ &= \int_0^{\rho}\int_0^1 (1-s)^2\left|u'''(x+vs)v\right|\,\mathrm{d}s\,v^{1-\alpha}\,\mathrm{d}v \\ &\le \int_0^{\rho}\int_0^1 \left|u'''(x+vs)\right|v\,\mathrm{d}s\,v^{1-\alpha}\,\mathrm{d}v \\ &\le \int_0^{\rho}\int_x^{x+v}\left|u'''(t)\right|\mathrm{d}t\,v^{1-\alpha}\,\mathrm{d}v \\ &= \int_0^{\rho}\left(\int_{x-1}^{x+1}\left|u'''(t)\right|\chi_{[x,x+v]}\,\mathrm{d}t\right)v^{1-\alpha}\,\mathrm{d}v.\end{aligned}$$

By using Hölder's inequality, we have

$$\begin{aligned}\int_0^{\rho}\left(\int_{x-1}^{x+1}\left|u'''(t)\right|\chi_{[x,x+v]}\,\mathrm{d}t\right)v^{1-\alpha}\,\mathrm{d}v &\le \int_0^{\rho}\|u'''\|_{L^p([x-1,x+1])}\|\chi_{[x,x+v]}\|_{L^{p'}([x-1,x+1])}\,v^{1-\alpha}\,\mathrm{d}v \\ &= \|u'''\|_{L^p([x-1,x+1])}\int_0^{\rho}\left(\int_x^{x+v}1^{p'}\,\mathrm{d}t\right)^{1/p'}v^{1-\alpha}\,\mathrm{d}v \\ &= \|u'''\|_{L^p([x-1,x+1])}\int_0^{\rho}v^{1-\alpha+1/p'}\,\mathrm{d}v \\ &= \|u'''\|_{L^p([x-1,x+1])}\frac{\rho^{2-\alpha+1/p'}}{2-\alpha+1/p'}.\end{aligned}$$

[2]Because we are calculating limit for $\rho \to 0$, we can use this restriction for ρ.

For the second integral we have

$$\begin{aligned}
\left|\int_{-\rho}^{0} v \int_{0}^{1} (1-s)^2 u'''(x+vs)\,\mathrm{d}s\,|v|^{1-\alpha}\,\mathrm{d}v\right| &= \left|\int_{-\rho}^{0}\int_{0}^{1} (1-s)^2 u'''(x+vs)\,v\,|v|^{1-\alpha}\,\mathrm{d}s\,\mathrm{d}v\right| \\
&\leq \int_{-\rho}^{0}\int_{0}^{1} \left|(1-s)^2 u'''(x+vs)\,v\,|v|^{1-\alpha}\right| \mathrm{d}s\,\mathrm{d}v \\
&= \int_{-\rho}^{0}\int_{0}^{1} (1-s)^2 \left|u'''(x+vs)\right| |v|\,\mathrm{d}s\,|v|^{1-\alpha}\,\mathrm{d}v \\
&\leq \int_{-\rho}^{0}\int_{0}^{1} \left|u'''(x+vs)\right| |v|\,\mathrm{d}s\,|v|^{1-\alpha}\,\mathrm{d}v \\
&= \int_{-\rho}^{0}\int_{0}^{1} -\left|u'''(x+vs)\right| v\,\mathrm{d}s\,|v|^{1-\alpha}\,\mathrm{d}v \\
&= \left|\begin{array}{ll} w=-v & \mathrm{d}w=-\mathrm{d}v \\ L=\rho, & H=0 \end{array}\right| \\
&= -\int_{\rho}^{0}\int_{0}^{1} \left|u'''(x-ws)\right| w\mathrm{d}s\,|w|^{1-\alpha}\,\mathrm{d}w \\
&= \int_{0}^{\rho}\int_{0}^{1} \left|u'''(x-ws)\right| w\mathrm{d}s\,w^{1-\alpha}\,\mathrm{d}w.
\end{aligned}$$

After introducing following substitution, we obtain

$$\begin{aligned}
\int_{0}^{\rho}\int_{0}^{1} \left|u'''(x-ws)\right| w\mathrm{d}s\,w^{1-\alpha}\,\mathrm{d}w &= \left|\begin{array}{ll} t=x-ws & \mathrm{d}t=-w\mathrm{d}s \\ L=x, & H=x-w \end{array}\right| \\
&= \int_{0}^{\rho}\int_{x}^{x-w} -\left|u'''(t)\right| \mathrm{d}t\,w^{1-\alpha}\,\mathrm{d}w \\
&= \int_{0}^{\rho}\int_{x-w}^{x} \left|u'''(t)\right| \mathrm{d}t\,w^{1-\alpha}\,\mathrm{d}w \\
&= \int_{0}^{\rho}\int_{x-1}^{x+1} \left|u'''(t)\right| \chi_{[x-w,x]}\,\mathrm{d}t\,w^{1-\alpha}\,\mathrm{d}w.
\end{aligned}$$

Again, by using Hölder's inequality, we have

$$\begin{aligned}
\int_{0}^{\rho}\int_{x-1}^{x+1} \left|u'''(t)\right| \chi_{[x-w,x]}\,\mathrm{d}t\,w^{1-\alpha}\,\mathrm{d}w &\leq \|u'''\|_{L^p([x-1,x+1])} \int_{0}^{\rho} \left(\int_{x-w}^{x} 1^{p'}\,\mathrm{d}t\right)^{1/p'} w^{1-\alpha}\,\mathrm{d}w \\
&= \|u'''\|_{L^p([x-1,x+1])} \int_{0}^{\rho} w^{1-\alpha+1/p'}\,\mathrm{d}w \\
&= \|u'''\|_{L^p([x-1,x+1])} \frac{\rho^{2-\alpha+1/p'}}{2-\alpha+1/p'}.
\end{aligned}$$

By that we have shown that (2.10) holds. Next, it remains to evaluate the remaining integral in (2.7). One can easily calculate that

$$u'(x)\int_{-\rho}^{\rho} \text{p.v.}\ \frac{v}{|v|^{1+\alpha}}\,\mathrm{d}v = 0,$$

due to the oddness of the function

$$\frac{v}{|v|^{1+\alpha}}.$$

Combining all our results, we have shown that

$$\int_{-\rho}^{\rho} \text{p.v.} \ \frac{u(x+v)-u(x)}{|v|^{1+\alpha}}\,\mathrm{d}v \approx u''(x)\frac{\rho^{2-\alpha}}{2-\alpha}. \tag{2.11}$$

To evaluate integral (2.5), we simply set $\rho = h/2$. We arrive at

$$\int_{-h/2}^{h/2} \text{p.v.} \ \frac{u(x+v)-u(x)}{|v|^{1+\alpha}}\,\mathrm{d}v \approx h^2 u''(x)\frac{1}{h^\alpha}\frac{1}{2-\alpha}\frac{1}{2^{2-\alpha}}.$$

So far, we have evaluated the second integral of (2.4). Now, let's focus on the remaining two integrals. Firstly, we will evaluate the first integral

$$\int_{-L_1-h/2}^{-h/2} \frac{u(x+v)-u(x)}{|v|^{1+\alpha}}\,\mathrm{d}v.$$

We can approximate this integral by the midpoint rule, getting

$$\begin{aligned}\int_{-L_1-h/2}^{-h/2} \frac{u(x+v)-u(x)}{|v|^{1+\alpha}}\,\mathrm{d}v &= \sum_{m=1}^{N_1} \int_{-h/2-(m-1)h}^{-h/2-mh} \frac{u(x+v)-u(x)}{|v|^{1+\alpha}}\,\mathrm{d}v \\ &\approx \sum_{m=1}^{N_1} \frac{u(x-mh)-u(x)}{(mh)^{1+\alpha}}h \\ &= \frac{1}{h^\alpha}\sum_{m=1}^{N_1} \frac{u(x-mh)-u(x)}{m^{1+\alpha}},\end{aligned}$$

where the approximation symbol means, that we are omitting the error of the midpoint rule

$$\int_{k_k}^{x_{k+1}} \phi(x)\,\mathrm{d}x = h\phi\left(x_k+\frac{h}{2}\right) + \frac{h^3}{24}\phi'''\left(\xi_k^R\right),$$

where $\xi_k^R \in (x_k, x_{k+1})$. In the same way, we can approximate the remaining integral

$$\int_{h/2}^{L_2+h/2} \frac{u(x+v)-u(x)}{|v|^{1+\alpha}}\,\mathrm{d}v$$

of (2.4). We get

$$\int_{h/2}^{L_2+h/2} \frac{u(x+v)-u(x)}{|v|^{1+\alpha}}\,\mathrm{d}v \approx \frac{1}{h^\alpha}\sum_{m=1}^{N_2} \frac{u(x+mh)-u(x)}{m^{1+\alpha}}.$$

Combining all the results from this section we arrive at

$$\begin{aligned}J_3(x) &= \int_{-L_1-h/2}^{L_2+h/2} \text{p.v.} \ \frac{u(x+v)-u(x)}{|v|^{1+\alpha}}\,\mathrm{d}v \\ &\approx \frac{1}{h^\alpha}\sum_{m=1}^{N_1} \frac{u(x-mh)-u(x)}{m^{1+\alpha}} + h^2u''(x)\frac{1}{h^\alpha}\frac{1}{2-\alpha}\frac{1}{2^{2-\alpha}} + \frac{1}{h^\alpha}\sum_{m=1}^{N_2} \frac{u(x+mh)-u(x)}{m^{1+\alpha}} \\ &= \frac{1}{h^\alpha}\left(\sum_{m=1}^{N_1} \frac{u(x-mh)-u(x)}{m^{1+\alpha}} + h^2u''(x)\frac{1}{2-\alpha}\frac{1}{2^{2-\alpha}} + \sum_{m=1}^{N_2} \frac{u(x+mh)-u(x)}{m^{1+\alpha}}\right).\end{aligned}$$

By setting

$$\sigma = \frac{1}{2-\alpha}\frac{1}{2^{2-\alpha}},$$

we arrive at

$$J_3(x) \approx \frac{1}{h^\alpha}\left(\sum_{m=1}^{N_1}\frac{u(x-mh)-u(x)}{m^{1+\alpha}} + h^2u''(x)\sigma + \sum_{m=1}^{N_2}\frac{u(x+mh)-u(x)}{m^{1+\alpha}}\right).$$

2.1.2 Calculation of $J_1(x)$ and $J_2(x)$

It remains to evaluate the terms

$$J_1(x) = -u(x)\int_{-\infty}^{-L_1-h/2}\frac{1}{|v|^{1+\alpha}}\,\mathrm{d}v,$$
$$J_2(x) = -u(x)\int_{L_2+h/2}^{+\infty}\frac{1}{|v|^{1+\alpha}}\,\mathrm{d}v.$$

We will start with $J_1(x)$. By simple calculation we obtain

$$\begin{aligned}
J_1(x) &= -u(x)\int_{-\infty}^{-L_1-h/2}\frac{1}{|v|^{1+\alpha}}\,\mathrm{d}v \\
&= -u(x)\int_{-\infty}^{-L_1-h/2}\frac{1}{(-v)^{1+\alpha}}\,\mathrm{d}v \\
&= -u(x)\left[\frac{1}{\alpha(-v)^\alpha}\right]_{-\infty}^{-L_1-h/2} \\
&= -u(x)\left[\frac{1}{\alpha(-v)^\alpha}\right]_{-\infty}^{-h\left(N_1+\frac{1}{2}\right)} \\
&= -\frac{1}{h^\alpha}u(x)\frac{1}{\alpha}\left(\frac{1}{N_1+\frac{1}{2}}\right)^\alpha.
\end{aligned}$$

By introducing the following term

$$\sigma_{(q)} = \frac{1}{\alpha}\left(\frac{1}{q+\frac{1}{2}}\right)^\alpha,$$

we arrive at

$$J_1(x) = -\frac{1}{h^\alpha}u(x)\sigma_{(N_1)}.$$

By the same fashion, we get

$$J_2(x) = -\frac{1}{h^\alpha}u(x)\sigma_{(N_2)}.$$

Notice that in [25, pp. 55] the author of the book has approximations of the terms $J_1(x)$, $J_2(x)$, compared to our equality. The reason is that the author is taking into the assumption general boundary conditions, thus the term $u(x+v)$ in the integrals is not in his case necessarily equal to zero.

2.1.3 Final evaluation of $J(x)$

So far, we have approximated the terms $J_1(x), J_2(x), J_3(x)$. Putting everything together, we have

$$\begin{aligned} J(x) &= J_1(x) + J_3(x) + J_2(x) \\ &\approx \frac{1}{h^\alpha}\left(-u(x)\sigma_{(N_1)} + \sum_{m=1}^{N_1} \frac{u(x-mh)-u(x)}{m^{1+\alpha}}\right. \\ &\left. + h^2 u''(x)\sigma + \sum_{m=1}^{N_2} \frac{u(x+mh)-u(x)}{m^{1+\alpha}} - u(x)\sigma_{(N_2)}\right), \end{aligned} \tag{2.12}$$

where

$$\begin{aligned} \sigma &= \frac{1}{2-\alpha}\frac{1}{2^{2-\alpha}}, \\ \sigma_{(q)} &= \frac{1}{\alpha}\left(\frac{1}{q+\frac{1}{2}}\right)^\alpha. \end{aligned}$$

One can see that the two sums in (2.12) can be further rearranged as follows

$$\begin{aligned} \sum_{m=1}^{N_1} \frac{u(x-mh)-u(x)}{m^{1+\alpha}} + \sum_{m=1}^{N_2} \frac{u(x+mh)-u(x)}{m^{1+\alpha}} &= \sum_{m=-N_1}^{-1} \frac{u(x+mh)-u(x)}{(-m)^{1+\alpha}} + \sum_{m=1}^{N_2} \frac{u(x+mh)-u(x)}{m^{1+\alpha}} \\ &= \sum_{m=-N_1}^{N_2}{}' \frac{u(x+mh)-u(x)}{|m|^{1+\alpha}} \\ &= -u(x)\sum_{m=-N_1}^{N_2}{}' \frac{1}{|m|^{1+\alpha}} + \sum_{m=-N_1}^{N_2}{}' \frac{u(x+mh)}{|m|^{1+\alpha}}, \end{aligned}$$

where the prime after the sum means that the singular term for $m = 0$ is omitted. After introducing the following notation

$$\begin{aligned} S(x) &= \sum_{m=-N_1}^{N_2}{}' \frac{u(x+mh)}{|m|^{1+\alpha}}, \\ \phi_{(N_1,N_2)} &= \sum_{m=-N_1}^{N_2}{}' \frac{1}{|m|^{1+\alpha}}, \end{aligned}$$

the equation (2.12) can we rewritten as

$$J(x) \approx \frac{1}{h^\alpha}\left(-u(x)\sigma_{(N_1)} + S(x) + h^2 u''(x)\sigma - u(x)\phi_{(N_1,N_2)} - u(x)\sigma_{(N_2)}\right). \tag{2.13}$$

Further more, second derivative on the right-hand side of (2.13) can be approximated by second-order centered finite-difference formula

$$u''(x) \approx \frac{u(x-h)-2u(x)+u(x+h)}{h^2}. \tag{2.14}$$

As before, the approximation symbol means that we are omitting the error term of the second-order centered scheme. Depending on the smoothness of u, we can either expand u at x as

follows

$$u(x-h) = u(x) - hu'(x) + h^2\frac{u''(x)}{2} - h^3\frac{u'''(\xi_1)}{6},$$
$$u(x+h) = u(x) + hu'(x) + h^2\frac{u''(x)}{2} + h^3\frac{u'''(\xi_2)}{6},$$

where $\xi_1 \in (x-h, x)$, $\xi_2 \in (x, x+h)$. By adding these terms together, we arrive at (2.14) with an error term

$$h\frac{u'''(\xi_2) - u'''(\xi_1)}{6}.$$

In the case, in which u is even smoother, we can use following expansion

$$u(x-h) = u(x) - hu'(x) + h^2\frac{u''(x)}{2} - h^3\frac{u'''(x)}{6} + h^4\frac{u^{(4)}(\xi_1)}{24},$$
$$u(x+h) = u(x) + hu'(x) + h^2\frac{u''(x)}{2} + h^3\frac{u'''(x)}{6} + h^4\frac{u^{(4)}(\xi_2)}{24},$$

where $\xi_1 \in (x-h, x)$, $\xi_2 \in (x, x+h)$. Again, by adding these terms together we arrive at (2.14) with an error term

$$h^2\frac{u^{(4)}(\xi_1) + u^{(4)}(\xi_2)}{24}.$$

After the substitution of (2.14) into (2.13), we get

$$J(x) \approx \frac{1}{h^\alpha}\Big(-u(x)\sigma_{(N_1)} + S(x) + \sigma(u(x-h) - 2u(x) + u(x+h)) \\ -u(x)\phi_{(N_1,N_2)} - u(x)\sigma_{(N_2)}\Big). \quad (2.15)$$

For more compact way, which also gives us a hint how the matrix for the disretized fraction Laplacian will look like, we can rewrite (2.15) into the final form

$$J(x) \approx \frac{1}{h^\alpha}\sum_{m=-N_1}^{N_2}\mathcal{A}_m^{(\alpha)}u(x+hm), \quad (2.16)$$

where

$$\mathcal{A}_0^{(\alpha)} = -\phi_{(N_1,N_2)} - 2\sigma - \sigma_{(N_1)} - \sigma_{(N_2)}, \quad (2.17)$$
$$\mathcal{A}_{\pm1}^{(\alpha)} = 1 + \sigma, \quad (2.18)$$
$$\mathcal{A}_m^{(\alpha)} = \frac{1}{|m|^{1+\alpha}}. \quad (2.19)$$

Elements $\mathcal{A}_0^{(\alpha)}$ represent self-contribution, elements $\mathcal{A}_{\pm1}^{(\alpha)}$ represent nearest neighbor contributions and $\mathcal{A}_m^{(\alpha)}$ represent contributions from the rest of the grid-points. Putting everything together, we have

$$(-\Delta)^{\alpha/2}u(x) = c_{1,\alpha}\int_{-\infty}^{+\infty}\frac{u(x+v) - u(x)}{|v|^{1+\alpha}}\,\mathrm{d}v = c_{1,\alpha}J(x) \approx c_{1,\alpha}\frac{1}{h^\alpha}\sum_{m=-N_1}^{N_2}\mathcal{A}_m^{(\alpha)}u(x+hm). \quad (2.20)$$

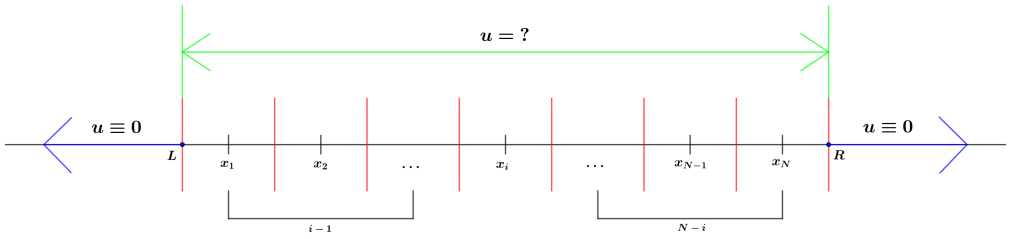

Figure 2.2: Relation between index i and N_1, N_2.

2.2 Construction of the matrix for discretized fractional Laplace operator

With the help of previous section, where the discretization of the fraction Laplace operator was discussed, the matrix of the operator will be constructed. To obtain the matrix, we will use equation (2.16) together with (2.17), (2.18), (2.19).

Recall that in our work we are considering equidistant spatial discretization of an interval (L, R), where $-\infty < L < R < +\infty$, with a number of nodes $N \in \mathbb{N}$ and step

$$h = \frac{R - L}{N}.$$

Because of this discretization, we are solving for a vector

$$\mathbf{u} = (u_1, u_2, \ldots, u_N),$$

where

$$u_i = u(L + (i-1)h) \text{ for } i = 1, \ldots, N.$$

Values of the fractional Laplace operator in these discrete values have then the form

$$\bar{\mathbf{u}} = (\bar{u}_1, \bar{u}_2, \ldots, \bar{u}_N),$$

where

$$\bar{u}_i = (-\Delta)^{\alpha/2} u(L + (i-1)h) \text{ for } i = 1, \ldots, N.$$

Then, following discrete form of the fractional Laplace operator holds

$$\bar{\mathbf{u}} = c_{1,\alpha} \frac{1}{h^\alpha} \tilde{\mathbf{A}}^{(\alpha)} \cdot \mathbf{u}, \tag{2.21}$$

where $\tilde{\mathbf{A}}^{(\alpha)} \in \mathbb{R}^{N \times N}$. To be able to utilize relations (2.17), (2.18), (2.19) we need to realize that for our situation, in which we have N nodes, for ith equation of (2.21), which corresponds to ith node, these relations hold

$$N_1 = i - 1, \tag{2.22}$$
$$N_2 = N - i, \tag{2.23}$$

for $i = 1, \ldots, N$. This situation is depicted in Figure 2.2. Substituting (2.22), (2.23) into (2.17), (2.18), (2.19) we get

$$A_{i,i}^{(\alpha)} = -\phi_{(i-1,N-i)} - 2\sigma - \sigma_{(i-1)} - \sigma_{(N-i)}, \tag{2.24}$$

$$A_{i,i\pm1}^{(\alpha)} = 1 + \sigma, \tag{2.25}$$

$$A_{i,j}^{(\alpha)} = \frac{1}{|i-j|^{1+\alpha}} \text{ for } j = 1, \ldots, i-2 \tag{2.26}$$

$$\text{and } j = i+2, \ldots, N,$$

where

$$\phi_{(n_1,n_2)} = \sum_{m=-n_1}^{n_2}{}' \frac{1}{|m|^{1+\alpha}}, \tag{2.27}$$

$$\sigma_{(q)} = \frac{1}{\alpha}\left(\frac{1}{q+\frac{1}{2}}\right)^{\alpha}, \tag{2.28}$$

$$\sigma = \frac{1}{2-\alpha}\frac{1}{2^{2-\alpha}}. \tag{2.29}$$

Apart from the matrix $\tilde{\mathbf{A}}^{(\alpha)}$ being a square matrix, another important property of the matrix $\tilde{\mathbf{A}}^{(\alpha)}$ is it being symmetrical. This can be easily seen directly from the terms (2.25), (2.26).

Finally, using (2.24), (2.25), (2.26), (2.27), (2.28), (2.29) the matrix $\tilde{\mathbf{A}}^{(\alpha)}$ can be constructed. Please, note that as a final step there is a need to multiply the constructed matrix by -1, that is

$$\mathbf{A}^{(\alpha)} = -\tilde{\mathbf{A}}^{(\alpha)},$$

because the author of [25] works with

$$\Delta^{\alpha/2} u(x),$$

while we are working with

$$(-\Delta)^{\alpha/2} u(x).$$

This final matrix $\mathbf{A}^{(\alpha)}$ is then the core for all the methods which will be described in following sections of this text.

In our implementation we are actually computing the normalized matrix $\mathbf{A}^{(\alpha)}$, that is matrix multiplied by the normalization constant $c_{1,\alpha}$. For further purposes, let's introduce following notation

$$\mathbf{A}_c^{(\alpha)} = c_{1,\alpha}\mathbf{A}^{(\alpha)}, \tag{2.30}$$

where as introduced before

$$c_{1,\alpha} = \alpha \frac{2^{\alpha-1}}{\sqrt{\pi}} \frac{\Gamma\left(\frac{1+\alpha}{2}\right)}{\Gamma\left(\frac{2-\alpha}{2}\right)}.$$

Our Matlab written function which computes the matrix $\mathbf{A}_c^{(\alpha)}$ is called *frac_lap_scaled_matrix_1D.m*. Pseudocode describing the algorithm follows.

Input:

$n \in \mathbb{N}$ (number of interior nodes in partition of interval $[L, R]$)

$\alpha \in (0, 2)$ (fractional order of $(-\Delta)^{\alpha/2}$)

Output:

$\mathbf{A}$ (matrix corresponding to discretized fractional Laplacian)

Begin

01 Calculation of $\mathbf{A}_{diag}$

% Calculation of the diagonal part of the matrix

02 Calculation of $\mathbf{A}_{sub\_super\_diag}$

% Calculation of the subdiagonal and superdiagonal part of the matrix

03 Calculation of $\mathbf{A}_{rest}$

% Calculation of the remaining upper part of the matrix

04 Calculation of $\mathbf{A}_{rest} \leftarrow \mathbf{A}_{rest} + \mathbf{A}'_{rest}$

% Calculation of the lower part of the matrix (using symmetry)

05 Calculation of $\mathbf{A} \leftarrow \mathbf{A}_{diag} + \mathbf{A}_{sub\_super\_diag} + \mathbf{A}_{rest}$

Putting calculated matrices together

06 $\mathbf{A} \leftarrow -c_{1,\alpha}\mathbf{A}$

07 Return $\mathbf{A}$

End

Example 2.1. To have an idea how the matrix of the discretized fractional Laplacian looks like and how it differs for different values of fractional order α, let us assume several scenarios, one for which the value of α is close to 0, one for which the value of alpha is in the middle of the fractional order interval and one for which the value is close to 2. We will assume an interval $(-1, 1)$, that is $L = -1$, $R = 1$, $N = 8$, together with fractional orders $\alpha = 0.001$, $\alpha = 1$ and $\alpha = 1.99$. By the usage of (2.24), (2.25), (2.26), (2.27), (2.28), (2.29) together with multiplying obtained matrix $\mathbf{A}^{(\alpha)}$ by a coefficient $c_{1,\alpha}$, that is

$$\mathbf{A}_c^{(\alpha)} = c_{1,\alpha}\mathbf{A}^{(\alpha)},$$

which is implemented in our function *frac_lap_scaled_matrix_1D.m*, one will get following matrices

$$\mathbf{A}_c^{(0.001)} = \begin{pmatrix} 1.0002 & -0.0006 & -0.0002 & -0.0002 & -0.0001 & -0.0001 & -0.0001 & -0.0001 \\ -0.0006 & 1.0001 & -0.0006 & -0.0002 & -0.0002 & -0.0001 & -0.0001 & -0.0001 \\ -0.0002 & -0.0006 & 1.0001 & -0.0006 & -0.0002 & -0.0002 & -0.0001 & -0.0001 \\ -0.0002 & -0.0002 & -0.0006 & 1.0001 & -0.0006 & -0.0002 & -0.0002 & -0.0001 \\ -0.0001 & -0.0002 & -0.0002 & -0.0006 & 1.0001 & -0.0006 & -0.0002 & -0.0002 \\ -0.0001 & -0.0001 & -0.0002 & -0.0002 & -0.0006 & 1.0001 & -0.0006 & -0.0002 \\ -0.0001 & -0.0001 & -0.0001 & -0.0002 & -0.0002 & -0.0006 & 1.0001 & -0.0006 \\ -0.0001 & -0.0001 & -0.0001 & -0.0001 & -0.0002 & -0.0002 & -0.0006 & 1.0002 \end{pmatrix},$$

$$\mathbf{A}_c^{(1)} = \begin{pmatrix} 1.4786 & -0.4775 & -0.0796 & -0.0354 & -0.0199 & -0.0127 & -0.0088 & -0.0065 \\ -0.4775 & 1.3725 & -0.4775 & -0.0796 & -0.0354 & -0.0199 & -0.0127 & -0.0088 \\ -0.0796 & -0.4775 & 1.3673 & -0.4775 & -0.0796 & -0.0354 & -0.0199 & -0.0127 \\ -0.0354 & -0.0796 & -0.4775 & 1.3664 & -0.4775 & -0.0796 & -0.0354 & -0.0199 \\ -0.0199 & -0.0354 & -0.0796 & -0.4775 & 1.3664 & -0.4775 & -0.0796 & -0.0354 \\ -0.0127 & -0.0199 & -0.0354 & -0.0796 & -0.4775 & 1.3673 & -0.4775 & -0.0796 \\ -0.0088 & -0.0127 & -0.0199 & -0.0354 & -0.0796 & -0.4775 & 1.3725 & -0.4775 \\ -0.0065 & -0.0088 & -0.0127 & -0.0199 & -0.0354 & -0.0796 & -0.4775 & 1.4786 \end{pmatrix},$$

$$\mathbf{A}_c^{(1.99)} = \begin{pmatrix} 1.9996 & -0.9939 & -0.0012 & -0.0004 & -0.0002 & -0.0001 & 0.0000 & 0.0000 \\ -0.9939 & 1.992 & -0.9939 & -0.0012 & -0.0004 & -0.0002 & -0.0001 & 0.0000 \\ -0.0012 & -0.9939 & 1.9918 & -0.9939 & -0.0012 & -0.0004 & -0.0002 & -0.0001 \\ -0.0004 & -0.0012 & -0.9939 & 1.9918 & -0.9939 & -0.0012 & -0.0004 & -0.0002 \\ -0.0002 & -0.0004 & -0.0012 & -0.9939 & 1.9918 & -0.9939 & -0.0012 & -0.0004 \\ -0.0001 & -0.0002 & -0.0004 & -0.0012 & -0.9939 & 1.9918 & -0.9939 & -0.0012 \\ 0.0000 & -0.0001 & -0.0002 & -0.0004 & -0.0012 & -0.9939 & 1.992 & -0.9939 \\ 0.0000 & 0.0000 & -0.0001 & -0.0002 & -0.0004 & -0.0012 & -0.9939 & 1.9996 \end{pmatrix}.$$

As mentioned, we can see that the matrix is indeed symmetrical. This property is useful while constructing the matrix, because we can just compute half of the elements of the matrix. By that we are saving computational time. On the other hand, we observe that our matrix is a full matrix, that is all elements are nonzero, which require $O(N^2)$ memory to store. Moreover, for solving linear equations with full matrices, Matlab uses an algorithm that is of $O(N^3)$ time complexity. In contrast, the matrix corresponding to ordinary Laplace operator has the banded sparse form

$$\mathbf{B} = \begin{pmatrix} 2 & -1 & 0 & 0 & 0 & 0 & 0 & 0 \\ -1 & 2 & -1 & 0 & 0 & 0 & 0 & 0 \\ 0 & -1 & 2 & -1 & 0 & 0 & 0 & 0 \\ 0 & 0 & -1 & 2 & -1 & 0 & 0 & 0 \\ 0 & 0 & 0 & -1 & 2 & -1 & 0 & 0 \\ 0 & 0 & 0 & 0 & -1 & 2 & -1 & 0 \\ 0 & 0 & 0 & 0 & 0 & -1 & 2 & -1 \\ 0 & 0 & 0 & 0 & 0 & 0 & -1 & 2 \end{pmatrix},$$

and time and memory efficient algorithms can be used. Thus, problems involving fractional Laplacian are much more difficult to treat numerically compared to problems involving classical Laplacian. Further more, let us note that the matrix $\mathbf{A}_c^{(1)}$, which corresponds to discretizaton of fractional Laplacian $(-\Delta)^{1/2}$, is not matrix $\mathbf{B}$ taken to the power $\frac{1}{2}$. Indeed,

$$\mathbf{B}^{\frac{1}{2}} = \begin{pmatrix} 1.3582 & -0.3879 & -0.0644 & -0.0231 & -0.0108 & -0.0056 & -0.0030 & -0.0013 \\ -0.3879 & 1.2938 & -0.4110 & -0.0752 & -0.0288 & -0.0138 & -0.0069 & -0.0030 \\ -0.064 & -0.4110 & 1.2830 & -0.4166 & -0.0782 & -0.0301 & -0.0138 & -0.0056 \\ -0.0231 & -0.0752 & -0.4166 & 1.2800 & -0.4179 & -0.0782 & -0.0288 & -0.0108 \\ -0.0108 & -0.0288 & -0.0782 & -0.4179 & 1.2800 & -0.4166 & -0.0752 & -0.0231 \\ -0.0056 & -0.0138 & -0.0301 & -0.0782 & -0.4166 & 1.2830 & -0.4110 & -0.0644 \\ -0.0030 & -0.0069 & -0.0138 & -0.0288 & -0.0752 & -0.4110 & 1.2938 & -0.3879 \\ -0.0013 & -0.0030 & -0.0056 & -0.0108 & -0.0231 & -0.0644 & -0.3879 & 1.3582 \end{pmatrix}.$$

Finally, let us point out that for the fractional order α going to zero, the fractional Laplacian goes to identity operator and on the other hand, for the fractional order α going to 2, the

fractional Laplacian goes to ordinary Laplacian operator, i.e.,

$$\lim_{\alpha \to 0^+} (-\Delta)^{\alpha/2} u = u,$$
$$\lim_{\alpha \to 2^-} (-\Delta)^{\alpha/2} u = -\Delta u,$$

as shown in [31, Proposition 5.3.]. This can be observed on the matrices $\mathbf{A}^{(0.001)}$ and $\mathbf{A}^{(1.99)}$, where we can see that the former is close to a unitary matrix and the latter is close the matrix corresponding to the ordinary Laplace operator. This agreement with theoretical fact is a kind of numerical verification that our discretization procedure was done correctly.

2.3 Stationary problems with fractional Laplacian

So far, we have been focusing on discretizing the fractional Laplacian. We have constructed the matrix $\mathbf{A}_c^{(\alpha)}$, which will be in the core of our numerical algorithms described in this and following section of the text. In this part of the text, stationary problems will be solved. Firstly, we will start with a problem with a right-hand side of the form $f = f(x)$. After that, we will move on to a problem with more general right-hand sides which will be dependent on the solution u itself and a parameter. More specifically, we will be working with the right-hand side of the form $f = \lambda f(x, u)$, where $\lambda \in \mathbb{R}$ is the parameter. For solving this type of problem, Newton's method will be used. Also, for this type of the right-hand side, bifurcation diagrams will be introduced, from which we will be able to see how the solution changes with respect to the parameter λ. For generating these bifurcation diagrams, simple continuation algorithm will be implemented.

Please, note that for problems involving fractional Laplacian the solution is not known in general, only for special cases, see e.g. [4, 11, 13]. Because of that we cannot really compare every solution of the numerical experiment obtained by our methods with the exact one, thus we cannot always directly evaluate the error of the methods.

2.3.1 Right-hand side independent of u

We will start with a case for which the right-hand side has the form $f = f(x)$, that is we are solving the following problem

$$\begin{cases} (-\Delta)^{\alpha/2} u(x) = f(x) \text{ in } \Omega, \\ u(x) = 0 \text{ in } \mathbb{R} \backslash \Omega, \end{cases}$$

where $\alpha \in (0, 2)$, $\Omega = (L, R)$ for $-\infty < L < R < +\infty$. Our Matlab written function for this type of problem is called *frac_laplace_1D.m*. This function calls the function *frac_lap_scaled_matrix_1D.m*, which was introduced in the previous Section 2.2. Pseudocode describing the Matlab function follows.

Input:

L	(left boundary of the domain)
R	(right boundary of the domain)
$n \in \mathbb{N}$	(number of nodes in partition of interval $[L, R]$)
$f = f(x)$	(source term f)
$\alpha \in (0, 2)$	(fractional order of $(-\Delta)^{\alpha/2}$)

Output:

solution	(solution vector)
grid	(vector of the gridpoints)

Begin

01 $h \leftarrow (R - L)/n$
02 **grid** $\leftarrow (L + h/2) : h : (R - h/2)$
03 **A** $\leftarrow$ *frac_lap_scaled_matrix_1D(n,α)*
04 **A** $\leftarrow \frac{1}{h^\alpha}$**A**
05 **b** $\leftarrow f($**grid**$)$
06 **solution** $\leftarrow$ **A**$\backslash$**b**
07 Return **solution**, **A**, **grid**

End

As mentioned before, we can see that we are indeed calling our function *frac_lap_scaled_matrix_1D.m* to obtain the matrix corresponding to the frational Laplacian. After that we are simply calculating the vector of the right-hand side and only then we solve the disretized system.

To get better understanding how the fractional Laplacian behaves, we will start with a simplest case, namely $f(x) = 1$, on which we will observe how the solution changes with respect to fractional order $\alpha \in (0, 2)$. Since the solution is known explicitly in this case, we can compare numerical solution with the true solution given by explicit formula and verify correctness of our numerical approach at least for this very special case.

Example 2.2. As said, let us solve the following problem

$$\begin{cases} (-\Delta)^{\alpha/2} u(x) = 1 \text{ in } (-1, 1), \\ \qquad\qquad u(x) = 0 \text{ in } \mathbb{R}\backslash(-1, 1). \end{cases} \tag{2.31}$$

In this case we will solve for $N = 200$ and for $\alpha = 0.001$, $\alpha = 0.1$, $\alpha = 1$, $\alpha = 1.9$. Solutions for these values of α are plotted in Figure 2.3. Explicit solutions are known by [4, Eq. (5.4.)], [13, pp. 89] and are given by the following formula

$$u^*(x) = \frac{\Gamma\left(\frac{1}{2}\right)}{2^\alpha \Gamma\left(\frac{1+\alpha}{2}\right) \Gamma\left(1 + \frac{\alpha}{2}\right)} \left[1 - x^2\right]_+^{\frac{\alpha}{2}}, \tag{2.32}$$

in our notation.

We can see that with α close to zero, the solution looks square-like and is close to the right-hand side, as can be seen in figure where the orange curve describes the right-hand side of our

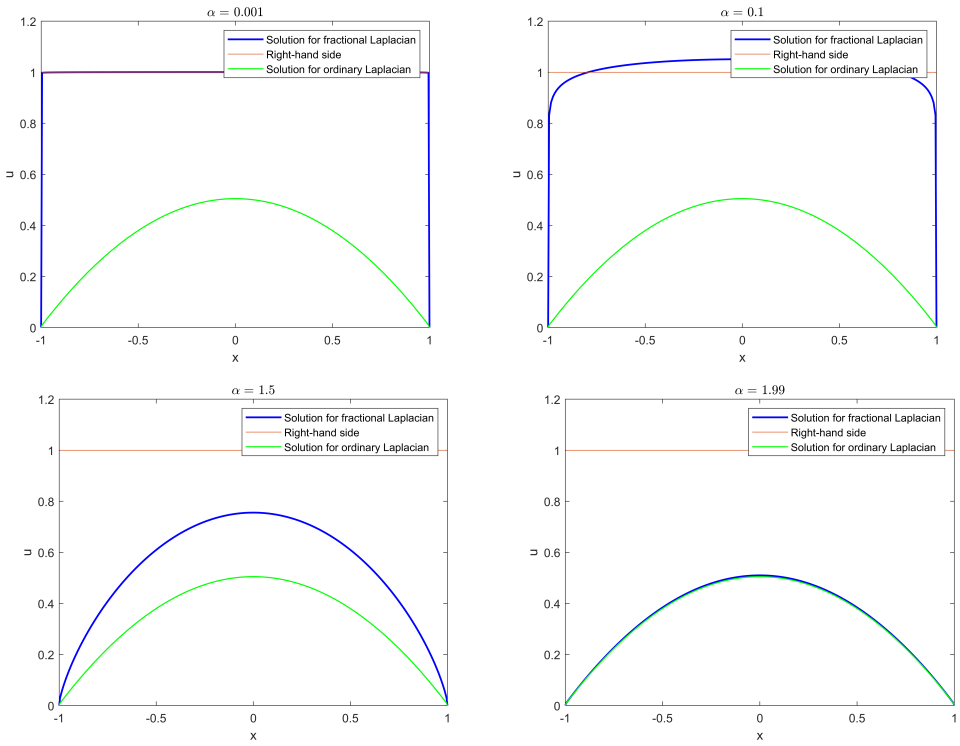

Figure 2.3: Solutions for different values of α of (2.31) together with the right-hand side (orange curve) and with the solution for the ordinary Laplacian problem (2.33) (green curve).

problem. The reason for that is that, as mentioned before, for α close to zero, the fractional Laplacian goes to the identity operator. Also, we can observe that the derivatives at the boundaries for α close to zero go to plus, or minus, infinity because of the zero boundary condition. With increasing values of α, the derivative at the boundaries decreases, in absolute value. Also, the solution is getting closer to the solution of the problem with the ordinary Laplacian, that is

$$\begin{cases} -\Delta u(x) = 1 \text{ in } (-1,1), \\ \quad u(x) = 0 \text{ for } x = -1,\ x = 1, \end{cases} \tag{2.33}$$

as can be seen in figure, where the green curve corresponds to the solution of the (2.33).

Also, in Figures 2.4, 2.5 we are providing the absolute error, that is

$$e_{absolute} = u^* - u,$$

where u is our numerical solution and u^* is the exact solution given by (2.32). Together with the absolute error we are providing the relative error given by

$$e_{relative} = \frac{u^* - u}{u^*}.$$

For the second example, we will choose more interesting right-hand side for which the solution for smaller values of α will behave in more interesting way. Let us note, that we do not have

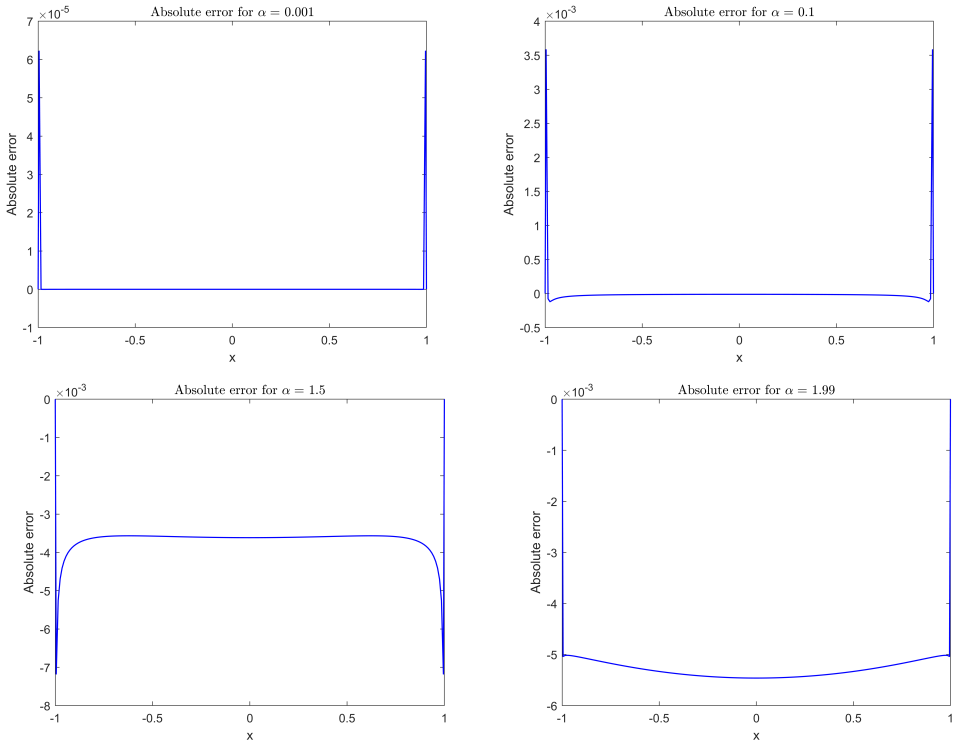

Figure 2.4: Absolute error for different values of α of (2.31).

any explicit formula for this solution and we also do not know if the solution is in $C^3(-1,1)$. So we cannot claim anything about accuracy of the approximation of the true solution by our numerical solution.

Example 2.3. Let us take a look at the following problem

$$\begin{cases} (-\Delta)^{\alpha/2} u(x) = x^2 + 1 \text{ in } (-1,1), \\ \qquad u(x) = 0 \text{ in } \mathbb{R}\backslash(-1,1). \end{cases} \tag{2.34}$$

Again, we are solving for $N = 200$ and for $\alpha = 0.001$, $\alpha = 0.1$, $\alpha = 1$, $\alpha = 1.99$. Solutions are plotted in Figure 2.6.

Again, for the derivatives close to the boundaries we can see similar behavior as in the previous example. For the cases $\alpha = 0.05$, $\alpha = 0.1$, we can see that the shape of the solution resembles the shape of the right-hand side of the problem (orange curve), as it was expected. However, the values of the solution tend to zero at the boundaries due to Dirichlet condition enforced by the outside of domain $(-1,1)$. For the solutions for $\alpha = 1$, $\alpha = 1.99$ we are expecting to obtain results which are close to the solution of the same problem with the ordinary Laplacian, that is the following problem

$$\begin{cases} -\Delta u(x) = x^2 + 1 \text{ in } (-1,1), \\ \quad u(x) = 0 \text{ for } \text{ for } x = -1,\ x = 1. \end{cases} \tag{2.35}$$

Solution corresponding to the problem (2.35) is also plotted in Figure 2.6 with a green color.

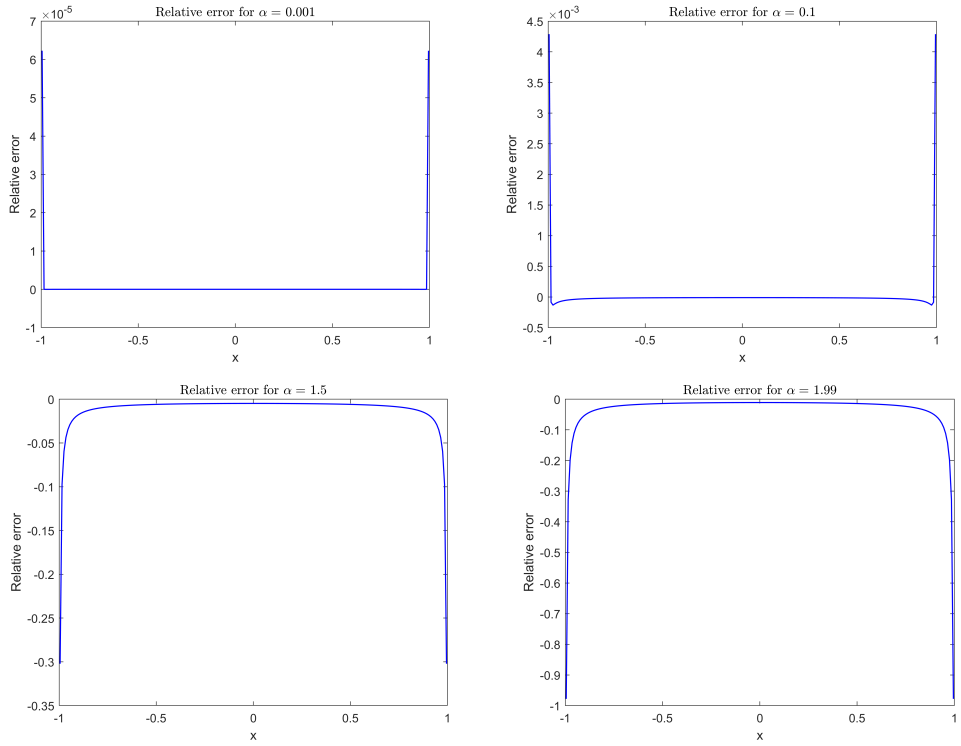

Figure 2.5: Relative error for different values of α of (2.31).

2.3.2 Nonlinear right-hand side dependent on parameter

In this section we consider right-hand side of the form $f = \lambda f(x, u)$, where $\lambda \in \mathbb{R}$ is a parameter. The problem we are solving has the following form

$$\begin{cases} (-\Delta)^{\alpha/2} u(x) = \lambda f(x, u) \text{ in } \Omega, \\ u(x) = 0 \text{ in } \mathbb{R} \backslash \Omega, \end{cases} \tag{2.36}$$

where $\alpha \in (0, 2)$, $\Omega = (L, R)$ for $-\infty < L < R < +\infty$, $\lambda \in \mathbb{R}$.

As mentioned at the beginning of this chapter, for solving this problem involving u on the right-hand side, Newton's method will be used. Firstly, we need to discretize (2.36). Using the finite differences method, we arrive at

$$\frac{1}{h^\alpha} \mathbf{A}_c^{(\alpha)} \mathbf{u} = \lambda \mathbf{F}(\mathbf{u}), \tag{2.37}$$

where $\mathbf{u} \in \mathbb{R}^N$ is a vector of values of the solution u evaluated at the $N \in \mathbb{N}$ discretization points belonging to Ω, $\mathbf{A}_c^{(\alpha)}$ is given by (2.30) and $\mathbf{F} \colon \mathbb{R}^N \to \mathbb{R}^N$ corresponds to the right-hand side function f by the following formula

$$[\mathbf{F}(\mathbf{u})]_j = f(x_j, u(x_j)),$$

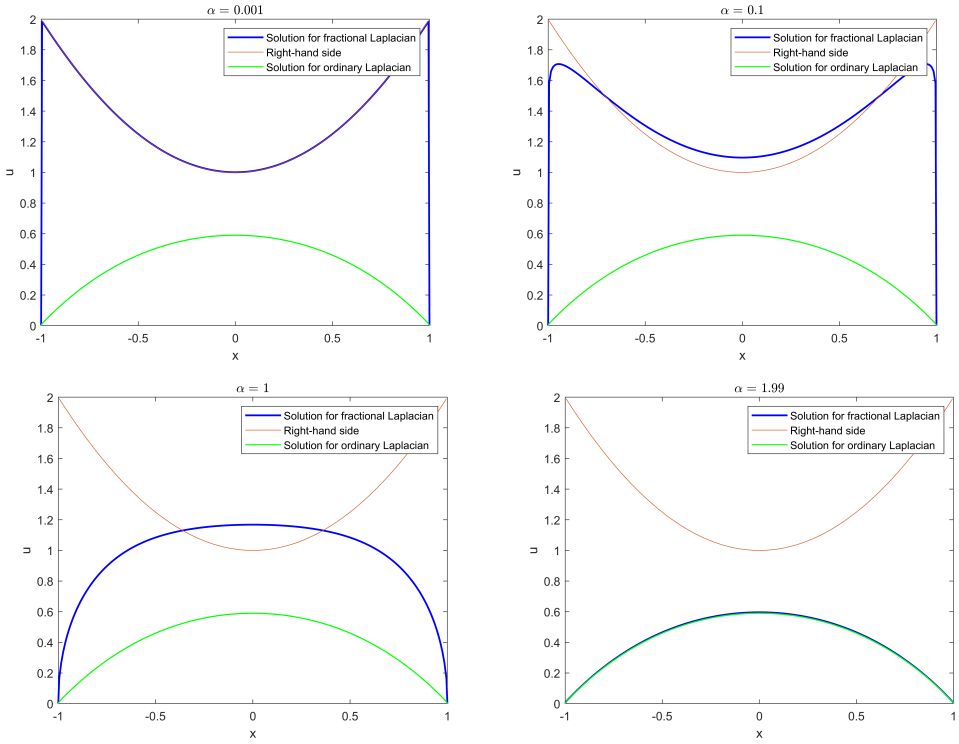

Figure 2.6: Solutions for different values of α of (2.34) together with the right-hand side (orange curve) and with the solution for the ordinary Laplacian problem (2.35) (green curve).

where $[\mathbf{F}(\mathbf{u})]_j$ stands for j-th component of the function $F\colon \mathbb{R}^N \to \mathbb{R}^N$ and

$$x_j = L + (j-1)h + \frac{h}{2} \text{ for } j = 1, 2, 3, \ldots, N.$$

After rearranging (2.37), we get

$$\frac{1}{h^\alpha}\mathbf{A}_c^{(\alpha)}\mathbf{u} - \lambda\mathbf{F}(\mathbf{u}) =: g(\mathbf{u}) = o,$$

where $g\colon \mathbb{R}^n \to \mathbb{R}^n$. Now, we have reformulated our original problem into a form for which the Newton's method can be used, producing successive approximations of our original problem (2.36). The successive approximations are then given by

$$\mathbf{u}_{k+1} = \mathbf{u}_k - \mathbf{J}_g(\mathbf{u}_k)^{-1} g(\mathbf{u}_k),$$

where $\mathbf{J}_g$ is the Jacobian matrix of g. Further more, the Jacobian matrix $\mathbf{J}_g$ is given by

$$\mathbf{J}_g = \frac{1}{h^\alpha}\mathbf{A}_c^{(\alpha)} - \lambda\mathbf{J}_F,$$

where $\mathbf{A}_c^{(\alpha)}$ is our matrix corresponding to dicretized fractional Laplacian and $\mathbf{J}_F$ is the Jacobian matrix of f.

Regarding the Newton's method, let us point out that the method is sensitive to the initial guess $\mathbf{u}_0$. Meaning, if the initial guess $\mathbf{u}_0$ is far from the solution, the successive iterations of the method may not converge to the solution. On the other hand, if the initial guess $\mathbf{u}_0$ is close enough, the method converges quadratically (under some assumptions) to the solution of the problem.

Our Matlab written solver for problems of the type (2.36), implementing the Newton's method (lines 11, 25, 40), is called *frac_laplace_newton_1D.m*. Pseudocode of this algorithm, which was inspired by [7], will follow.

Input:

L	(left boundary of the domain)
R	(right boundary of the domain)
$n \in \mathbb{N}$	(number of nodes in partition of interval $[L, R]$)
λ_{middle}	(parameter λ_{middle}, $\lambda_{middle} < \lambda_{max}$)
λ_{max}	(upper boundary of interval for λ parameter)
$m_1 \in \mathbb{N}$	(number of discretization points for partition of interval $(\lambda_{bif}, \lambda_{middle})$, where λ_{bif} is defined in the algorithm section)
$m_2 \in \mathbb{N}$	(number of discretization points for partition of interval $(\lambda_{middle}, \lambda_{max})$)
$6 < r < 15$	(10^{-r} is the tolerance in the Newton iteration)
$f = f(x, u)$	(source term f)
$f_u = f_u(x, u)$	(derivative f_u of source term f)
$u_{init} = u_{init}(x)$	(initial guess for Newton method for $\lambda = \lambda_{middle}$)
$\alpha \in (0, 2)$	(fractional order of $(-\Delta)^{\alpha/2}$)

Output:

S	(matrix of parameters λ (first column) with norms of corresponding norms of the solutions $\lvert\mathbf{u}\rvert_\infty$ (second column))
U	(matrix of solutions (each column corresponds to a solution for each λ_i))
grid	(vector of the gridpoints)
λ_{bif}	(bifurcation point)

Begin

01 $h \leftarrow (R - L)/n$
02 $\mathbf{grid} \leftarrow (L + h/2) : h : (R - h/2)$
03 $\mathbf{A} \leftarrow frac\_lap\_scaled\_matrix\_1D(n, \alpha)$
04 $\mathbf{A} \leftarrow \frac{1}{h^\alpha}\mathbf{A}$
05 $\mathbf{u}_{init} \leftarrow u_{init}(\mathbf{grid})$
06 $\lambda_{bif} \leftarrow min(eig(\mathbf{A}))$
07 Creation of matrices $\mathbf{S_1}$, $\mathbf{S_2}$, $\mathbf{U_1}$, $\mathbf{U_2}$
08 $[\mathbf{b}]_j \leftarrow f(x_j, u_j)$ for $j = 1, \ldots, n$
09 $\mathbf{u} \leftarrow \mathbf{u}_{init}$

$\mathbf{res} \leftarrow \mathbf{A}\mathbf{u} - \lambda_{middle}\mathbf{b}$
While $|\mathbf{res}|_\infty > 10^{-r}$ do
    % Newton loop for $\lambda = \lambda_{middle}$
    $[\mathbf{J_F}]_{i,j} \leftarrow f_u(x_j, u_j)$ for $j = 1, \ldots, n$
    $[\mathbf{J_F}]_{i,j} \leftarrow 0$ for $i \neq j,\ i, j = 1, \ldots, n$
    $\mathbf{J} \leftarrow \mathbf{A} - \lambda_{middle}\mathbf{J_F}$
    $\mathbf{u}_{diff} \leftarrow \mathbf{J} \backslash (-\mathbf{res})$
    $\mathbf{u} \leftarrow \mathbf{u}_{diff} + \mathbf{u}$
    $[\mathbf{b}]_j \leftarrow f(x_j, u_j)$ for $j = 1, \ldots, n$
    $\mathbf{res} \leftarrow \mathbf{A}\mathbf{u} - \lambda_{middle}\mathbf{b}$
EndWhile
$\mathbf{S_2} \leftarrow Append(\mathbf{S_2}, (\lambda_{middle}, |\mathbf{u}_{\lambda_{middle}}|_\infty))$
$\mathbf{U_2} \leftarrow Append(\mathbf{U_2}, \mathbf{u}_{\lambda_{middle}})$
For $i := 1 : m_2$ do
    % Apply Newton iterations to $\mathbf{A}\mathbf{u} - \mu_i\mathbf{F}(\mathbf{u}) = o$ for $\mu_i \in (\lambda_{middle}, \lambda_{max}]$
    $\mu_i \leftarrow \lambda_{middle} + \frac{i(\lambda_{max} - \lambda_{middle})}{m_2}$
    $\mathbf{u} \leftarrow \mathbf{u}_{i-1}$
    $[\mathbf{b}]_j \leftarrow f(x_j, u_j)$ for $j = 1, \ldots, n$
    $\mathbf{res} \leftarrow \mathbf{A}\mathbf{u} - \mu_i\mathbf{b}$
    While $|\mathbf{res}|_\infty > 10^{-r}$ do
        % Newton loop for $\lambda = \mu_i$
        $[\mathbf{J_F}]_{i,j} \leftarrow f_u(x_j, u_j)$ for $j = 1, \ldots, n$
        $[\mathbf{J_F}]_{i,j} \leftarrow 0$ for $i \neq j,\ i, j = 1, \ldots, n$
        $\mathbf{J} \leftarrow \mathbf{A} - \mu_i\mathbf{J_F}$
        $\mathbf{u}_{diff} \leftarrow \mathbf{J} \backslash (-\mathbf{res})$
        $\mathbf{u} \leftarrow \mathbf{u}_{diff} + \mathbf{u}$
        $[\mathbf{b}]_j \leftarrow f(x_j, u_j)$ for $j = 1, \ldots, n$
        $\mathbf{res} \leftarrow \mathbf{A}\mathbf{u} - \mu_i\mathbf{b}$
    EndWhile
    $\mathbf{S_2} \leftarrow Append(\mathbf{S_2}, (\mu_i, |\mathbf{u}_i|_\infty))$
    $\mathbf{U_2} \leftarrow Append(\mathbf{U_2}, \mathbf{u}_i)$
EndFor
For $i := 1 : m_1$ do
    % Apply Newton iterations to $\mathbf{A}\mathbf{u} - \mu_i\mathbf{F}(\mathbf{u}) = o$ for $\mu_i \in [\lambda_{bif}, \lambda_{middle})$
    $\mu_i \leftarrow \lambda_{middle} - \frac{i(\lambda_{middle} - \lambda_{bif})}{m_1}$
    $\mathbf{u} \leftarrow \mathbf{u}_{i+1}$
    $[\mathbf{b}]_j \leftarrow f(x_j, u_j)$ for $j = 1, \ldots, n$
    $\mathbf{res} \leftarrow \mathbf{A}\mathbf{u} - \mu_i\mathbf{b}$
    While $|\mathbf{res}|_\infty > 10^{-r}$ do
        % Newton loop for $\lambda = \mu_i$
        $[\mathbf{J_F}]_{i,j} \leftarrow f_u(x_j, u_j)$ for $j = 1, \ldots, n$
        $[\mathbf{J_F}]_{i,j} \leftarrow 0$ for $i \neq j,\ i, j = 1, \ldots, n$
        $\mathbf{J} \leftarrow \mathbf{A} - \mu_i\mathbf{J_F}$
        $\mathbf{u}_{diff} \leftarrow \mathbf{J} \backslash (-\mathbf{res})$
        $\mathbf{u} \leftarrow \mathbf{u}_{diff} + \mathbf{u}$
        $[\mathbf{b}]_j \leftarrow f(x_j, u_j)$ for $j = 1, \ldots, n$

46 $\quad\quad$ **res** $\leftarrow \mathbf{Au} - \mu_i \mathbf{b}$
47 $\quad$ EndWhile
48 $\quad$ $\mathbf{S_1} \leftarrow Append(\mathbf{S_1}, (\mu_i, |\mathbf{u}_i|_\infty))$
$\quad\quad$ $\mathbf{U_1} \leftarrow Append(\mathbf{U_1}, \mathbf{u}_i)$
49 EndFor
50 $\mathbf{S} \leftarrow Append(\mathbf{S_1}, \mathbf{S_2})$
51 $\mathbf{U} \leftarrow Append(\mathbf{U_1}, \mathbf{U_2})$
52 Return **S**, **U**, **grid**, λ_{bif},
End

Our Matlab written function for creating bifurcation diagrams requires that the function $\mathbf{F}\colon \mathbb{R}^N \to \mathbb{R}^N$ is twice continuously differentiable, since we use Newton's method.

Let us note that if $\mathbf{F}(0) = 0$, then $\mathbf{u} = 0$ is a solution of (2.37) for any $\lambda \in \mathbb{R}$. This is the so called line of trivial solutions. It may happen that nontrivial solutions bifurcate (separate) from this line of trivial solutions. If this bifurcation happens at a particular value of λ, this value of λ is called bifurcation point, see [9, Def. 1.1] for exact definition. Let, moreover, the function $\mathbf{F}$ satisfy the following additional assumptions $\mathbf{F}(\mathbf{u}) = \mathbf{u} + \mathbf{H}(\mathbf{u})$ and $\mathbf{H}\colon \mathbb{R}^N \to \mathbb{R}^N$ is twice continuously differentiable, $\mathbf{H}(0) = 0$, and

$$\lim_{|\mathbf{u}|\to 0} \frac{\mathbf{H}(\mathbf{u})}{|\mathbf{u}|} = 0\,.$$

Let $\lambda_0 \neq 0$ is a bifurcation point of nonzero solutions of (2.37). Then, under above stated additional assumptions, λ_0 is an eigenvalue of the matrix $\frac{1}{h^\alpha}\mathbf{A}_c^{(\alpha)}$, [9, Lemma 3.2]. Our continuation algorithm is designed in such a way that it is checking if the least eigenvalue of $\frac{1}{h^\alpha}\mathbf{A}_c^{(\alpha)}$ is a bifurcation point. This is motivated by the fact that bifurcations of positive solutions are of particular interest in practice and at the same time bifurcation of positive solutions of the original problem (2.36) usually happens at λ_1, which is the principal (smallest) eigenvalue of the corresponding eigenvalue problem for $(-\Delta)^{\alpha/2}$ on (L, R) [7, pp. 19] and [14]. We numerically approximate λ_1 as the smallest eigenvalue of the discretized fractional Laplacian (notice that in the sixth step of the algorithm λ_{bif} is computed as least eigenvalue of $\mathbf{A}$, which is $\frac{1}{h^\alpha}\mathbf{A}_c^{(\alpha)}$, indeed).

We mentioned that for the problems for which the right-hand side is dependent on a parameter, there will be a bifurcation diagram for which the simple continuation algorithm will be used. The simple continuation algorithm can be seen in the pseudocode. Notice, that we are going through two *For* cycles (starting at line 20 and line 35). In the first cycle, solutions for $\lambda \in (\lambda_{middle}, \lambda_{max}]$ are being calculated. In the second cycle, solutions for $\lambda \in (\lambda_{bif}, \lambda_{middle}]$ are being calculated. Before these two cycle, the solution for $\lambda = \lambda_{middle}$ is calculated as a starting point for the calculation of the solutions for remaining lambdas.

The idea of our simple continuation algorithm is that for a calculation of a solution for $\lambda = \lambda_i$, we are using solution corresponding to the neighboring value of λ, either $\lambda = \lambda_{i-1}$ or $\lambda = \lambda_{i+1}$, as an initial guess. As said before, firstly we are going through a *For* cycle which calculates solutions for $\lambda \in (\lambda_{middle}, \lambda_{max}]$, that is we are going in the positive direction for the values of λ. Because of that, for finding a solution for $\lambda = \lambda_i$ we are choosing solution corresponding to λ_{i-1} as the initial guess. In the case of the second *For* cycle, that is solutions

for $\lambda \in (\lambda_{bif}, \lambda_{middle}]$, we are going in the negative direction for the values of λ. Thus, we are taking the solution corresponding to λ_{i+1} as the initial guess.

For the first two numerical experiments we will take a look at right-hand side

$$f(\lambda, x, u) = \lambda u(1-u),$$

which can be found in [7, pp. 22].

Example 2.4. Consider the following problem

$$\begin{cases} (-\Delta)^{0.9} u(x) = \lambda u(1-u) \text{ in } (0,1), \\ u(x) = 0 \text{ in } \mathbb{R}\backslash(0,1). \end{cases} \tag{2.38}$$

As in previous examples, we will solve for $N = 200$. Then, we set $\lambda_{middle} = 10$, $\lambda_{max} = 60$, $m_1 = 50$, $m_2 = 30$, $r = 7$, $u_{init}(x) = 1$. For the fractional order we will set $\alpha = 1.8$.

In the Figure 2.7 we can see the bifurcation diagram for the problem (2.38). As described before, firstly we calculate the solution for $\lambda = \lambda_{middle}$, which in figure corresponds to point number 1. After that, we are calculating solutions for $\lambda \in (\lambda_{middle}, \lambda_{max}]$. Some of these solutions are depicted in figure by points 2, 3, 4, 5, 6. After that, we are calculating solutions for $\lambda \in [\lambda_{bif}, \lambda_{middle})$, in figure points 7, 8. Please note, that we are plotting only nontrivial solutions, that is in Figure 2.7 is missing line which coincides with x-axes. Solutions corresponding to the points highlighted in the bifurcation diagram 2.7, can be seen in Figure 2.8.

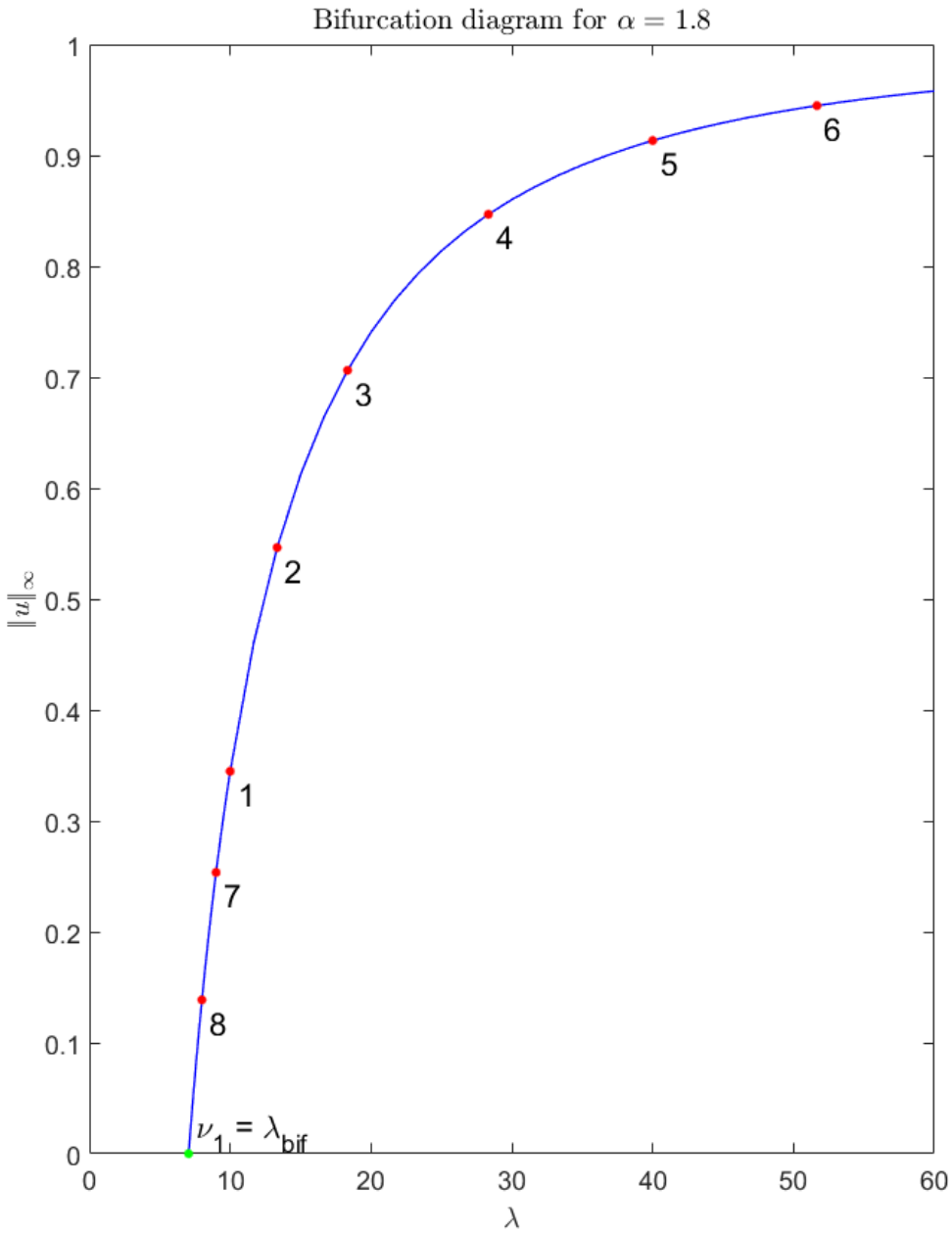

Figure 2.7: Bifurcation diagram for the problem (2.38).

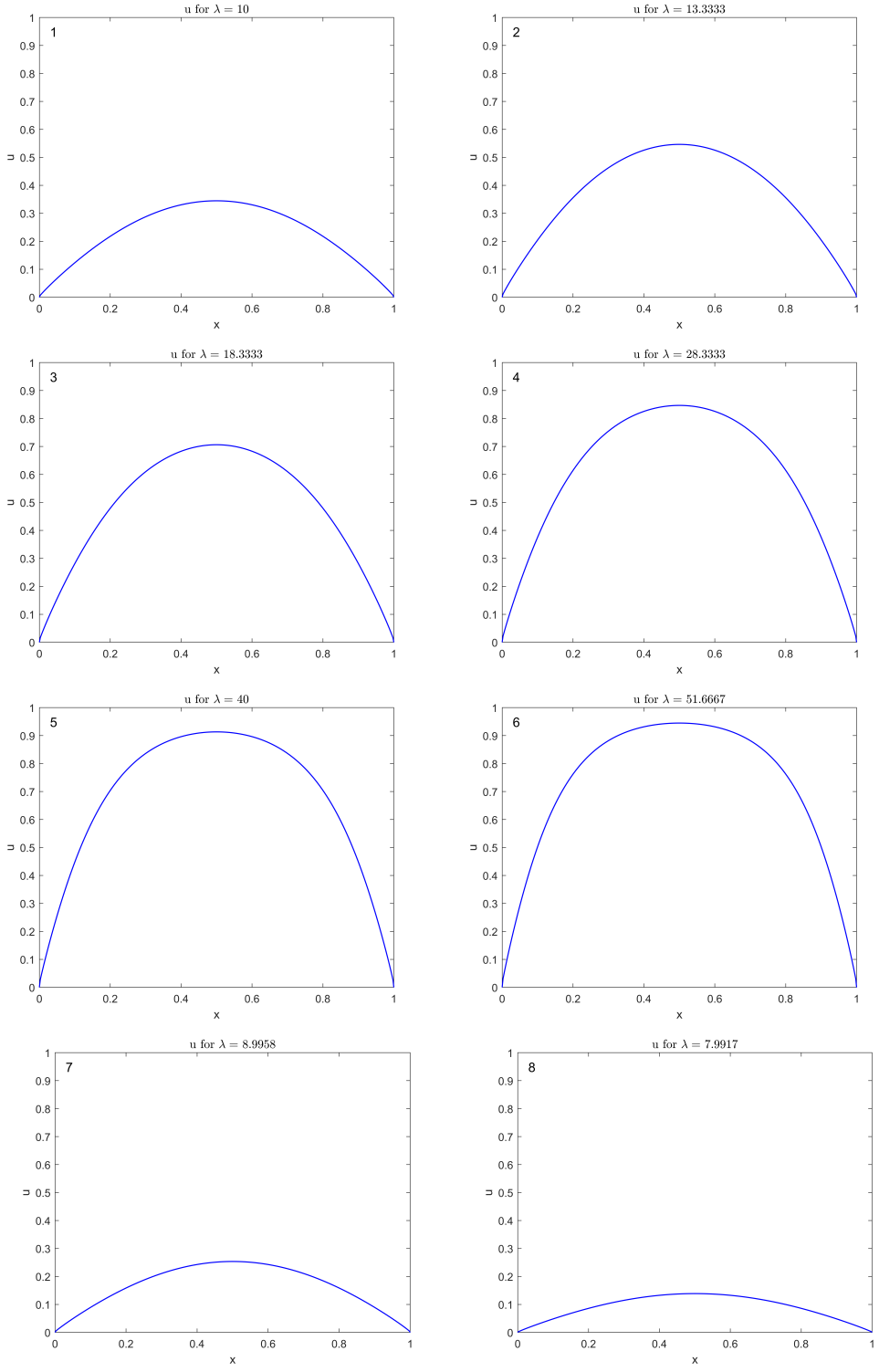

Figure 2.8: Solutions of (2.38) for different values of λ.

For the next example we will consider the same setting as for the previous example with a difference in the choice of the fractional order α. For this case we will set $\alpha = 0.1$.

Example 2.5. Consider the following problem

$$\begin{cases} (-\Delta)^{0.05} u(x) = \lambda u(1-u) \text{ in } (0,1), \\ \qquad\qquad u(x) = 0 \text{ in } \mathbb{R}\backslash(0,1). \end{cases} \tag{2.39}$$

Again, we will solve for $N = 200$. Then, we set $\lambda_{middle} = 10$, $\lambda_{max} = 60$, $m_1 = 50$, $m_2 = 30$, $r = 7$, $u_{init}(x) = 1$. For the fractional order, we will set $\alpha = 0.1$.

For this example we are choosing the sames values of λ to be highlighted in the bifurcation diagram and to be plotted as solutions corresponding to those values of λ as for the previous example. In Figure 2.9 we can see the bifurcation diagram corresponding to our problem (2.39). We can see that the highlighted points $1-8$ moved closer to each other compared to the previous example. This corresponds to the fact, that with decreasing value of fractional order α the norm of the solution grows faster with increasing value of parameter λ. This can be directly seen in Figure 2.10.

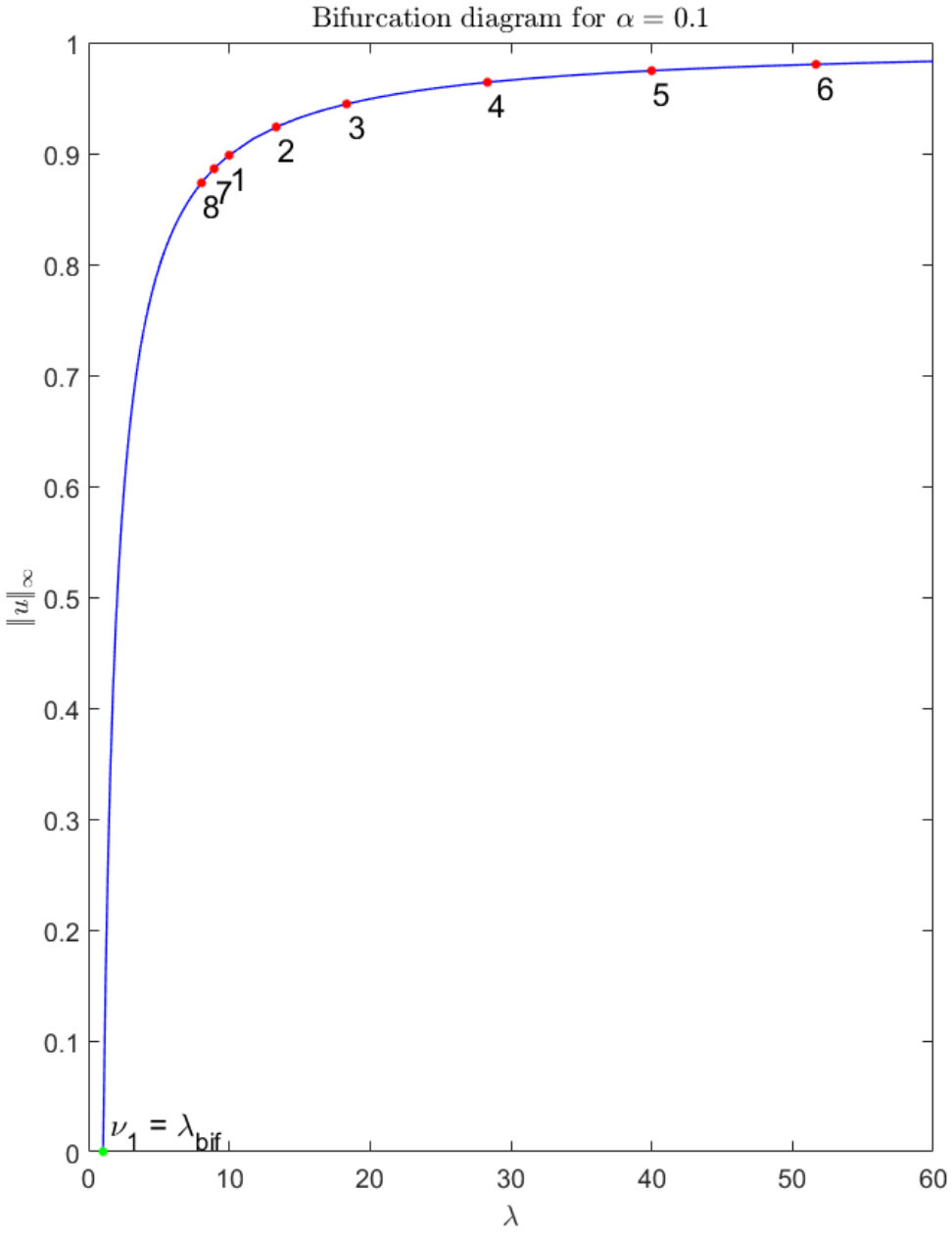

Figure 2.9: Bifurcation diagram for the problem (2.39).

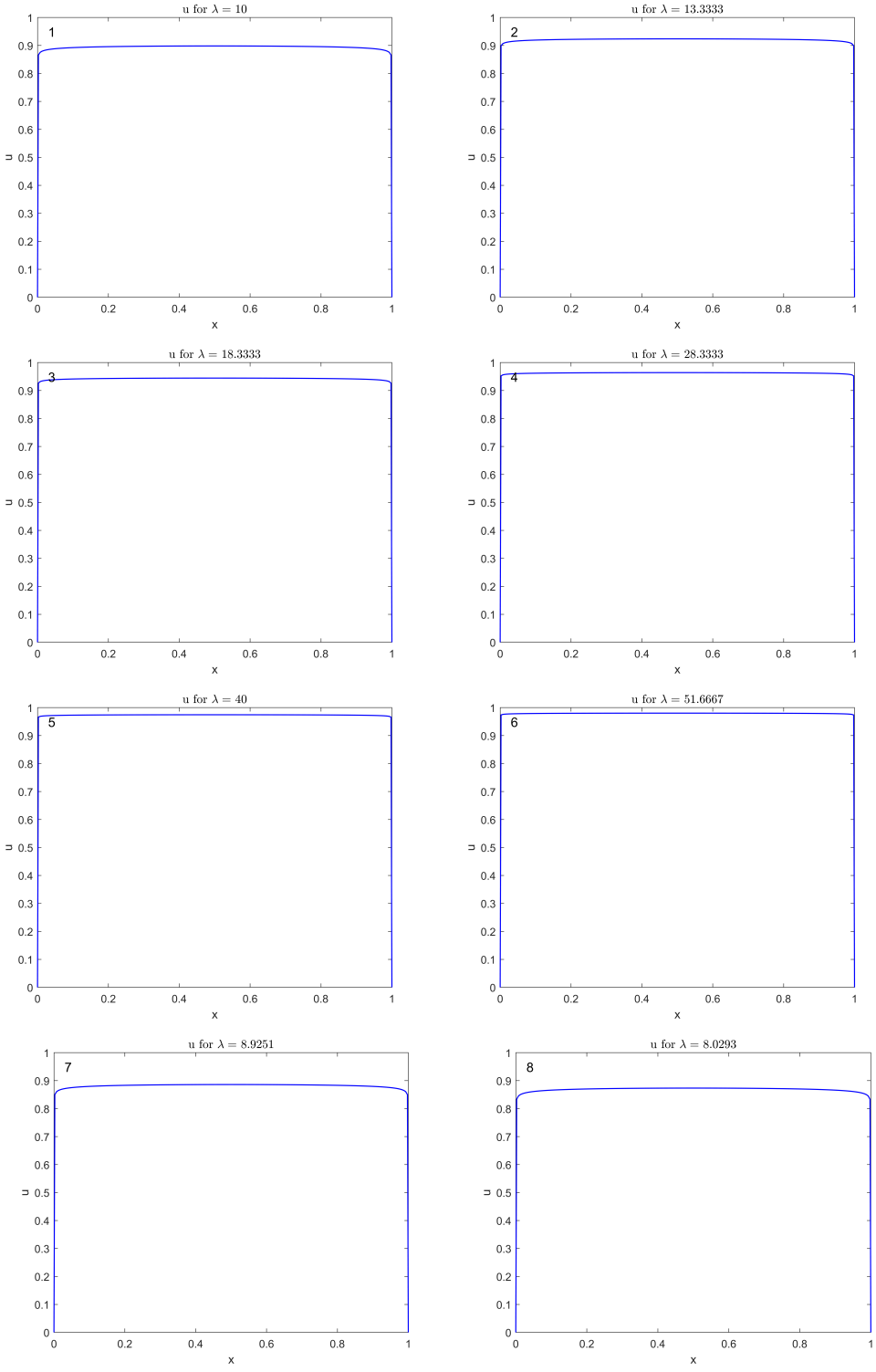

Figure 2.10: Solutions of (2.39) for different values of λ.

2.4 Evolutionary problems with fractional Laplacian

In this section, we will consider time dependent (evolutionary) problems. That is, we are looking at the following problem

$$\begin{cases} \dfrac{\partial u(t,x)}{\partial t} + (-\Delta)^{\alpha/2} u(t,x) = f(t,x,u) & \text{in } (T_0,T)\times\Omega, \\ u(t,x) = 0 & \text{in } (T_0,T)\times(\mathbb{R}\setminus\Omega), \\ u(T_0,x) = u_{init}(x) & \text{in } \Omega, \end{cases}$$

where $\alpha \in (0,2)$, $\Omega = (L,R)$ for $-\infty < L < R < +\infty$, $T_0 < T$. As in the stationary case, we will divide the problem into two cases. For the first case, we will consider a right-hand side of the form $f = f(t,x)$ and for the second case we will consider right-hand side of the form $f = f(t,x,u)$. For the former problem, we will develop linear solver based on implicit Euler method. For later case, we will combine this linear solver with the method of monotone iterations. The method of monotone iterations requires that $f(t,x,u) \leq f(t,x,v)$ whenever $u \leq v$ (f is nondecreasing in the third variable).

2.4.1 Right-hand side independent of u

As mentioned in the beginning of this section, we will firstly assume a right-hand side of the form $f = f(t,x)$, that is we are solving following problem

$$\begin{cases} \dfrac{\partial u(t,x)}{\partial t} + (-\Delta)^{\alpha/2} u(t,x) = f(t,x) & \text{in } (T_0,T)\times(L,R), \\ u(t,x) = 0 & \text{in } (T_0,T)\times(\mathbb{R}\setminus(L,R)), \\ u(T_0,x) = u_{init}(x) & \text{in } (L,R), \end{cases} \tag{2.40}$$

where $\alpha \in (0,2)$, $-\infty < L < R < +\infty$, $T_0 < T$. By expanding $u = u(t,x)$ into a Taylor series

$$u(t+\tau,x) = u(t,x) + \tau\frac{\partial u(t,x)}{\partial t} + \frac{\tau^2}{2}\frac{\partial^2 u(\xi,x)}{\partial t^2},$$

for $\xi \in (t, t+\tau)$, where $\tau > 0$ is a temporal step, we are able to express time derivative as follows

$$\frac{\partial u(t,x)}{\partial t} = \frac{u(t+\tau,x) - u(t,x)}{\tau} + \frac{\tau^2}{2}\frac{\partial^2 u(\xi,x)}{\partial t^2}. \tag{2.41}$$

Substituting (2.41), together with omitting the error term, into (2.40), we arrive at

$$\frac{u(t+\tau,x) - u(t,x)}{\tau} + (-\Delta)^{\alpha/2} u(t+\tau,x) \approx f(t+\tau,x). \tag{2.42}$$

Furthermore, by introducing $\mathbf{A}_c^{(\alpha)}$, which we defined as

$$\mathbf{A}_c^{(\alpha)} = c_{1,\alpha}\mathbf{A}^{(\alpha)},$$

as the discretized fractional Laplacian, together with the introduction of the following notation

$$u^n := u(t,x),$$
$$u^{n+1} := u(t+\tau,x),$$

we can rewrite (2.42) as

$$\frac{u^{n+1}-u^n}{\tau}+\frac{1}{h^\alpha}\mathbf{A}_c^{(\alpha)}u^{n+1}=f(t+\tau,x). \tag{2.43}$$

We can see that from the previous equation (2.43) we can explicitly express the term u^{n+1}, getting

$$\left(\mathbf{I}+\frac{\tau}{h^\alpha}\mathbf{A}_c^{(\alpha)}\right)u^{n+1}=\tau f(t+\tau,x)+u^n. \tag{2.44}$$

As a last step, we multiply (2.44) by

$$\left(\mathbf{I}+\frac{\tau}{h^\alpha}\mathbf{A}_c^{(\alpha)}\right)^{-1}.$$

Finally, we obtain

$$u^{n+1}=\left(\mathbf{I}+\frac{\tau}{h^\alpha}\mathbf{A}_c^{(\alpha)}\right)^{-1}\left(\tau f(t+\tau,x)+u^n\right). \tag{2.45}$$

At this point, we are able to solve our original problem (2.40). Our Matlab written solver for this problem is called *frac_laplace_evolution_1D.m*. Pseudocode follows.

Input:

$T0$	(initial time)
T	(end time)
τ	(temporal step)
$u_{init}(x)=u(T_0,x)$	(initial condition)
L	(left boundary of the domain)
R	(right boundary of the domain)
$n\in\mathbb{N}$	(number of nodes in partition of interval $[L,R]$)
$f=f(t,x)$	(source term f)
$\alpha\in(0,2)$	(fractional order of $(-\Delta)^{\alpha/2}$)

Output:

solutions	(matrix of solution (each column contains solution for certain time))
grid	(vector of the gridpoints)

Begin

01 $h\leftarrow(R-L)/n$
02 **grid** $\leftarrow(L+h/2):h:(R-h/2)$
03 $\mathbf{A}\leftarrow$ *frac_lap_scaled_matrix_1D*(n,α)
04 $\mathbf{A}\leftarrow\frac{1}{h^\alpha}\mathbf{A}$
05 $j\leftarrow(T-T_0)/\tau$
06 Calculation of $\mathbf{B}\leftarrow(\mathbf{I}+\tau\mathbf{A})^{-1}$
07 Creation of matrix **solutions**
08 **solutions** $\leftarrow Append($**solutions**$,u_{init})$
09 For $i:=2:j+1$ do
    % Calculation of the solution for each time step

10 **solutions**$(i) \leftarrow \mathbf{B}\,(\tau f(\mathbf{grid}, T_0 + i\tau) + \mathbf{solutions}(i-1))$
11 EndFor
12 Return **solutions**, **grid**
End

As for the stationary case with the right-hand side independent of u, we can see that our Matlab written function *frac_lap_scaled_matrix_1D* is called in order to obtain the matrix for the disretized fractional Laplacian (line 03). Main calculation is done on tenth line, where we use the formula (2.45).

As previously, examples will follow. The examples will concern simple right-hand side, namely a constant right-hand side. For both of these example the setup will be similar with only difference in the choice of fractional order α and the endtime T.

Example 2.6. As mentioned above, we will solve a problem with a constant right-hand side together with constant initial condition. We are solving following problem

$$\begin{cases} \dfrac{\partial u(t,x)}{\partial t} + (-\Delta)^{0.95} u(t,x) = 1 & \text{in } (0,10)\times(-1,1), \\ u(t,x) = 0 & \text{in } (0,10)\times(\mathbb{R}\setminus(-1,1)), \\ u(0,x) = 2 & \text{in } (-1,1), \end{cases} \tag{2.46}$$

where we set $\alpha = 1.9$, $T_0 = 0$, $T = 10$, $L = -1$, $R = 1$. As for previous examples, we are setting $N = 200$. For a temporal step we are choosing $\tau = 0.01$.

Solution of (2.46) for different time steps together with the solution of stationary version of the problem, that is

$$\begin{cases} (-\Delta)^{0.95}\tilde{u}(x) = 1 & \text{in } (-1,1), \\ \tilde{u}(x) = 0 & \text{in } \mathbb{R}\setminus(-1,1), \end{cases} \tag{2.47}$$

can be seen in Figure 2.11. We can see that with increasing time the solution of (2.46) approaches the solution of the stationary version of the problem, as one would expect. This can be also seen in Figure 2.12, where the norm of the difference of

$$u_{diff}(x) = u(t,x) - \tilde{u}(x) \text{ in } x \in (-1,1) \text{ for } t \in (0,10) \text{ fixed},$$

where u solves (2.46) and $\tilde{u}$ solves (2.47), is plotted. We can see that with increasing time the norm is approaching zero. Because of the error terms introduced by the numerical method, the difference will never reach zero completely.

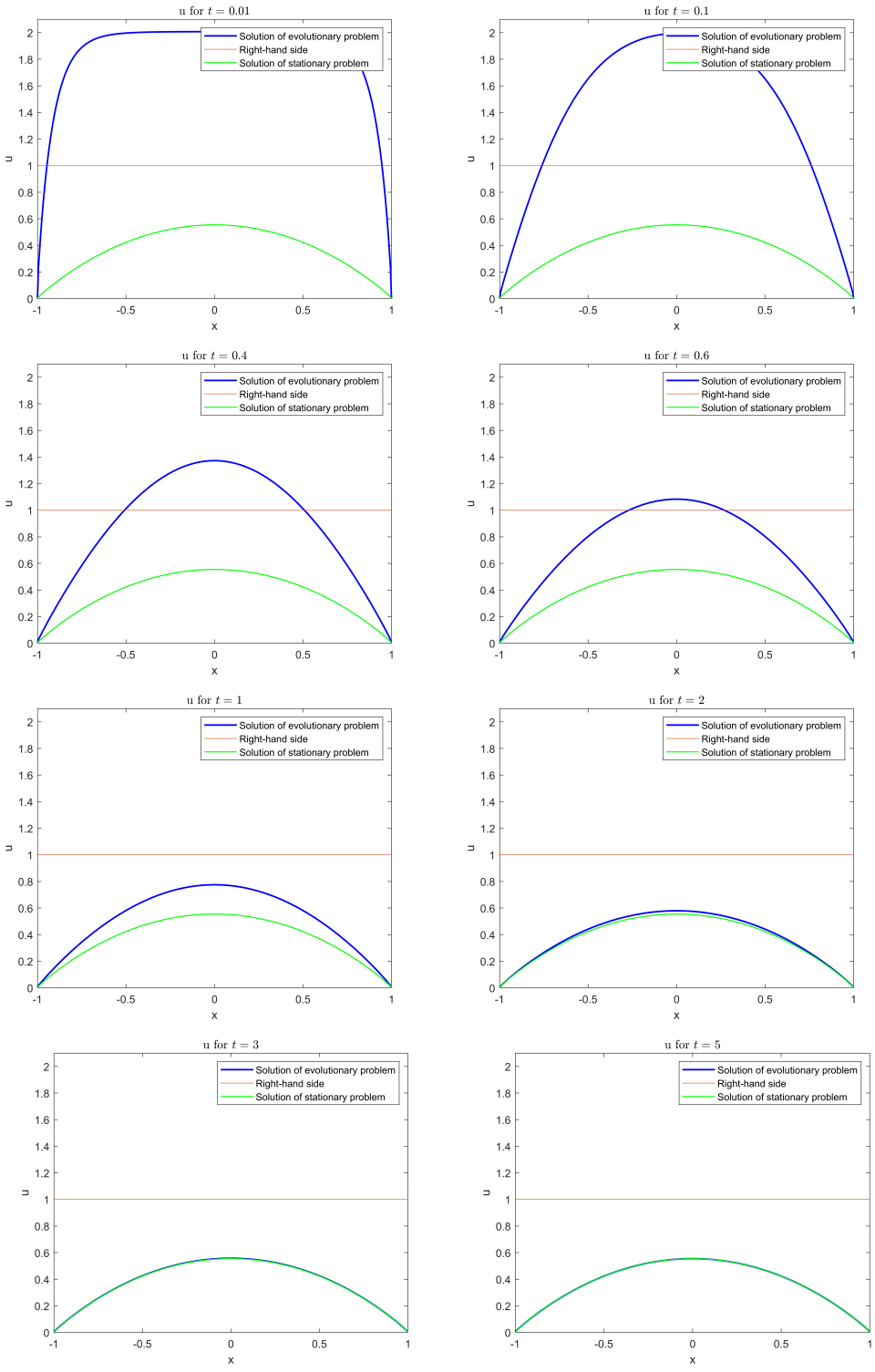

Figure 2.11: Solution of (2.46) at different time steps (blue curve) together with the solution of (2.47) (green curve) and with the right-hand side (orange curve).

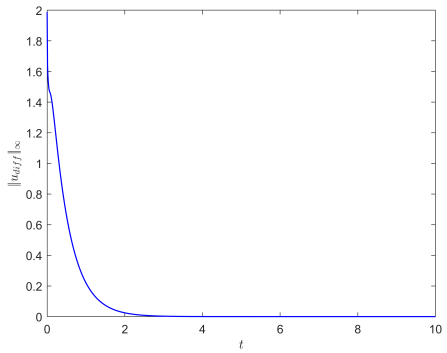

Figure 2.12: Norm of the difference $u_{diff} = u - \tilde{u}$, where u solves (2.46) and $\tilde{u}$ solves (2.47).

Example 2.7. For the next example we will assume similar scenario with a difference in a choice of the fractional order α and T. Let's set $\alpha = 0.1$ and $T = 15$. The reason for setting larger value of T is, that in the case of lower α it takes longer to reach the steady state of the problem. Putting everything together, we are solving following problem

$$\begin{cases} \dfrac{\partial u(t,x)}{\partial t} + (-\Delta)^{0.05} u(t,x) = 1 & \text{in } (0,15) \times (-1,1), \\ u(t,x) = 0 & \text{in } (0,15) \times (\mathbb{R} \setminus (-1,1)), \\ u(0,x) = 2 & \text{in } (-1,1). \end{cases} \tag{2.48}$$

Solution of the problem is plotted in Figure 2.17. As in the previous example, we are also plotting the solution of the corresponding stationary problem

$$\begin{cases} (-\Delta)^{0.05} \tilde{u}(x) = 1 & \text{in } (-1,1), \\ \tilde{u}(x) = 0 & \text{in } \mathbb{R} \setminus (-1,1). \end{cases} \tag{2.49}$$

Also, in Figure 2.18 we are including a plot the following difference

$$u_{diff}(x) = u(t,x) - \tilde{u}(x) \text{ in } x \in (-1,1) \text{ for } t \in (0,15) \text{ fixed},$$

where u solves (2.48) and $\tilde{u}$ solves (2.49).

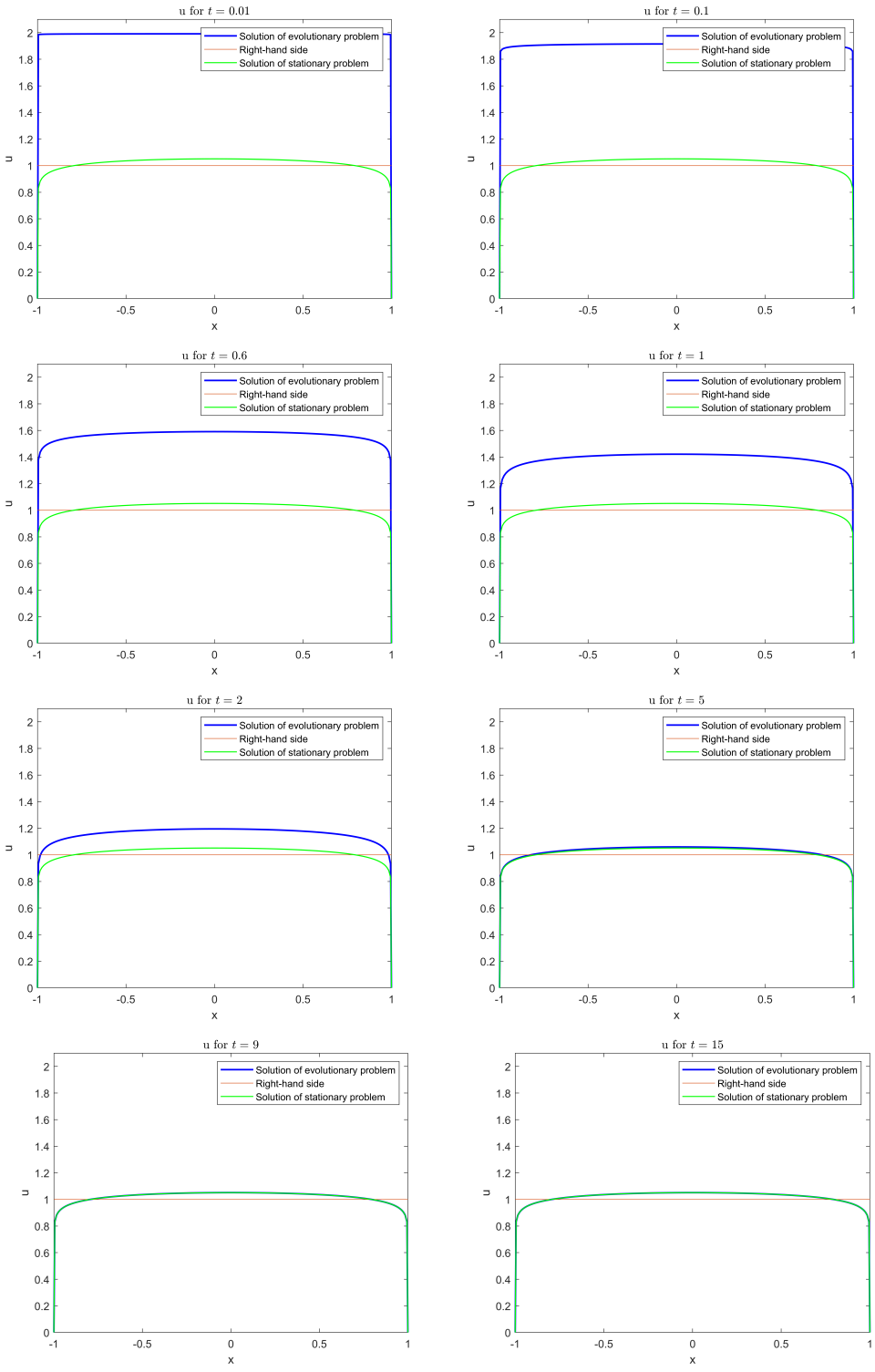

Figure 2.13: Solution of (2.48) at different time steps (blue curve) together with the solution of (2.49) (green curve) and with the right-hand side (orange curve).

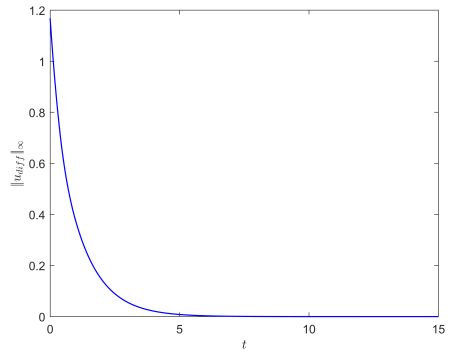

Figure 2.14: Norm of the difference $u_{diff} = u - \tilde{u}$, where u solves (2.48) and $\tilde{u}$ solves (2.49).

2.4.2 Right-hand side dependent on u

In the last section related to the one dimensional case, we will consider evolutionary problem with more general right-hand side which can be dependent on u, i.e. $f = f(t, x, u)$. The problem under consideration is of the form

$$\begin{cases} \dfrac{\partial u(t,x)}{\partial t} + (-\Delta)^{\alpha/2} u(t,x) = f(t,x,u) & \text{in } (T_0, T) \times (L, R), \\ u(t,x) = 0 & \text{in } (T_0, T) \times (\mathbb{R} \setminus (L, R)), \\ u(T_0, x) = u_{init}(x) & \text{in } (L, R), \end{cases} \tag{2.50}$$

where $\alpha \in (0, 2)$, $-\infty < L < R < +\infty$, $T_0 < T$.

To solve this kind of problem, method of monotone iterations will be used. For that, let's reformulate (2.50) as a sequence of initial-boundary value problems

$$\begin{cases} \dfrac{\partial u_m(t,x)}{\partial t} + (-\Delta)^{\alpha/2} u_m(t,x) = h(t,x) := f(t,x,u_{m-1}) & \text{in } (T_0, T) \times (L, R), \\ u_m(t,x) = 0 & \text{in } (T_0, T) \times (\mathbb{R} \setminus (L, R)), \\ u_m(T_0, x) = u_{\text{init}}(x) & \text{in } (L, R), \end{cases} \tag{2.51}$$

where the subscript $m \in \mathbb{N}$ indicates the index related to the sequence of solutions. Related to the method of monotone iterations, let us introduced so called upper and lower solutions, denoted as $\overline{u}$ and $\underline{u}$, respectively. Please note, that $\overline{u}$ can be also called as a supersolution and $\underline{u}$ as a subsolution. To call a function as an upper solution following inequality must hold

$$\begin{cases} \dfrac{\partial \overline{u}(t,x)}{\partial t} + (-\Delta)^{\alpha/2} \overline{u}(t,x) \geq f(t,x,\overline{u}) & \text{in } (T_0, T) \times (L, R), \\ \overline{u}(t,x) \geq 0 & \text{in } (T_0, T) \times (\mathbb{R} \setminus (L, R)), \\ \overline{u}(T_0, x) \geq u_{\text{init}}(x) & \text{in } (L, R), \end{cases}$$

for the lower solution opposite inequality holds, that is

$$\begin{cases} \dfrac{\partial \underline{u}(t,x)}{\partial t} + (-\Delta)^{\alpha/2}\underline{u}(t,x) \leq f(t,x,\underline{u}) & \text{in } (T_0,T)\times(L,R), \\ \underline{u}(t,x) \leq 0 & \text{in } (T_0,T)\times(\mathbb{R}\setminus(L,R)), \\ \underline{u}(T_0,x) \leq u_{\text{init}}(x) & \text{in } (L,R). \end{cases}$$

It can be shown (this theory is quite complicated and exceeds possibilities of this master's thesis, see, e.g., [3]), that if certain assumptions are fulfilled, then there exists a solution u of (2.50) which satisfies following inequality

$$\underline{u}(t,x) \leq u(t,x) \leq \overline{u}(t,x) \text{ in } [T_0,T]\times(L,R).$$

As an initial guess for the solution one can use

$$u_1 := \underline{u}.$$

Then one proceeds iteratively obtaining u_m from u_{m-1} by solving linear problem (2.51) with right-hand side independent of u_m. Since we assume here that f is nondecreasing in the third variable, the maximum principle (see, e.g., [19]) yields the following ordering for the iterated sequence of solutions

$$\underline{u} = u_1 \leq u_2 \leq u_3 \leq \cdots \leq \overline{u}.$$

Under certain conditions, this sequence is converging to a solution (see, e.g., [3]).

For practical purposes, one can set a tolerance $\epsilon > 0$ for the stopping condition of the method, that is the iteration method stops if

$$\|u_{i+1} - u_i\|_\infty < \epsilon,$$

where $i = 1, 2, 3, \ldots$.

Because of the complexity of the evolutionary problem and because of our abilities, we are not able to fully described the theory behind the monotone iteration method for the evolutionary problem of a reaction-diffusion type with fractional order operator. To get more detailed and precise description, we refer interested reader to the following literature [3, 19].

As in the previous section, after discretization we obtain

$$u_m^{n+1} = \left(\mathbf{I} + \frac{\tau}{h^\alpha}\mathbf{A}_c^\alpha\right)^{-1}(\tau f(t+\tau, x, u_{m-1}^n) + u_m^n),$$

where the subscript $m \in \mathbb{N}$ denotes m-th element of the sequence of solutions of the problem (2.51) and $n \in \mathbb{N}$ denotes n-th node of the grid.

Our solver for problem (2.50) written in Matlab is called *frac_laplace_lin_parabolic_solver_1D.m*. As usually, pseudocode follows.

Input:

ϵ	(tolerance for the monotone iterative method)
$T0$	(initial time)
T	(end time)
τ	(temporal step)
$u_{init}(x) = u(T_0, x)$	(initial condition)
$u_{subsolution}(t,x)$	(subsolution for the monotone iterative method)
L	(left boundary of the domain)

R	(right boundary of the domain)
$n \in \mathbb{N}$	(number of nodes in partition of interval $[L, R]$)
$f = f(t, x, u)$	(source term f)
$\alpha \in (0, 2)$	(fractional order of $(-\Delta)^{\alpha/2}$)

Output:

solutions	(matrix of solution (each column contains solution for certain time))
grid	(vector of the gridpoints)

Begin

01 $h \leftarrow (R - L)/n$
02 $\mathbf{grid} \leftarrow (L + h/2) : h : (R - h/2)$
03 $\mathbf{A} \leftarrow frac\_lap\_scaled\_matrix\_1D(n, \alpha)$
04 $\mathbf{A} \leftarrow \frac{1}{h^\alpha}\mathbf{A}$
05 $j \leftarrow (T - T_0)/\tau$
06 Creation of the matrix **F**
% Each column correspond to the values at discretization grid points at certain time step of right-hand side f
07 For $i := 1 : m$ do
% Calculation of the right-hand side for each time step
08 $\mathbf{F} \leftarrow f(\mathbf{grid}, T_0 + i\tau, u_{sobsolution}(\mathbf{grid}, T_0 + i\tau))$
09 EndFor
10 Calculation of $\mathbf{B} \leftarrow (\mathbf{I} + \tau\mathbf{A})^{-1}$
11 Creation of matrix **solutions**
12 $\mathbf{solutions} \leftarrow Append(\mathbf{solutions}, u_{init})$
13 While $\|\mathbf{solutions}^{m+1} - \mathbf{solutions}^{m}\|_\infty > \epsilon$ do
14 For $i := 2 : j + 2$ do
15 $\mathbf{solutions}(i) \leftarrow \mathbf{B}\,(\tau\mathbf{F}(i-1) + \mathbf{solutions}(i-1))$
% Main calculation
16 EndFor
17 For $i := 1 : m$ do
18 $\mathbf{F} \leftarrow f(\mathbf{grid}, T_0 + i\tau, \mathbf{solutions}(i))$
% Update of the matrix **F** corresponding to the right-hand side
19 EndFor
20 EndWhile
21 Return **solutions**, **grid**

End

Example 2.8. In this example, we are choosing starting time $T_0 = 0$ as in the previous examples. For the endtime we are setting $T = 5$. The temporal step is set as in the previous examples, that

is $\tau = 0.001$. Different domain on which the problem is solved is assumed, specifically we are choosing $L = 0$, $R = 1$ with the same number of nodes $N = 200$. For the initial condition we are choosing constant function equal to zero. The subsolution is equal to the initial condition. The right-hand side function has the form $f(t, x, u) = \sqrt{|u|} + 1$. For the tolerance we are setting $\epsilon = 10^{-6}$. Finally, for the fractional order we are choosing $\alpha = 1.9$. Combining all together, we are solving

$$\begin{cases} \dfrac{\partial u(t,x)}{\partial t} + (-\Delta)^{0.95} u(t,x) = \sqrt{|u|} + 1 & \text{in } (0,5) \times (0,1), \\ u(t,x) = 0 & \text{in } (0,5) \times (\mathbb{R} \setminus (0,1)), \\ u(0,x) = u_{init}(x) := 0 & \text{in } (0,1). \end{cases} \tag{2.52}$$

It is straightforward to check that the constant function $\underline{u}(t, x) = 0$ is subsolution of (2.52). We can choose solution of the following stationary problem

$$\begin{cases} (-\Delta)^{0.95} \tilde{u}(x) = \sqrt{|\tilde{u}|} + 1 & \text{in } (0,1), \\ \tilde{u}(x) = 0 & \text{in } \mathbb{R} \setminus (0,1), \end{cases} \tag{2.53}$$

as supersolution $\overline{u}(t, x) = \tilde{u}(x)$ for any $t \in [0, 5)$ and $x \in (0, 1)$. This solution exists, it is nonzero and nonnegative by similar argument as in [3]. By a straightforward calculation, we can see that the equation and boundary condition in (2.52) are satisfied. For initial condition, we get $\overline{u}(0, x) = \tilde{u}(x) \geq 0$ for any $x \in (0, 1)$. So our function $\overline{u}(t, x) = \tilde{u}(x)$ for any $t \in [0, 5)$ and $x \in (0, 1)$ is supersolution of (2.52).

Solutions for few time steps can be seen in Figure 2.15. As in the section concerning the evolutionary problem with simple right-hand side, we are also plotting solution for the stationary version of the problem (2.52).

As expected, we can observe that with increasing time the solution of (2.52) is approaching the solution of the corresponding stationary problem (2.53). This fact can be also seen in Figure 2.16, where we are plotting the norm of the difference

$$u_{diff}(x) = u(t, x) - \tilde{u}(x) \text{ in } (0, 1) \text{ for } t \in (0, 5) \text{ fixed},$$

where u solves (2.52) and $\tilde{u}$ solves (2.53).

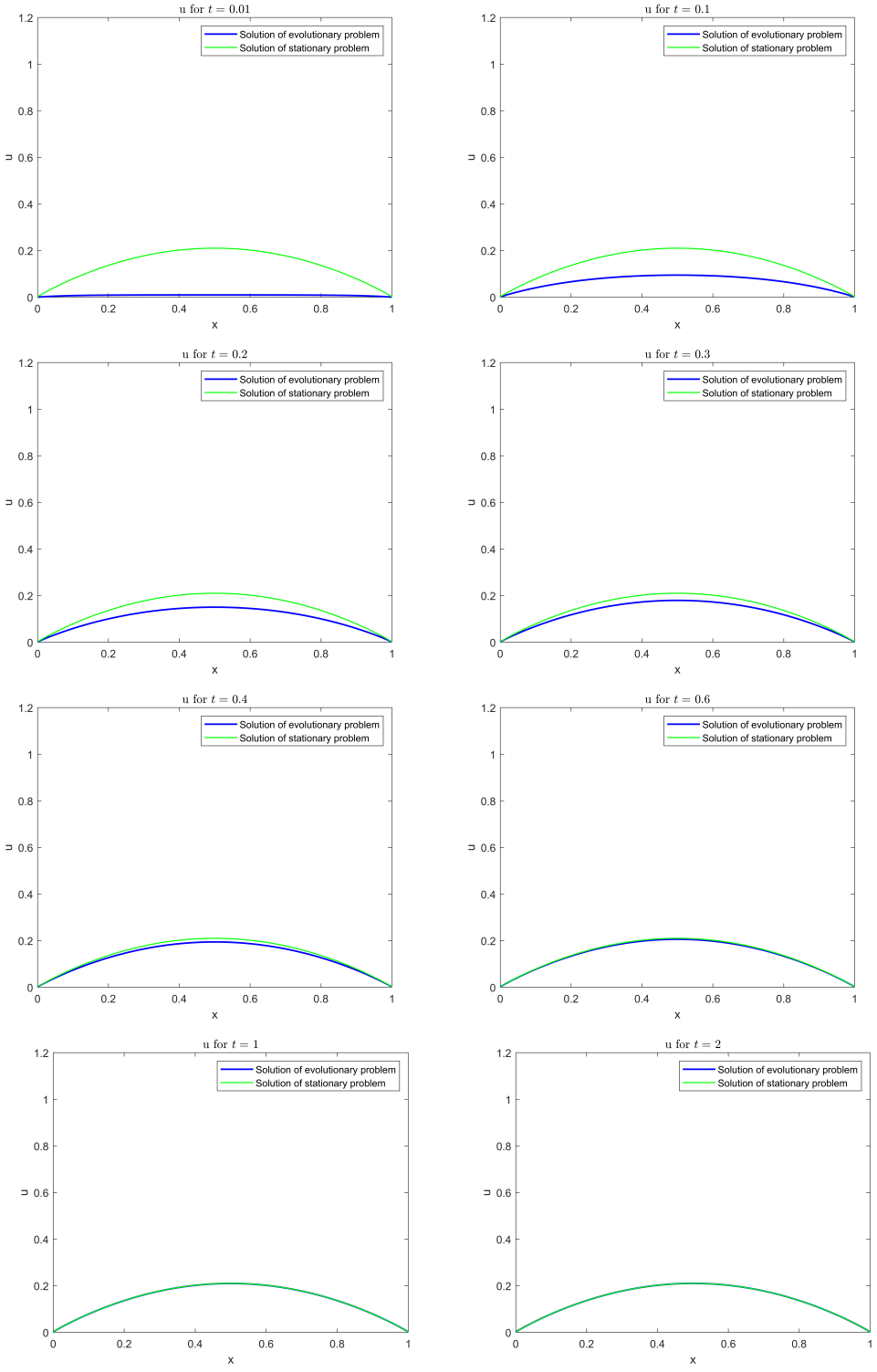

Figure 2.15: Solutions of (2.52) at different time steps (blue curve) together with the solution of (2.53).

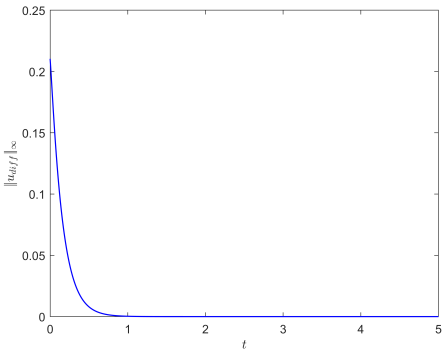

Figure 2.16: Norm of the difference $u_{diff} = u - \tilde{u}$, where u solves (2.52) and $\tilde{u}$ solves (2.53).

Example 2.9. In this example, we will change the fractional order to $\alpha = 0.1$ together with final time T, which we set to $T = 15$. Problem we are solving has the following form

$$\begin{cases} \dfrac{\partial u(t,x)}{\partial t} + (-\Delta)^{0.05} u(t,x) = \sqrt{u} + 1 & \text{in } (0,15) \times (0,1), \\ u(t,x) = 0 & \text{in } (0,15) \times (\mathbb{R} \setminus (0,1)), \\ u(0,x) = u_{init}(x) := 0 & \text{in } (0,1), \end{cases} \tag{2.54}$$

together with the subsolution $\underline{u}(t,x) = 0$. As in the previous Example 2.8, we can choose solution of the problem (2.55) as a supersolution $\overline{u}(t,x) = \tilde{u}(x)$ for any $t \in [0,15)$ and $x \in (0,1)$.

The solution of the problem is plotted in Figure 2.17, together with the solution of the corresponding stationary problem

$$\begin{cases} (-\Delta)^{0.05} \tilde{u}(x) = \sqrt{|\tilde{u}|} + 1 & \text{in } (0,1), \\ \tilde{u}(x) = 0 & \text{in } \mathbb{R} \setminus (0,1). \end{cases} \tag{2.55}$$

As before, we observe that the solution for the evolutionary problem (2.54) is approaching the solution of the stationary problem. The norm of the difference

$$u_{diff}(x) = u(t,x) - \tilde{u}(x) \text{ in } (0,1) \text{ for } t \in (0,15) \text{ fixed},$$

is then plotted in Figure 2.18.

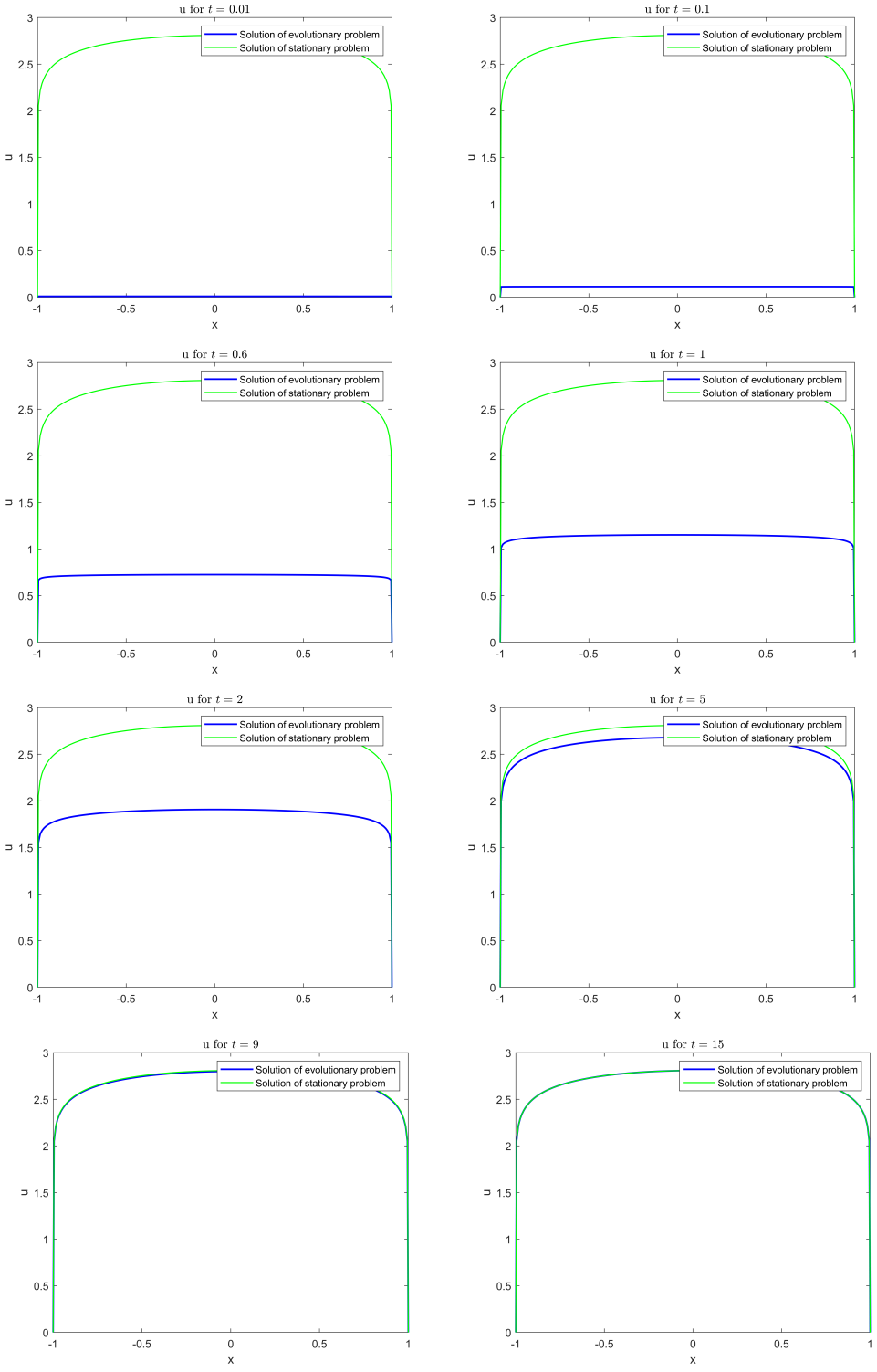

Figure 2.17: Solutions of (2.54) at different time steps (blue curve) together with the solution of (2.55).

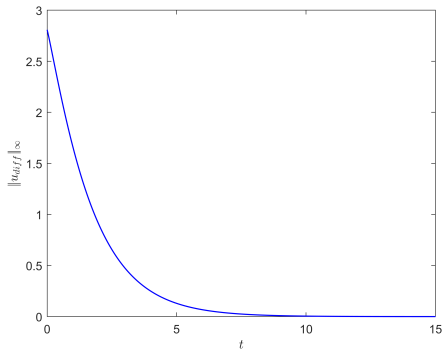

Figure 2.18: Norm of the difference $u_{diff} = u - \tilde{u}$, where u solves (2.54) and $\tilde{u}$ solves (2.55).

Numerical study of Fractional Laplacian in bounded domains in two dimensions

3

This chapter of the text is devoted to the study of the fractional Laplacian in two dimensions. As in the previous chapter, the main source used for writing this chapter is the monograph [25, Chapt. 6]. Again, we are taking over the process of discretizing the operator. Although, in the two dimensional case, we are not as thorough as in the one dimensional case. The reason for that is that because of the higher dimension, the Taylor expansions in higher dimensions would be necessary which would lead to lengthy calculations. Instead of this lengthy calculations, we borrow the formulas from [25] and focus on domains other than rectangle. The implementation details for handling such domains are not provided in [25]. Thus we implemented them by ourselves with some help of [21], where such domains were considered in connection with the usual Laplacian. Moreover, because of the error of the discretization is not even discussed in the monograph [25], we will not be able to comment on the errors introduced by the discretization process.

As in the previous chapter, first section of this chapter will concern discretization of the fractional Laplace in two dimensions. As mentioned, we will not arrive at formulas describing each of the elements of the matrix. We will arrive at an equation, from which it is possible to construct the matrix.

Next section will be then devoted to study of stationary problems involving the fractional Laplacian, namely

$$\begin{cases} (-\Delta)^{\alpha/2} u(x,y) = \lambda f(x,y,u) \text{ in } \Omega, \\ u(x,y) = 0 \text{ in } \mathbb{R}^2 \backslash \Omega, \end{cases}$$

where $\alpha \in (0,2)$, $\lambda \in \mathbb{R}$, $\Omega \subset \mathbb{R}^2$. Again, we will start with the case, where right-hand side does not depend on the solution u itself and the parameter λ. That is, we will be looking at

$$\begin{cases} (-\Delta)^{\alpha/2} u(x,y) = f(x,y) \text{ in } \Omega, \\ u(x,y) = 0 \text{ in } \mathbb{R}^2 \backslash \Omega. \end{cases}$$

As in the previous one dimensional case, for this type of problems, in the core of the numerical method is the construction of the matrix corresponding to the fractional Laplacian, discretizing the right-hand side and only then solving the system of linear equations. In the following section, the original nonlinear problem involving λ and u on the right-hand side, will be studied. Again, we will be implementing Newton's method with the simple continuation algorithm.

Lastly, the following evolutionary problem will be of our interest

$$\begin{cases} \dfrac{\partial u(t,x,y)}{\partial t} + (-\Delta)^{\alpha/2} u(t,x,y) = f(t,x,y,u) & \text{in } (T_0,T)\times\Omega, \\ u(t,x,y) = 0 & \text{in } (T_0,T)\times(\mathbb{R}\setminus\Omega), \\ u(T_0,x,y) = u_{init}(x,y) & \text{in } \Omega, \end{cases}$$

where where $\alpha \in (0,2)$, $\Omega \subset \mathbb{R}^2$, $T_0 < T$. Firstly, we will be interested in the problem

$$\begin{cases} \dfrac{\partial u(t,x,y)}{\partial t} + (-\Delta)^{\alpha/2} u(t,x,y) = f(t,x,y) & \text{in } (T_0,T)\times\Omega, \\ u(t,x,y) = 0 & \text{in } (T_0,T)\times(\mathbb{R}\setminus\Omega), \\ u(T_0,x,y) = u_{init}(x,y) & \text{in } \Omega, \end{cases}$$

for which the right-hand side is independent of u. For this problem, Euler method will be used. Lastly, the original problem will be solved with the help of the method of monotone iterations.

As was the case for the one dimensional case, examples for each of the above mentioned problems will be included. Because the algorithms used for solving these issues are the same as for the one dimensional case, we will not be including the whole pseudocodes. We will focus only on the differences with respect to the pseudocodes from the previous chapter. The only differences between one- and two- dimensional cases are in the inputs of respective pseudocodes, since extra inputs related to the geometry of domain are needed in two dimensions (which was not needed in the case of one dimension).

3.1 Discretization matrix for fractional Laplacian

We will start with problem which is not involving the solution u in the right-hand side, that is following problem is considered

$$\begin{cases} (-\Delta)^{\alpha/2} u(x,y) = f(x,y) \text{ in } \Omega, \\ u(x,y) = 0 \text{ in } \mathbb{R}^2\setminus\Omega, \end{cases} \tag{3.1}$$

where $\alpha \in (0,2)$, $\lambda \in \mathbb{R}$, $\Omega \subset \mathbb{R}^2$. In our case, we are considering the domain Ω to be bounded Lipschitz domain in $\mathbb{R}^2$. The domain Ω will be, in our case, divided into rectangular cells with side lengths equal to $\Delta x, \Delta y > 0$. The solution will be then computed in the center of each of the rectangle. Each of this center of the corresponding rectangle will have assigned doublet of indices (i,j) for $i = 1,2,\ldots,N_1$ and $j = 1,2,\ldots,N_2$, as can be seen in Figure 3.1. As we mentioned above, because of the lengthy calculations which would be needed in order to obtain the discretization of the problem (3.1), we are directly introducing following equation [25, Eq. (6.8.5)]

$$c_{2,\alpha}\left(\frac{\pi}{2}\frac{1}{2-\alpha}\rho^{2-\alpha}(\nabla^2 u)_{i,j} + A_c {\sum_{m,n}}' \frac{u_{m,n}-u_{i,j}}{|\mathbf{x}_{m,n}-\mathbf{x}_{i,j}|^{2+\alpha}} - \chi_{i,j}u_{i,j}\right) = f_{i,j}, \tag{3.2}$$

where

$$\begin{aligned}
\pi\rho^2 &= A_c,\\
A_c &= \Delta x\Delta y,\\
\mathbf{x}_{i,j} &= (x_i, y_j),\\
\chi_{i,j} &= \int_{\Omega_c} \frac{1}{|\mathbf{x}-\mathbf{x}_{i,j}|^{2+\alpha}}\,\mathrm{d}\mathbf{x},\\
u_{i,j} &= u(x_i, y_j),\\
f_{i,j} &= f(x_i, y_j),
\end{aligned}$$

where Ω_c in the integral stands for the complement of the domain Ω, that is $\Omega_c = \mathbb{R}^2\backslash\Omega$. Furthermore, we can evaluate the value of $\chi_{i,j}$ by introducing an approximation [25, Eq. (6.8.9)]

$$\chi_{i,j} \approx A_c\left(\Psi_\alpha - {\sum_{m,n}}' \frac{1}{|\mathbf{x}_{m,n}-\mathbf{x}_{i,j}|^{2+\alpha}}\right), \tag{3.3}$$

where [25, Eq. (6.8.10)]

$$\Psi_\alpha = {\sum_{p,q=-\infty,\ldots,+\infty}}' \frac{1}{(p^2\Delta x^2 + q^2\Delta y^2)^{(2+\alpha)/2}}.$$

Substituting (3.3) into (3.2) and simplifying, we arrive at

$$c_{2,\alpha}\left(\frac{\pi}{2}\frac{1}{2-\alpha}\rho^{2-\alpha}(\nabla^2 u)_{i,j} - A_c\Psi_\alpha u_{i,j}\right) + A_c{\sum_{m,n}}' \frac{u_{m,n}}{|\mathbf{x}_{m,n}-\mathbf{x}_{i,j}|^{2+\alpha}} = f_{i,j}. \tag{3.4}$$

Furthermore, we can directly evaluate the term $(\nabla^2 u)_{i,j}$ as

$$(\nabla^2 u)_{i,j} = \frac{u_{i-1,j} + u_{i+1,j} - 4u_{i,j} + u_{i,j-1} + u_{i,j+1}}{h^2}, \tag{3.5}$$

where $h = \Delta x = \Delta y$ in a case of square cells. Furthermore, throughout this chapter we will consider a situation, for which $N := N_1 = N_2$ together with equidistant grid. After substituting (3.5) into (3.4) and rearranging, we arrive at

$$\begin{aligned}
c_{2,\alpha}\Bigg(&\frac{1}{2}\frac{1}{2-\alpha}\pi^{\alpha/2}(u_{i-1,j} + u_{i+1,j} - 4u_{i,j} + u_{i,j-1} + u_{i,j+1})\\
&+ {\sum_{m,n}}' \frac{u_{m,n}}{|(m-i)^2 + (n-j)^2|^{(2+\alpha)/2}} - \Sigma_\alpha u_{i,j}\Bigg) = h^\alpha f_{i,j},
\end{aligned} \tag{3.6}$$

where

$$\Sigma_\alpha = {\sum_{p,q=-\infty,\ldots,+\infty}}' \frac{1}{(p^2+q^2)^{(2+\alpha)/2}}.$$

Furthermore, we would like to emphasize, that terms $u_{p,q}$ in (3.6) are equal to zero if the node (p,q) lies outside of the domain Ω because of the zero Dirichlet boundary condition in (3.1). Finally, after consolidating the terms involving $u_{i,j}$, we get

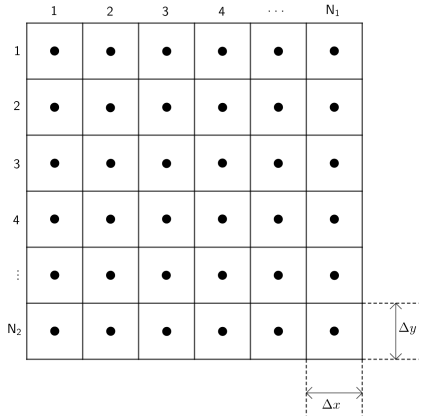

Figure 3.1: Two dimensional grid.

$$c_{2,\alpha}\left(-\left(\frac{2}{2-\alpha}\pi^{\alpha/2}+\Sigma_\alpha\right)u_{i,j} + \frac{1}{2}\frac{1}{2-\alpha}\pi^{\alpha/2}(u_{i-1,j}+u_{i+1,j}+u_{i,j-1}+u_{i,j+1}) + {\sum_{m,n}}' \frac{u_{m,n}}{|(m-i)^2+(n-j)^2|^{(2+\alpha)/2}}\right) = h^\alpha f_{i,j}. \quad (3.7)$$

In the following section we will utilize the equation (3.7) for the construction of the matrix corresponding to the discretized fractional Laplacian in two dimensions.

3.2 Construction of the matrix for discretized fractional Laplace operator

As mentioned before, the matrix corresponding to the discretized fractional Laplacian will be constructed from an equation, specifically from the equation (3.7). We will firstly introduce how the matrix is constructed on a square domain and after that we will consider more general domain. Only then, the pseudocode will follow.

The final matrix will be as in the one dimensional case denoted as

$$\mathbf{A}_c^{(\alpha)},$$

where as before, we will firstly arrive at the matrix

$$\tilde{\mathbf{A}}^{(\alpha)},$$

which will be multiplied by -1, getting

$$\mathbf{A}^{(\alpha)} = -\tilde{\mathbf{A}}^{(\alpha)}.$$

Only then, by multiplying the matrix $\mathbf{A}^{(\alpha)}$ by the coefficient $c_{2,\alpha}$, we will get the final matrix

$$\mathbf{A}_c^{(\alpha)} = c_{1,\alpha}\mathbf{A}^{(\alpha)}.$$

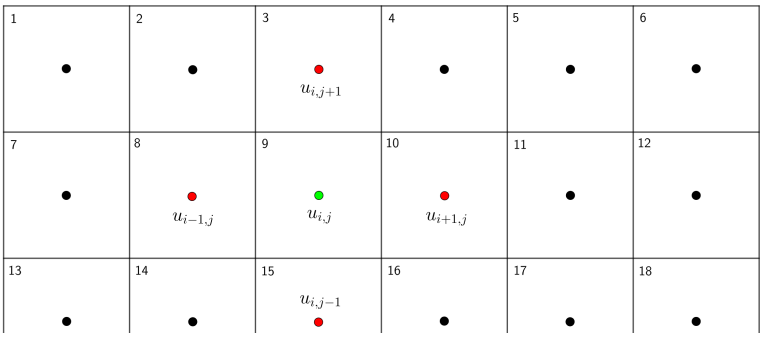

Figure 3.2: Indexing of the grid points.

Before obtaining the matrix $\tilde{\mathbf{A}}^{(\alpha)}$, we will firstly compute a matrix ${}_0\tilde{\mathbf{A}}^{(\alpha)}$. The meaning of this matrix will be described later. By omitting certain rows and columns of ${}_0\tilde{\mathbf{A}}^{(\alpha)}$, we will obtain the matrix $\tilde{\mathbf{A}}^{(\alpha)}$.

Firstly, let us assume that we have square domain, as shown in Figure 3.2, where part of the grid for $N = 6$ is depicted. Assume, that of our interest is a value of u at the coordinates (x_i, y_j), that is the value $u_{i,j}$, as depicted in Figure 3.2 by a green point. From (3.7) we can see that for the equation to hold, values at the neighboring cells (in Figure 3.2 red dots) need to be taken into account together with the values at the remaining points of the grid. In our case, we have N^2 grid points, meaning we have N^2 equations of the form (3.7). Apart from the coordinates (i, j), it is useful to introduce another labeling of the grid points. Let us introduces indices of the grid points, such that each grid point has an index k for $k = 1, \ldots, N^2$. We are choosing labeling, such that we are starting at the top-left corner and indexing by rows, as shown in Figure 3.2. This labeling is useful for us, because kth grid point, where $k = 1, \ldots, N^2$, corresponds to kth equation of the discretized system. Meaning, that in our case for which the grid point with coordinates $(2, 3)$ (green point in Figure 3.2) has an index $k = 9$, that is ninth equation of the system corresponds to the grid point with coordinates $(2, 3)$. Now, we are able to to construct each row of the matrix corresponding to the discretized fractional Laplacian. Again, if we would consider our situation depicted in Figure 3.2, ninth element of the ninth row would be equal to

$$A_{i,j} = -\left(\frac{2}{2-\alpha}\pi^{\alpha/2} + \Sigma_\alpha\right),$$

then third, eighth, tenth and fifteenth element of the ninth row would be equal to

$$A_{i,j+1} = A_{i-1,j} = A_{i+1,j} = A_{i,j-1} = \frac{1}{2}\frac{1}{2-\alpha}\pi^{\alpha/2},$$

and the remaining elements of the ninth row would be equal to

$$A_{m,n} = {\sum_{m,n}}' \frac{1}{|(m-i)^2 + (n-j)^2|^{(2+\alpha)/2}},$$

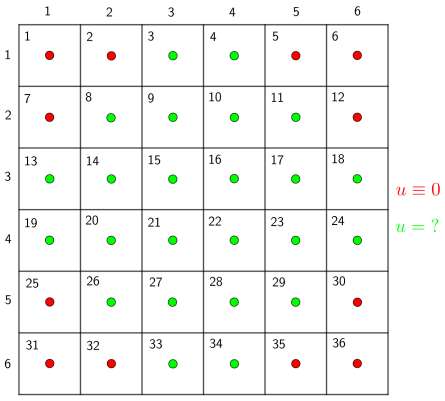

Figure 3.3: General domain.

where in our case $i = 2$, $j = 3$. Proceeding similarly for every other grid point, we would arrive at the matrix ${}_0\tilde{\mathbf{A}}^{(\alpha)}$.

Now, we will describe how the algorithm for construction of the matrix corresponding to the general grid, for example the one shown in Figure 3.3, works. As mentioned at the beginning of this section, the final matrix corresponding to the general grid, for example the one depicted in Figure 3.3, to which we will arrive is denoted by $\mathbf{A}_c^{(\alpha)}$. Meaning, that we do not need to solve, or to be more specific we cannot solve, for all of the grid points of the general grid, in the case of Figure 3.3 that is we cannot solve for all $N^2 = 36$ grid points. The reason for that is, that the right-hand side of the problem (3.1) is prescribed only on the domain Ω to which the green points correspond. So, we do not know what the fractional Laplacian of u is equal to in the red grid points, nevertheless the Dirichlet boundary condition is prescribed on these grid points, so we know that the solution is equal to zero there. Because of that, we are not constructing matrix of the size $N^2 \times N^2$ (for the case depicted in Figure 3.3 that is 36×36), but we are constructing matrix of the size $(N-M)^2 \times (N-M)^2$, where $N \in \mathbb{N}$ is the total number of grid points and $M \in \mathbb{N}$ is the number of grid points which does not lie in the domain Ω (for the case depicted in Figure 3.3 that is 24×24).

Taking all the above described into the consideration, we firstly construct the matrix ${}_0\tilde{\mathbf{A}}^{(\alpha)}$ of the size $N^2 \times N^2$ (that is we are including the grid points for which the zero Dirichlet condition is prescribed - red grid points) and then, we are omitting rows and columns corresponding to the grid points for which the zero Dirichlet condition is prescribed, obtaining the matrix $\tilde{\mathbf{A}}^{(\alpha)}$ of the size $(N-M)^2 \times (N-M)^2$. Finally, we multiply the matrix $\tilde{\mathbf{A}}^{(\alpha)}$ by $-c_{1,\alpha}$, obtaining the matrix $\mathbf{A}_c^{(\alpha)}$. Again, if we would consider the case which is depicted in Figure 3.3, we would construct the matrix of a size 36×36 and only then, we would omit kth row and kth column, where k is the index of the grid points lying outside of the domain Ω (red grid points), getting a matrix of a size 24×24.

Before introducing the reader to the pseudocode, there is a need to clarify our approach to how the domain together with the grid is entered to the algorithm. We are considering rectangular domain $\Omega_{square} = [L_x, R_x] \times [U_y, L_y]$, where $-\infty < L_x, R_x, U_y, L_y < +\infty$ together with $R_x - L_x = U_y - L_y$ to ensure equidistant discretization, for which the domain Ω, on which

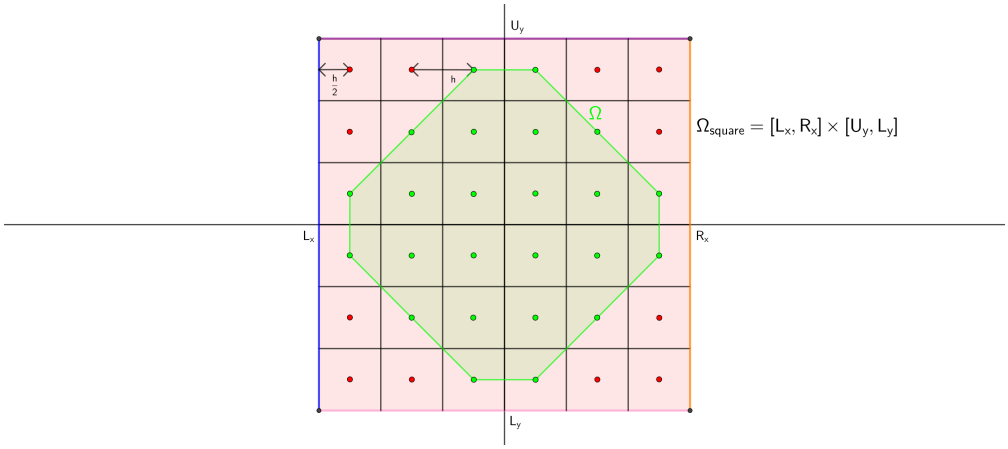

Figure 3.4: General domain Ω as a subset of a square domain $[L_x, R_x] \times [U_y, L_y]$.

the problem (3.1) is solved, is a subset of Ω_{square}, that is $\Omega \subset \Omega_{square}$. This situation is shown in Figure 3.4. Recall, that the number of grid points in the direction of the x axes is the same as in the direction of the y axes, that is $N = N_1 = N_2$. Then, the spatial step is equal to

$$h = \frac{R_x - L_x}{N} = \frac{U_y - L_y}{N}.$$

The domain Ω can be described by a matrix $\mathbf{G}$ of a size $N \times N$ with the following structure

$$G_{i,j} = \begin{cases} 1 \text{ if } x_{i,j} \in \Omega, \\ 0 \text{ otherwise.} \end{cases}$$

For example, for the case depicted in Figure 3.4 the matrix $\mathbf{G}$ would have the following form

$$\mathbf{G} = \begin{pmatrix} 0 & 0 & 1 & 1 & 0 & 0 \\ 0 & 1 & 1 & 1 & 1 & 0 \\ 1 & 1 & 1 & 1 & 1 & 1 \\ 1 & 1 & 1 & 1 & 1 & 1 \\ 0 & 1 & 1 & 1 & 1 & 0 \\ 0 & 0 & 1 & 1 & 0 & 0 \end{pmatrix}.$$

This approach can be also seen in [21, Figure 19]. Our Matlab written function which computes the matrix $\mathbf{A}_c^{(\alpha)}$ is called *frac_laplace_scaled_matrix_2D*. Pseudocode for the function follow.

Input:

L_x	(left boundary of the domain Ω_{square})
R_x	(right boundary of the domain Ω_{square})
U_y	(upper boundary of the domain Ω_{square})
L_y	(lower boundary of the domain Ω_{square})
$\mathbf{G}$	(grid matrix)
$\alpha \in (0,2)$	(fractional order of $(-\Delta)^{\alpha/2}$))

Output:

$\mathbf{A}$	(matrix corresponding to discretized fractional Laplacian)
x_coordinates	(vector of x coordinates of grid points which lie in Ω)
y_coordinates	(vector of y coordinates of grid points which lie in Ω)

Begin

01 Calculation of $\mathbf{A}_{diag}$
% Calculation of the diagonal part of the matrix

02 Calculation of $\mathbf{A}_{neighbors}$
% Calculation of the elements corresponding to the neighboring grid points $u_{i,j+1}$, $u_{i-1,j}$, $u_{i+1,j}$, $u_{i,j-1}$

03 Calculation of $\mathbf{A}_{rest}$
% Calculation of the remaining elements of the matrix

04 Calculation of $\mathbf{A} \leftarrow \mathbf{A}_{diag} + \mathbf{A}_{neighbors} + \mathbf{A}_{rest}$
Putting calculated matrices together

05 Omitting rows and columns corresponding to the grid points which do not lie in the domain Ω

06 Calculation of **x_coordinates**, **y_coordinates**

07 $\mathbf{A} \leftarrow -c_{2,\alpha}\mathbf{A}$

08 Return $\mathbf{A}$, **x_coordinates**, **y_coordinates**

End

Example 3.1. Assume, that we have a domain $\Omega = (-1,1) \times (-1,1)$ with $N = 3$, as shown in Figure 3.5. For the fractional order, we are choosing $\alpha = 0.01$, $\alpha = 1$, $\alpha = 1.99$. Notice, that matrix $\mathbf{G}$ corresponding to this domain and grid has the following form

$$\mathbf{G} = \begin{pmatrix} 1 & 1 & 1 \\ 1 & 1 & 1 \\ 1 & 1 & 1 \end{pmatrix}.$$

Because of that, we are not omitting any rows or columns, thus the matrix ${}_0\tilde{\mathbf{A}}^{(\alpha)}$ equals to the

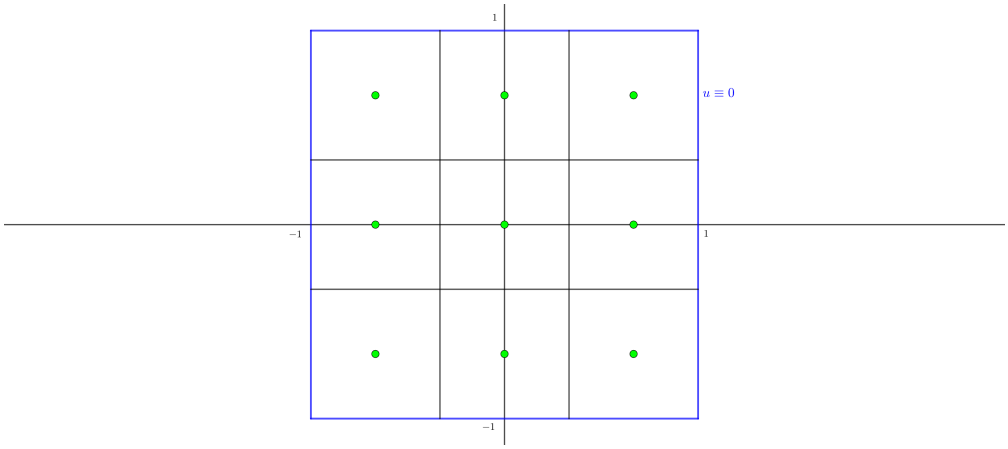

Figure 3.5: Grid for $\Omega = (-1,1) \times (-1,1)$ with $N = 3$.

matrix $\tilde{\mathbf{A}}^{(\alpha)}$. After multiplying the matrix $\tilde{\mathbf{A}}^{(\alpha)}$ by $-c_{2,\alpha}$, we obtain following matrices.

$$\mathbf{A}_c^{(0.01)} = \begin{pmatrix} 1.0069 & -0.002 & -0.0004 & -0.002 & -0.0008 & -0.0003 & -0.0004 & -0.0003 & -0.0002 \\ -0.002 & 1.0069 & -0.002 & -0.0008 & -0.002 & -0.0008 & -0.0003 & -0.0004 & -0.0003 \\ -0.0004 & -0.002 & 1.0069 & -0.0003 & -0.0008 & -0.002 & -0.0002 & -0.0003 & -0.0004 \\ -0.002 & -0.0008 & -0.0003 & 1.0069 & -0.002 & -0.0004 & -0.002 & -0.0008 & -0.0003 \\ -0.0008 & -0.002 & -0.0008 & -0.002 & 1.0069 & -0.002 & -0.0008 & -0.002 & -0.0008 \\ -0.0003 & -0.0008 & -0.002 & -0.0004 & -0.002 & 1.0069 & -0.0003 & -0.0008 & -0.002 \\ -0.0004 & -0.0003 & -0.0002 & -0.002 & -0.0008 & -0.0003 & 1.0069 & -0.002 & -0.0004 \\ -0.0003 & -0.0004 & -0.0003 & -0.0008 & -0.002 & -0.0008 & -0.002 & 1.0069 & -0.002 \\ -0.0002 & -0.0003 & -0.0004 & -0.0003 & -0.0008 & -0.002 & -0.0004 & -0.002 & 1.0069 \end{pmatrix},$$

$$\mathbf{A}_c^{(1)} = \begin{pmatrix} 2.0019 & -0.3002 & -0.0199 & -0.3002 & -0.0563 & -0.0142 & -0.0199 & -0.0142 & -0.007 \\ -0.3002 & 2.0019 & -0.3002 & -0.0563 & -0.3002 & -0.0563 & -0.0142 & -0.0199 & -0.0142 \\ -0.0199 & -0.3002 & 2.0019 & -0.0142 & -0.0563 & -0.3002 & -0.007 & -0.0142 & -0.0199 \\ -0.3002 & -0.0563 & -0.0142 & 2.0019 & -0.3002 & -0.0199 & -0.3002 & -0.0563 & -0.0142 \\ -0.0563 & -0.3002 & -0.0563 & -0.3002 & 2.0019 & -0.3002 & -0.0563 & -0.3002 & -0.0563 \\ -0.0142 & -0.0563 & -0.3002 & -0.0199 & -0.3002 & 2.0019 & -0.0142 & -0.0563 & -0.3002 \\ -0.0199 & -0.0142 & -0.007 & -0.3002 & -0.0563 & -0.0142 & 2.0019 & -0.3002 & -0.0199 \\ -0.0142 & -0.0199 & -0.0142 & -0.0563 & -0.3002 & -0.0563 & -0.3002 & 2.0019 & -0.3002 \\ -0.007 & -0.0142 & -0.0199 & -0.0142 & -0.0563 & -0.3002 & -0.0199 & -0.3002 & 2.0019 \end{pmatrix},$$

$$\mathbf{A}_c^{(1.99)} = \begin{pmatrix} 3.971 & -0.9895 & -0.0004 & -0.9895 & -0.0016 & -0.0003 & -0.0004 & -0.0003 & -0.0001 \\ -0.9895 & 3.971 & -0.9895 & -0.0016 & -0.9895 & -0.0016 & -0.0003 & -0.0004 & -0.0003 \\ -0.0004 & -0.9895 & 3.971 & -0.0003 & -0.0016 & -0.9895 & -0.0001 & -0.0003 & -0.0004 \\ -0.9895 & -0.0016 & -0.0003 & 3.971 & -0.9895 & -0.0004 & -0.9895 & -0.0016 & -0.0003 \\ -0.0016 & -0.9895 & -0.0016 & -0.9895 & 3.971 & -0.9895 & -0.0016 & -0.9895 & -0.0016 \\ -0.0003 & -0.0016 & -0.9895 & -0.0004 & -0.9895 & 3.971 & -0.0003 & -0.0016 & -0.9895 \\ -0.0004 & -0.0003 & -0.0001 & -0.9895 & -0.0016 & -0.0003 & 3.971 & -0.9895 & -0.0004 \\ -0.0003 & -0.0004 & -0.0003 & -0.0016 & -0.9895 & -0.0016 & -0.9895 & 3.971 & -0.9895 \\ -0.0001 & -0.0003 & -0.0004 & -0.0003 & -0.0016 & -0.9895 & -0.0004 & -0.9895 & 3.971 \end{pmatrix}.$$

Recall the following limits[31, Proposition 5.3.]

$$\lim_{\alpha \to 0^+} (-\Delta)^{\alpha/2} u = u,$$
$$\lim_{\alpha \to 2^-} (-\Delta)^{\alpha/2} u = -\Delta u.$$

We can see, that the matrix for $\alpha = 0.01$ is close to the identity matrix, which agrees with the limit above. On the other side of the spectrum, that is for $\alpha = 1.99$, we should obtain matrix which should be close to the matrix for the ordinary Laplacian on the domain Ω. Indeed, the matrix $\mathbf{B}$ corresponding to the ordinary Laplacian has the following form

$$\mathbf{B} = \begin{pmatrix} 4 & -1 & 0 & -1 & 0 & 0 & 0 & 0 & 0 \\ -1 & 4 & -1 & 0 & -1 & 0 & 0 & 0 & 0 \\ 0 & -1 & 4 & 0 & 0 & -1 & 0 & 0 & 0 \\ -1 & 0 & 0 & 4 & -1 & 0 & -1 & 0 & 0 \\ 0 & -1 & 0 & -1 & 4 & -1 & 0 & -1 & 0 \\ 0 & 0 & -1 & 0 & -1 & 4 & 0 & 0 & -1 \\ 0 & 0 & 0 & -1 & 0 & 0 & 4 & -1 & 0 \\ 0 & 0 & 0 & 0 & -1 & 0 & -1 & 4 & -1 \\ 0 & 0 & 0 & 0 & 0 & -1 & 0 & -1 & 4 \end{pmatrix}.$$

Comparing the matrix $\mathbf{B}$ with the matrix $\mathbf{A}_c^{(1.99)}$, we can see that the matrices are close to each other. In this way, we numerically verified that our numerical approach is in reasonable agreement with theoretical results.

3.3 Stationary problems with fractional Laplacian

As in the one dimensional case, we will start with the stationary problems. Firstly, we will consider problems with right-hand side independent of the solution u. For this type of problem, we will introduce several examples, for which we know the exact solution. Then, we will consider problem with the right-hand side which can be dependent on the solution u together with the right-hand side being multiplied by a parameter $\lambda \in \mathbb{R}$. For this type of problem, we will be again using Newton's method together with the simple continuation algorithm for plotting the bifurcation diagram.

3.3.1 Right-hand side independent of u

In this section, we will consider right-hand side of the form $f = f(x, y)$. Problem we are then solving has the following form

$$\begin{cases} (-\Delta)^{\alpha/2} u(x,y) = f(x,y) \text{ in } \Omega, \\ u(x,y) = 0 \text{ in } \mathbb{R}^2 \backslash \Omega. \end{cases}$$

Our Matlab written solver for this type of problems is called *frac_laplace_2D.m*. Its pseudocode follows.

Input:

L_x	(left boundary of the domain Ω_{square})
R_x	(right boundary of the domain Ω_{square})
U_y	(upper boundary of the domain Ω_{square})
L_y	(lower boundary of the domain Ω_{square})
$\mathbf{G}$	(grid matrix)
$f = f(x, y)$	(source term f)

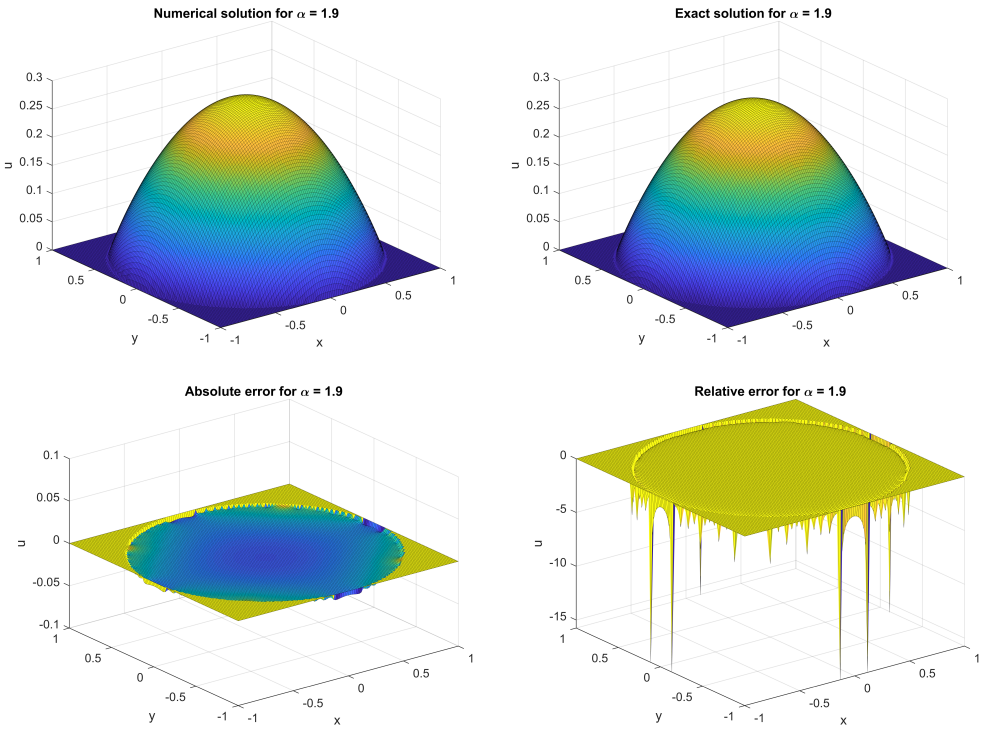

Figure 3.6: Numerical solution of (3.8), exact solution of (3.8), absolute and relative error for the solution.

$\alpha \in (0,2)$ (fractional order of $(-\Delta)^{\alpha/2}$))

Output:

solution (solution vector)

x_coordinates (vector of x coordinates of grid points which lie in Ω)

y_coordinates (vector of y coordinates of grid points which lie in Ω)

Begin

01 $n \leftarrow size(\mathbf{G})$

02 $h \leftarrow (R_x - L_x)/n$

03 $[\mathbf{A}, \mathbf{x\_coordinates}, \mathbf{y\_coordinates}] \leftarrow frac\_lap\_scaled\_matrix\_2D(L_x, R_x, U_y, L_y, \mathbf{G}, \alpha)$

04 $\mathbf{A} \leftarrow \frac{1}{h^\alpha}\mathbf{A}$

05 $\mathbf{b} \leftarrow f(\mathbf{x\_coordinates}, \mathbf{y\_coordinates})$

06 $\mathbf{solution} \leftarrow \mathbf{A} \backslash \mathbf{b}$

07 Return **solution**, **x_coordinates**, **y_coordinates**

End

Now, several examples, for which we know the exact solution, will follow. The knowledge

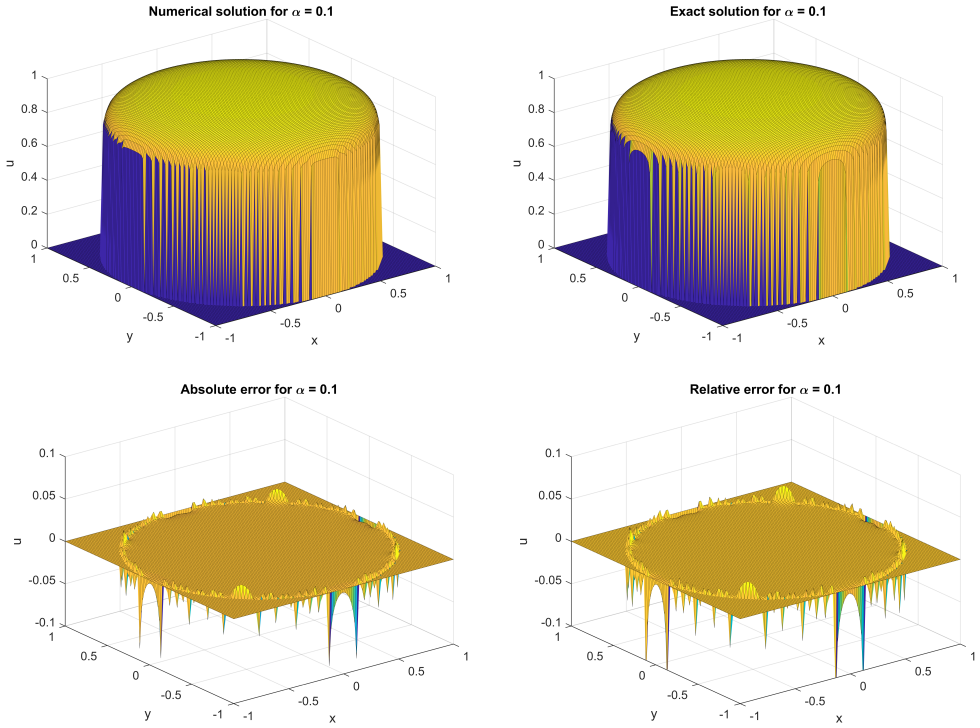

Figure 3.7: Numerical solution of (3.9), exact solution of (3.9), absolute and relative error for the solution.

of the exact solution allow us to evaluate and plot the absolute error together with the relative error of the solution.

Example 3.2. Consider circular domain $\Omega = B_1(0) := \{(x,y) \in \mathbb{R}^2 \colon x^2 + y^2 < 1\}$ together with the fractional order $\alpha = 1.9$. The number of grid points in the direction of both axes x and y is equal to $N = 120$, that is the grid contains $14,400$ grid points. For the right-hand side we are choosing $f \equiv 1$. The problem we are then solving has the following form

$$\begin{cases} (-\Delta)^{0.95} u(x,y) = 1 \text{ in } B_1(0), \\ \qquad\qquad u(x,y) = 0 \text{ in } \mathbb{R}^2 \backslash B_1(0). \end{cases} \tag{3.8}$$

Recall, that this is a special case of problem considered in Example 1.3 on page 3 for $d = 2$, $\alpha = 1.9$. The exact solution of the problem (3.8) is given by

$$u^*(\mathbf{x}) = \frac{1}{2^\alpha \Gamma\left(\frac{2+\alpha}{2}\right) \Gamma\left(1+\frac{\alpha}{2}\right)} \left[1 - |\mathbf{x}|^2\right]_+^{\alpha/2},$$

as shown in [4, Eq. (5.4.)], [13, pp. 89].

In Figure 3.6 we can see our numerical solution of the problem, together with the exact solution. Also, we are providing the absolute error

$$e_{absolute} = u^* - u,$$

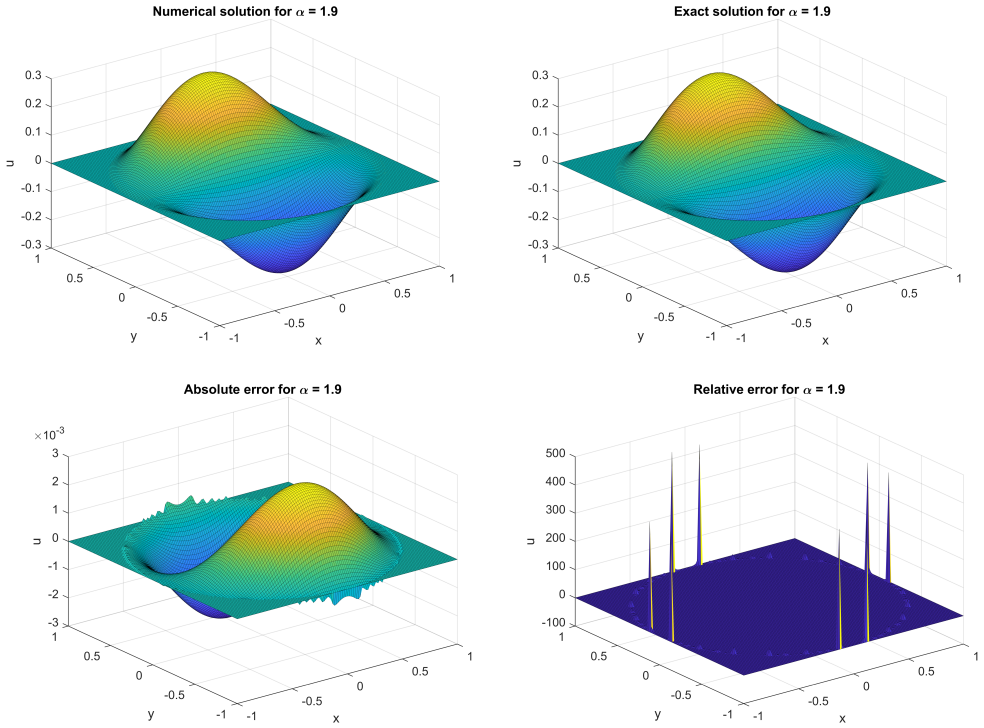

Figure 3.8: Numerical solution of (3.10), exact solution of (3.10), absolute and relative error for the solution.

together with the relative error

$$e_{relative} = \frac{u^* - u}{u^*}.$$

Example 3.3. For the next example, we will consider similar scenario as for the previous example with the difference of the choice for the fractional order α, where we set $\alpha = 0.1$. Following problem is being solved

$$\begin{cases} (-\Delta)^{0.05} u(x,y) = 1 \text{ in } B_1(0), \\ \qquad\qquad u(x,y) = 0 \text{ in } \mathbb{R}^2 \backslash B_1(0). \end{cases} \tag{3.9}$$

As before, we are plotting the numerical solution together with the exact solution. Also, absolute and relative error are plotted as well. Results can be seen in Figure 3.7.

For the next two examples we will consider right-hand side, for which the solution is known as well. The behavior of the solution is more interesting, because on a certain part of the domain the function is negative and on different part of the domain the function is positive. As before, we will consider two cases with the same setting expect of the fractional order α.

Example 3.4. Again, we will have a circular domain $\Omega = B_1(0) := \{(x,y) \in \mathbb{R}^2 \colon x^2 + y^2 < 1\}$. For the fractional order we are choosing $\alpha = 1.9$. The numbers of grid points in the direction of

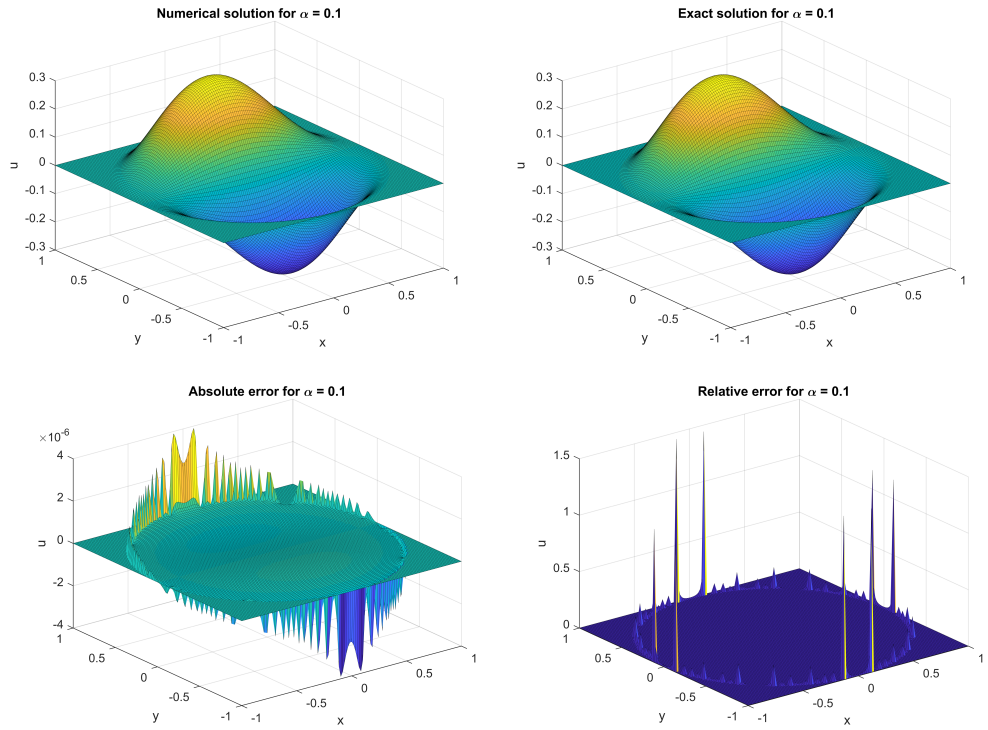

Figure 3.9: Numerical solution of (3.12), exact solution of (3.12), absolute and relative error for the solution.

both axes x and y are again equal to $N = 120$. We consider the following problem

$$\begin{cases} (-\Delta)^{0.95} u(x,y) = -y\,\Phi^{(4)}_{2,1.9}(|\mathbf{x}|^2) \text{ in } B_1(0)\,, \\ \qquad\qquad u(x,y) = 0 \text{ in } \mathbb{R}^2 \backslash B_1(0)\,, \end{cases} \tag{3.10}$$

where the function $\Phi^{(d+2)}_{p,\alpha}$ was defined in Example 1.4. By [10, Th. 1] (cf. Example 1.4), the solution of (3.10) has the following form

$$u^*(\mathbf{x}) = y\,(1 - |\mathbf{x}|^2)^2_+ \tag{3.11}$$

for $d = 2$ and $\mathbf{x} = (x, y)$. Numerical solution of the problem (3.10) obtained by our linear solver together with the exact solution of (3.11) is plotted in Figure 3.8. Again, we are plotting the absolute error $u_{absolute}$ and the relative error $e_{relative}$.

Example 3.5. Now, let us change the fractional order to $\alpha = 0.1$. The problem we are solving is

$$\begin{cases} (-\Delta)^{0.05} u(x,y) = -y\,\Phi^{(4)}_{2,0.1}(|\mathbf{x}|^2) \text{ in } B_1(0), \\ \qquad\qquad u(x,y) = 0 \text{ in } \mathbb{R}^2 \backslash B_1(0). \end{cases} \tag{3.12}$$

Solution of the problem (3.12) together with the exact solution, absolute error $e_{absolute}$ and relative error $e_{relative}$, are plotted in Figure 3.9.

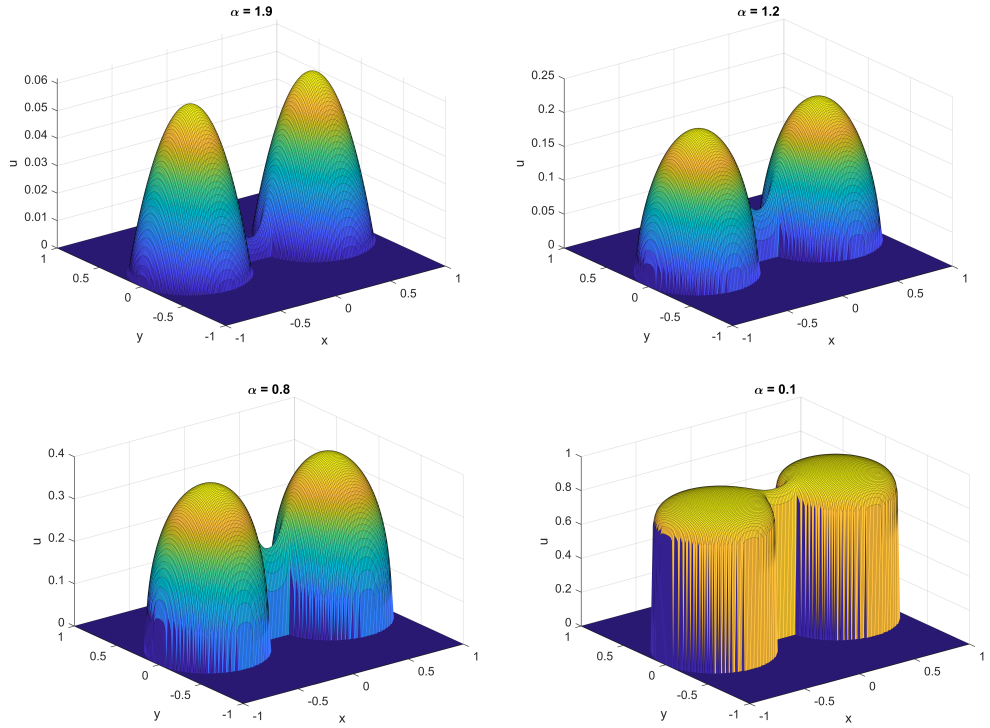

Figure 3.10: Solution of (3.13) for different values of α.

For the next example, we will demonstrate, that we are able to solve the problem involving fractional Laplacian on quite general domains $\Omega \subset \mathbb{R}^2$. More specifically, we will consider a domain, which consists of two circles which are connected by a rectangular section (so called dumbbell domain). This domain may be interpreted as a two lakes which are connected by a channel, which allows migration between the lakes.

Example 3.6. Let us consider a domain Ω, which consists of two circles connected by a rectangular section. The problem, we are then solving, has the following form

$$\begin{cases} (-\Delta)^{\alpha/2} u(x,y) = 1 \text{ in } \Omega, \\ \qquad\quad u(x,y) = 0 \text{ in } \mathbb{R}^2 \backslash \Omega, \end{cases} \tag{3.13}$$

for $\alpha = 1.9$, $\alpha = 1.2$, $\alpha = 0.8$, $\alpha = 0.1$. Solutions of the problem for corresponding values of α are plotted in Figure 3.10.

3.3.2 Nonlinear right-hand side dependent on parameter

This section of the text is dedicated to the right-hand side of the form $f = \lambda f(x,y,u)$, where $\lambda \in \mathbb{R}$ is a parameter. The problem we are solving then, has the following form

$$\begin{cases} (-\Delta)^{\alpha/2} u(x,y) = \lambda f(x,y,u) \text{ in } \Omega, \\ \qquad\quad u(x,y) = 0 \text{ in } \mathbb{R}^2 \backslash \Omega. \end{cases}$$

As in the one dimensional case, we will use Newton's algorithm for solving this type of a problem. The approach of deriving the Newton's method is the same as for the one dimensional case, thus we will not derive the iteration scheme again.

Our Matlab written function for solving the problem is called *frac_laplace_newton_12.m*. Regarding the pseudocode, it is not necessary to include the whole pseudocode, because the body of the pseudocode is the same as for the one dimensional case with a difference, that corresponding Matlab function *frac_laplace_scaled_matrix_2D.m* for the assembly of the matrix corresponding to the fractional Laplacian is called. Also, another difference is, that the right-hand side function, the derivative with respect to u of the right-hand function are a functions of x, y, u, instead of x, u. Lastly, the initial guess of the solution u_{init} is a function of x, y. Another differences concern the inputs of the algorithm, thus for the pseudocode we will include only the inputs of the algorithm.

Input:

L_x	(left boundary of the domain Ω_{square})
R_x	(right boundary of the domain Ω_{square})
U_y	(upper boundary of the domain Ω_{square})
L_y	(lower boundary of the domain Ω_{square})
$\mathbf{G}$	(grid matrix)
λ_{middle}	(parameter λ_{middle}, $\lambda_{middle} < \lambda_{max}$)
λ_{max}	(upper boundary of interval for λ parameter)
$m_1 \in \mathbb{N}$	(number of discretization points for partition of interval $(\lambda_{bif}, \lambda_{middle})$, where λ_{bif} is defined in the algorithm section)
$m_2 \in \mathbb{N}$	(number of discretization points for partition of interval $(\lambda_{middle}, \lambda_{max})$)
$6 < r < 15$	(10^{-r} is the tolerance in the Newton iteration)
$f = f(x, y, u)$	(source term f)
$f_u = f_u(x, y, u)$	(derivative f_u of source term f)
$u_{init} = u_{init}(x, y)$	(initial guess for Newton method for $\lambda = \lambda_{middle}$)
$\alpha \in (0, 2)$	(fractional order of $(-\Delta)^{\alpha/2}$))

Also, the simple continuation algorithm is implemented the same way as for the one dimensional case.

Example 3.7. Consider the following problem for $\alpha = 1.9$

$$\begin{cases} (-\Delta)^{0.95} u(x,y) = \lambda u(1-u) \text{ in } B_1(0), \\ u(x,y) = 0 \text{ in } \mathbb{R}^2 \backslash B_1(0), \end{cases} \tag{3.14}$$

where again $\Omega = B_1(0) := \{(x,y) \in \mathbb{R}^2 \colon x^2 + y^2 < 1\}$. For the number of grid points, we are solving for $N = 100$. Then, we set $\lambda_{middle} = 10$, $\lambda_{max} = 60$, $m_1 = 40$, $m_2 = 50$, $r = 7$, $u_{init}(x,y) = 1$.

We are including the bifurcation diagram, as depicted in Figure 3.11, together with a few solutions for several values of λ. These solutions are plotted in Figure 3.12.

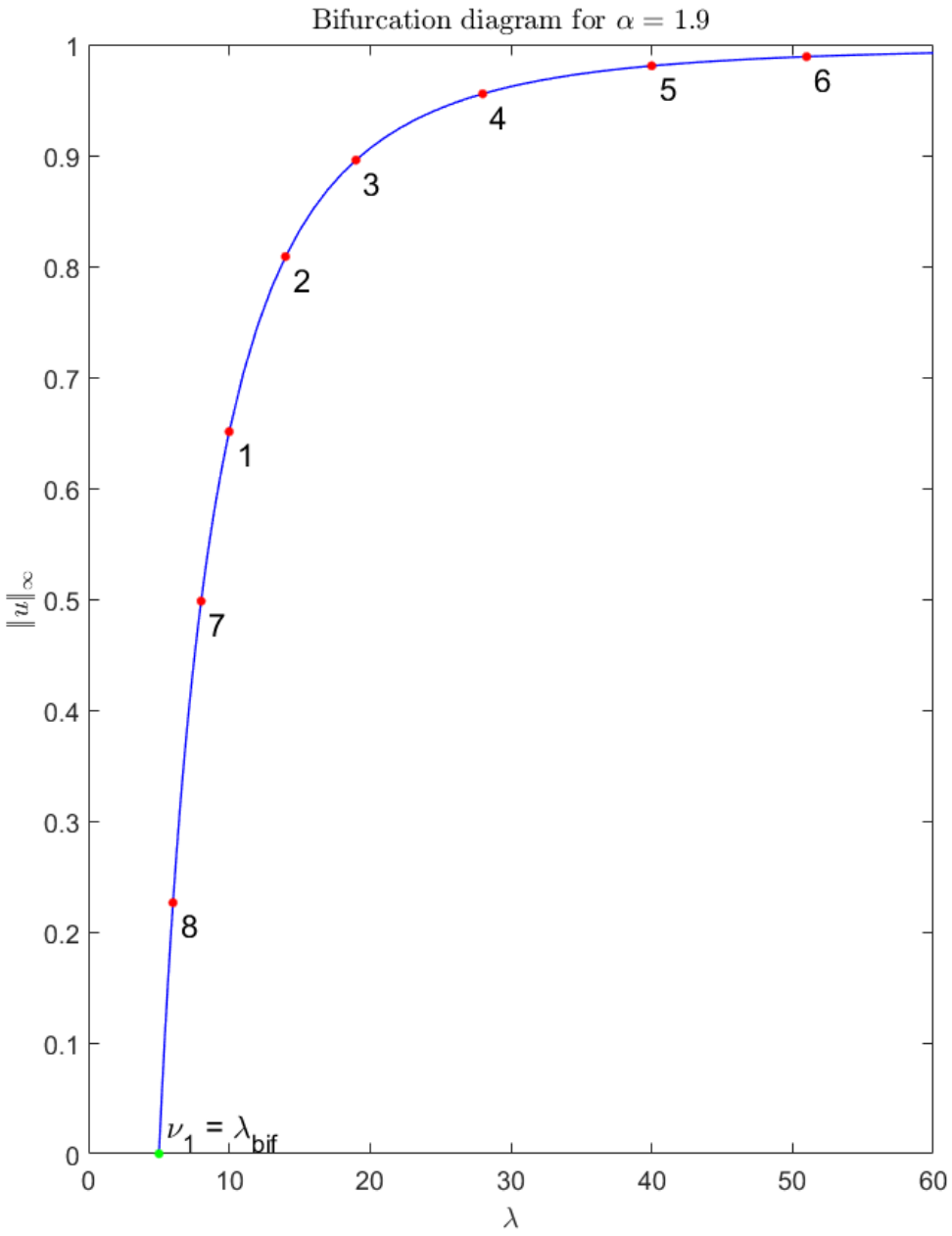

Figure 3.11: Bifurcation diagram for the problem (3.14).

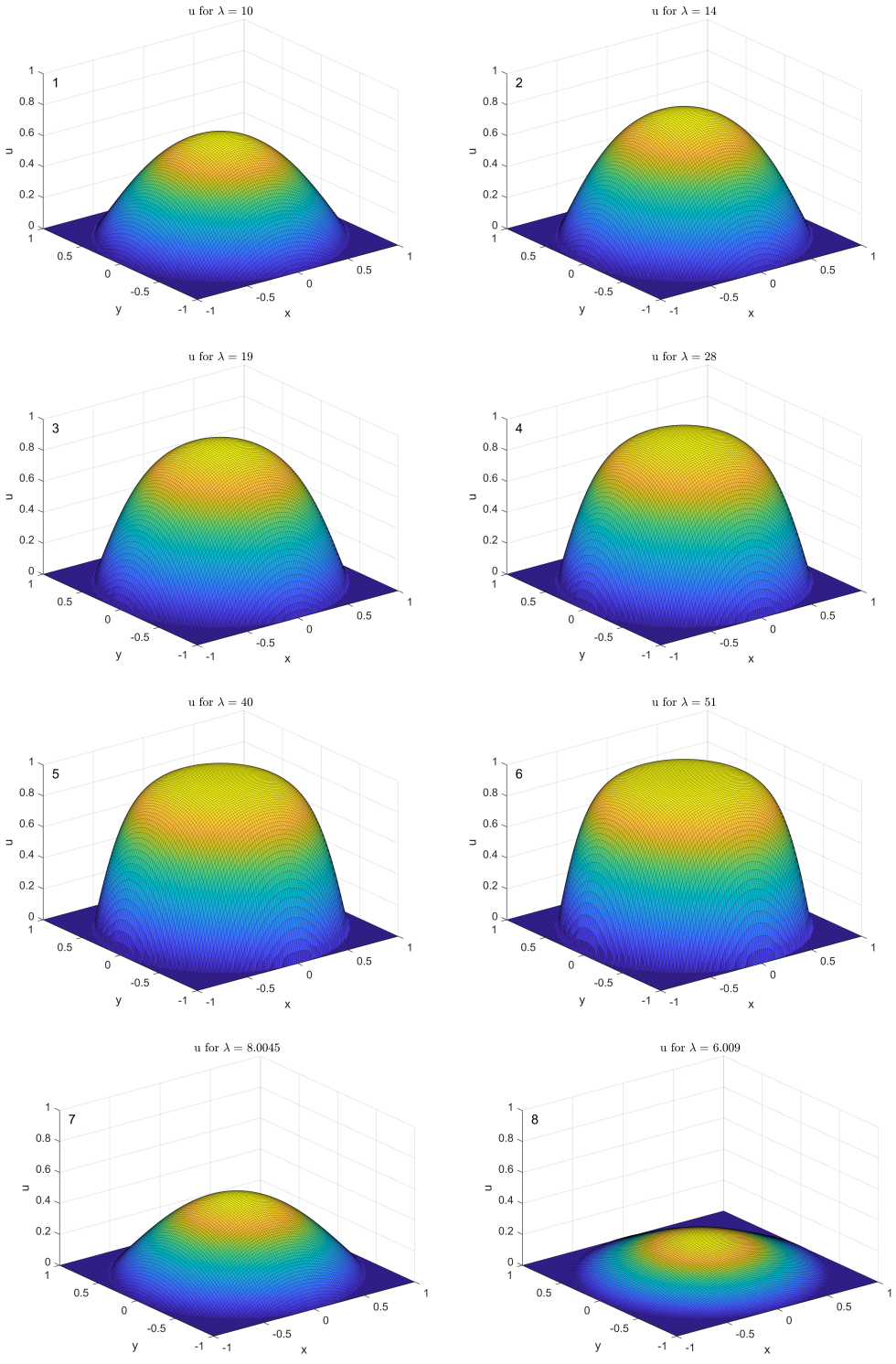

Figure 3.12: Solutions of (3.14) for different values of λ.

Example 3.8. Consider the problem solved in the previous example with a different value of the fractional order, specifically $\alpha = 0.1$. The problem, we are solving has the following form

$$\begin{cases} (-\Delta)^{0.05} u(x,y) = \lambda u(1-u) \text{ in } B_1(0), \\ u(x,y) = 0 \text{ in } \mathbb{R}^2 \backslash B_1(0). \end{cases} \tag{3.15}$$

Solution of the problem for several values of λ is plotted in Figure 3.14. The bifurcation diagram is then plotted in Figure 3.13.

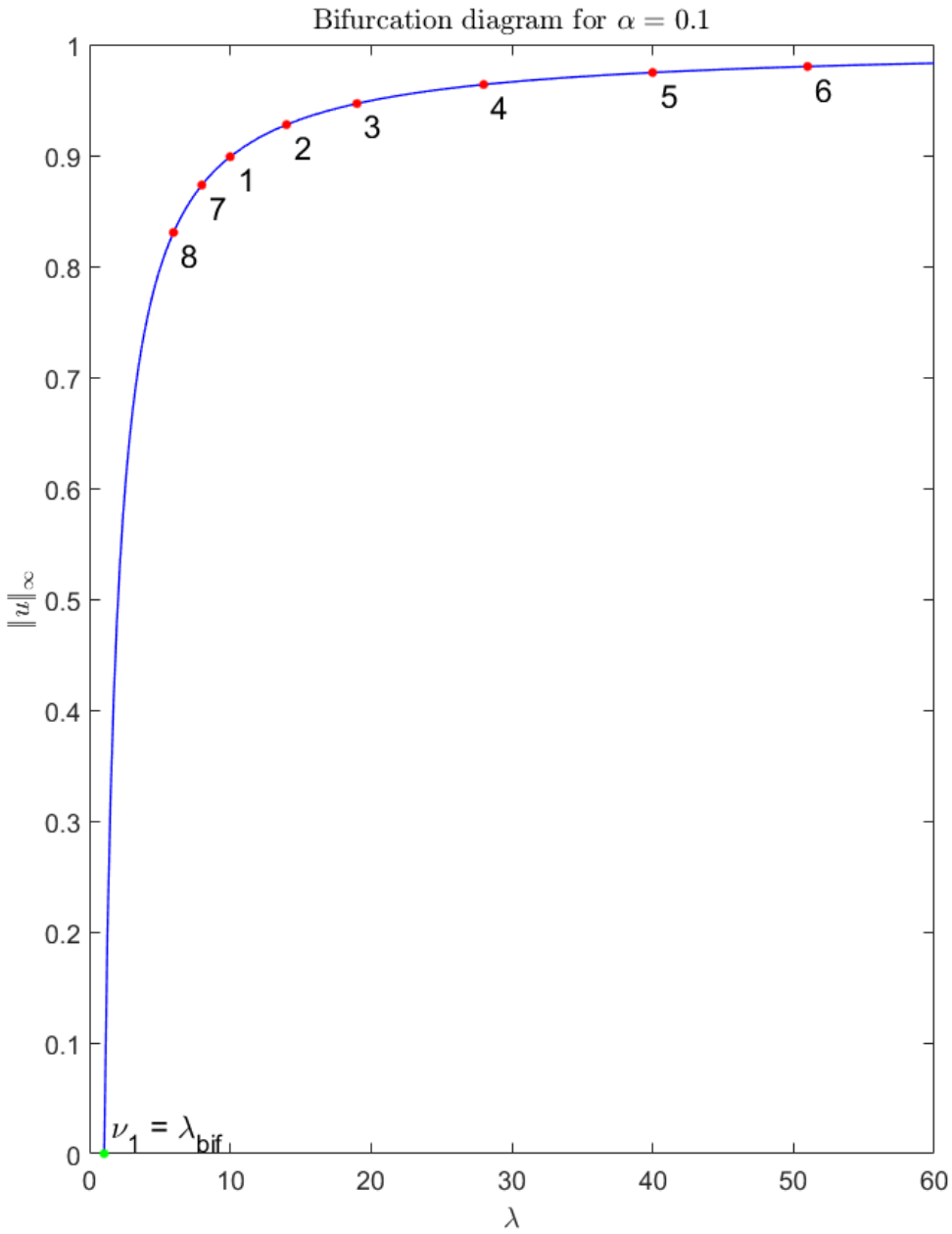

Figure 3.13: Bifurcation diagram for the problem (3.15).

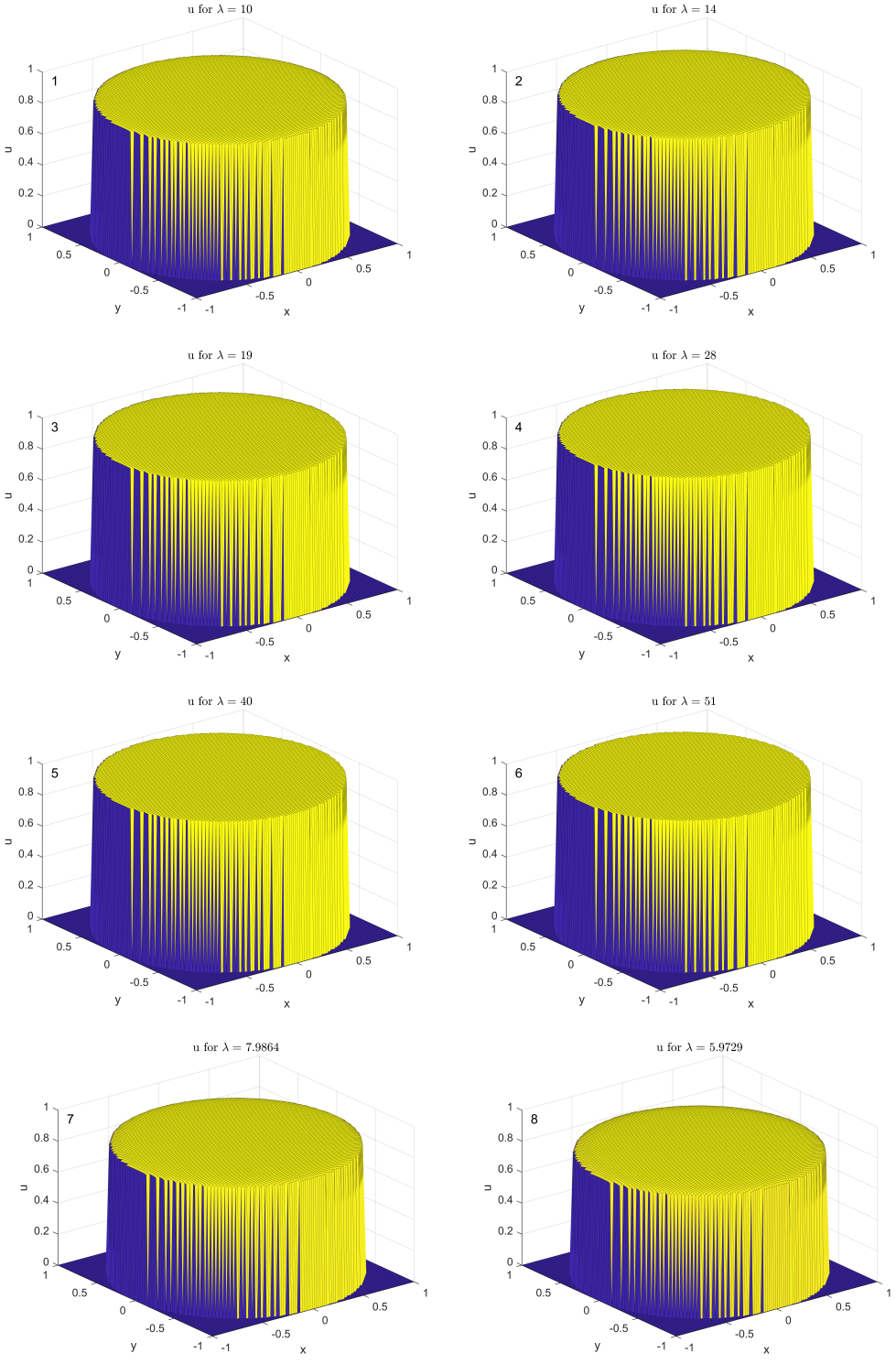

Figure 3.14: Solutions of (3.15) for different values of λ.

3.4 Evolutionary problems with fractional Laplacian

By introducing a transient term $\frac{\partial u}{\partial t}$ to the problem involving fractional Laplacian, we obtain evolutionary problem. We will begin with the problem involving right-hand side independent of u. For this type of a problem, Euler method will be used. After that, we will move on to the problem, for which the right-hand side can be dependent on u. As for the one dimensional, for that type of a problem, method of monotone iterations will be used.

3.4.1 Right-hand side independent of u

For the case of evolutionary problem with the right-hand side independent of u, we are solving

$$\begin{cases} \dfrac{\partial u(t,x,y)}{\partial t} + (-\Delta)^{\alpha/2} u(t,x,y) = f(t,x,y) & \text{in } (T_0,T)\times\Omega, \\ u(t,x,y) = 0 & \text{in } (T_0,T)\times(\mathbb{R}^2\setminus\Omega), \\ u(T_0,x,y) = u_{init}(x,y) & \text{in } \Omega. \end{cases} \tag{3.16}$$

Similarly as for the one dimensional case, we will use implicit Euler method for solving this type of problem. By the same fashion, firstly we would discretize the problem, then we would approximate the time derivative by the difference scheme and only then we would consolidate the term u^{n+1}, which denotes the solution at the next time step, i.e. $u^{n+1} := u(t+\tau,x,y)$, where $\tau > 0$ is the temporal step. Following this procedure, we would again arrive at

$$u^{n+1} = \left(\mathbf{I} + \frac{\tau}{h^\alpha}\mathbf{A}_c^{(\alpha)}\right)^{-1}\left(\tau f(t+\tau,x,y) + u^n\right).$$

Our Matlab written linear solver for the problem (3.16) is called *frac_laplace_evolution_2D.m*. The main body of the pseudocode for the algorithm is the same as for the on dimension case, thus we will not be including it, but as in the case of the stationary problem with right-hand side dependent on u, we will include just the inputs of the algorithm.

Input:

$T0$	(initial time)
T	(end time)
τ	(temporal step)
$u_{init}(x,y) = u(T_0,x,y)$	(initial condition)
L_x	(left boundary of the domain Ω_{square})
R_x	(right boundary of the domain Ω_{square})
U_y	(upper boundary of the domain Ω_{square})
L_y	(lower boundary of the domain Ω_{square})
$\mathbf{G}$	(grid matrix)
$f = f(t,x,y)$	(source term f)
$\alpha \in (0,2)$	(fractional order of $(-\Delta)^{\alpha/2}$))

Two examples will follow. In each of them, we will consider the same right-hand side. For the first example, fractional order close to 2 will be chosen, for the second example we will

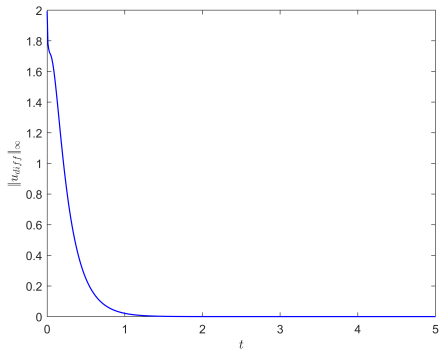

Figure 3.15: Norm of the difference $u_{diff} = u - \tilde{u}$, where u solves (3.17) and $\tilde{u}$ solves (3.18).

set fractional order close to 0. We will plot the solution for several time steps, together with including a graph of the norm of the difference of the solution for the evolutionary problem and solution for corresponding stationary problem.

Example 3.9. Consider an evolutionary problem with the right-hand side $f \equiv 1$, together with the fractional order $\alpha = 1.9$. The problem has the following form

$$\begin{cases} \dfrac{\partial u(t,x,y)}{\partial t} + (-\Delta)^{0.95} u(t,x,y) = 1 & \text{in } (0,5) \times B_1(0), \\ u(t,x,y) = 0 & \text{in } (0,5) \times (\mathbb{R}^2 \setminus B_1(0)), \\ u(0,x,y) = 2 & \text{in } B_1(0), \end{cases} \tag{3.17}$$

where $T_0 = 0$, $T = 5$, $\Omega = B_1(0) := \{(x,y) \in \mathbb{R}^2 \colon x^2 + y^2 < 1\}$. For the number of grid points, both in the direction of x axes and y axes, we set $N = 120$, for the spatial step we set $\tau = 0.01$.

In Figure 3.16 we can solution of (3.17) for several time steps. In the following Figure 3.15 we can see a norm of

$$u_{diff}(x,y) = u(t,x,y) - \tilde{u}(x,y) \text{ in } B_1(0) \text{ for } t \in (0,5) \text{ fixed},$$

where $\tilde{u}$ solves the stationary problem

$$\begin{cases} (-\Delta)^{0.95} \tilde{u}(x,y) = 1 & \text{in } B_1(0), \\ \tilde{u}(x,y) = 0 & \text{in } (\mathbb{R}^2 \setminus B_1(0)). \end{cases} \tag{3.18}$$

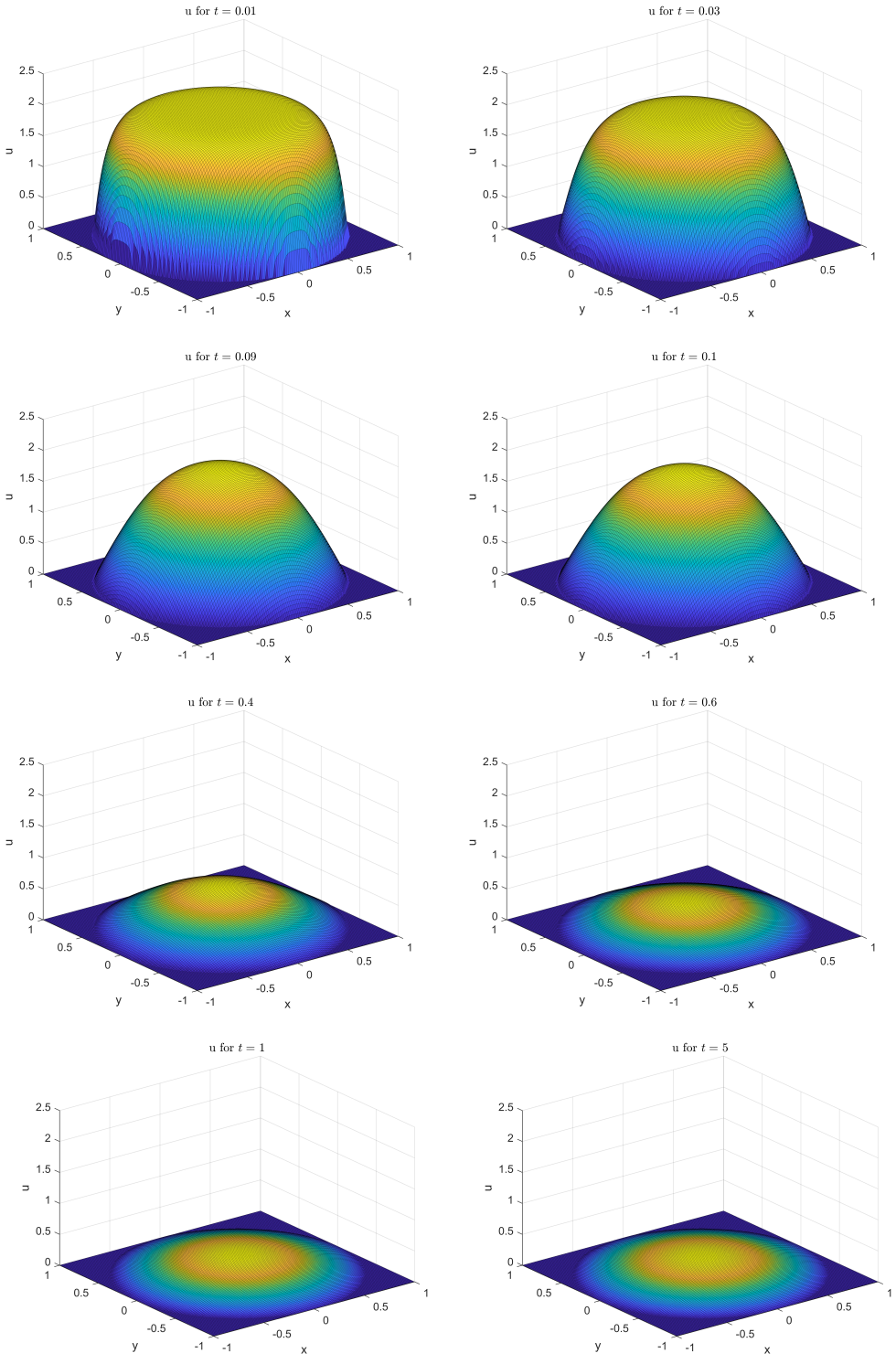

Figure 3.16: Solution of (3.17) at different time steps.

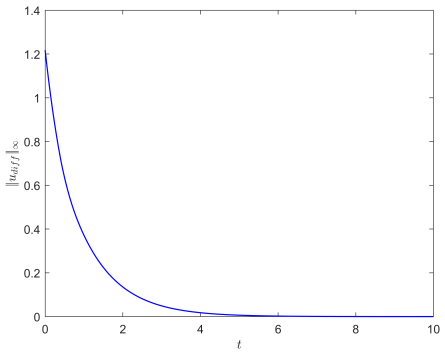

Figure 3.17: Norm of the difference $u_{diff} = u - \tilde{u}$, where u solves (3.19) and $\tilde{u}$ solves (3.20).

Example 3.10. Let us consider the previous example with different value of fractional order, specifically $\alpha = 0.1$. Together with the fractional order, we set different value of T to $T = 10$. Problem we are then solving has the following form

$$\begin{cases} \dfrac{\partial u(t,x,y)}{\partial t} + (-\Delta)^{0.05} u(t,x,y) = 1 & \text{in } (0,10) \times B_1(0), \\ u(t,x,y) = 0 & \text{in } (0,10) \times (\mathbb{R}^2 \setminus B_1(0)), \\ u(0,x,y) = 2 & \text{in } B_1(0), \end{cases} \tag{3.19}$$

Together with this problem, consider the stationary version of the problem, that is

$$\begin{cases} (-\Delta)^{0.05} \tilde{u}(x,y) = 1 & \text{in } B_1(0), \\ \tilde{u}(x,y) = 0 & \text{in } (\mathbb{R}^2 \setminus B_1(0)). \end{cases} \tag{3.20}$$

Solution of (3.19) for several time steps is plotted in Figure 3.18. In Figure 3.18, we are again plotting the difference of the solution of (3.20) and the solution of (3.20).

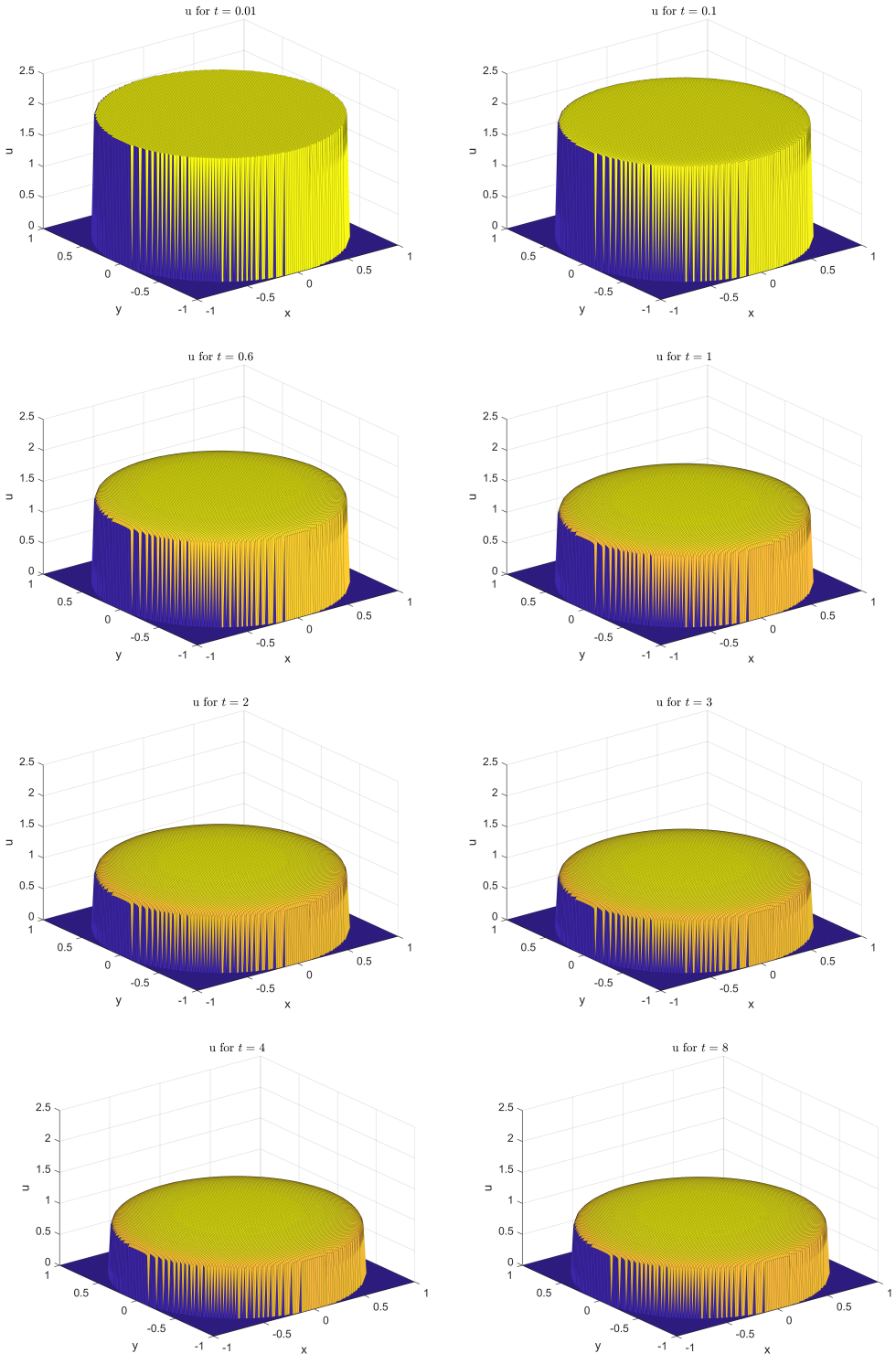

Figure 3.18: Solution of (3.19) at different time steps.

3.4.2 Right-hand side dependent on u

Lastly, we consider the evolutionary problem involving fractional Laplacian with right-hand side dependent on the solution u, i.e.

$$\begin{cases} \dfrac{\partial u(t,x,y)}{\partial t} + (-\Delta)^{\alpha/2} u(t,x,y) = f(t,x,y,u) & \text{in } (T_0,T)\times\Omega, \\ u(t,x,y) = 0 & \text{in } (T_0,T)\times(\mathbb{R}^2\setminus\Omega), \\ u(T_0,x,y) = u_{init}(x,y) & \text{in } \Omega. \end{cases} \tag{3.21}$$

Similarly as for the one dimensional case, the method of monotone iterations will be used. As before, we would firstly reformulate the problem (3.21) as a sequence of initial-boundary value problems of the form

$$\begin{cases} \dfrac{\partial u_m(t,x,y)}{\partial t} + (-\Delta)^{\alpha/2} u_m(t,x,y) = h(t,x,y) := f(t,x,y,u_{m-1}) & \text{in } (T_0,T)\times\Omega, \\ u_m(t,x,y) = 0 & \text{in } (T_0,T)\times(\mathbb{R}^2\setminus\Omega), \\ u_m(T_0,x,y) = u_{\text{init}}(x,y) & \text{in } \Omega, \end{cases} \tag{3.22}$$

where $m \in \mathbb{N}$ indicates the index related to the sequence of solutions. Then, on the problem (3.22) the method of the monotone iterations would be used. Because the method was introduced in the chapter concerning the one dimensional case, we will not be describing the method again.

After discretizing the problem (3.21), we would arrive at

$$u_m^{n+1} = \left(\mathbf{I} + \frac{\tau}{h^\alpha}\mathbf{A}_c^\alpha\right)^{-1} (\tau f(t+\tau,x,y,u_{m-1}^n) + u_m^n),$$

where the subscript $m \in \mathbb{N}$ denotes m-th element of the sequence of solutions of the problem (3.22) and $n \in \mathbb{N}$ denotes n-th node of the grid.

Our Matlab written solver for problems (3.21) is called *frac_laplace_lin_parabolic_solver_2D.m*. Again, we will not include the whole pseudocode of the algorithm, because the algorithm is the same as for the one dimension case. Nevertheless, we will list the inputs for the algorithm, which differ from the one dimensional case.

Input:

ϵ	(tolerance for the monotone iterative method)
$T0$	(initial time)
T	(end time)
τ	(temporal step)
$u_{init}(x,y) = u(T_0,x,y)$	(initial condition)
$u_{subsolution}(t,x,y)$	(subsolution for the monotone iterative method)
L_x	(left boundary of the domain Ω_{square})
R_x	(right boundary of the domain Ω_{square})

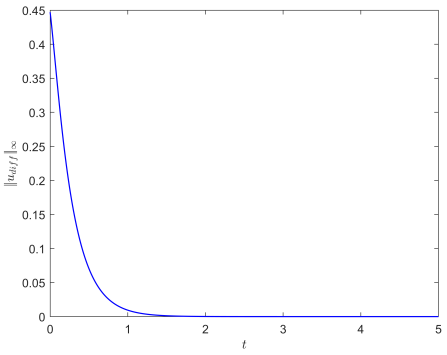

Figure 3.19: Norm of the difference $u_{diff} = u - \tilde{u}$, where u solves (3.23) and $\tilde{u}$ solves (3.24).

U_y	(upper boundary of the domain Ω_{square})
L_y	(lower boundary of the domain Ω_{square})
$\mathbf{G}$	(grid matrix)
$f = f(t,x,y,u)$	(source term f)
$\alpha \in (0,2)$	(fractional order of $(-\Delta)^{\alpha/2}$))

Examples for the right-hand side of the form $f(t,x,y,u) = 1 + \sqrt{|u|}$, which was also included in the examples for the one dimensional evolutionary problem, will follow.

Example 3.11. Let us consider a problem on a circular domain $\Omega = B_1(0) := \{(x,y) \in \mathbb{R}^2 \colon x^2 + y^2 < 1\}$ with the right-hand side $f(t,x,y,u) = 1 + \sqrt{|u|}$. Further, we are setting $\epsilon = 10^{-6}$, $T_0 = 0$, $T = 5$, $\tau = 0.01$, $N = 120$ and for the fractional order we set $\alpha = 1.9$. Then, the problem we are solving has the following form

$$\begin{cases} \dfrac{\partial u(t,x,y)}{\partial t} + (-\Delta)^{0.95} u(t,x,y) = \sqrt{|u|} + 1 & \text{in } (0,5) \times B_1(0), \\ u(t,x,y) = 0 & \text{in } (0,5) \times (\mathbb{R}^2 \setminus B_1(0)), \\ u(0,x,y) = u_{init}(x,y) := 0 & \text{in } B_1(0), \end{cases} \tag{3.23}$$

together with subsolution $\underline{u}(t,x,y) = 0$ and supersolution $\overline{u}(t,x,y) = \tilde{u}(x,y)$, where $\tilde{u}$ is the solution of the stationary problem (3.24). For further discussion regarding the subsolution and supersulotin, we refer the reader to Example 2.8.

Solution of the problem (3.23) for several time steps is plotted in Figure 3.20. As for the evolutionary problem with the right-hand side independent of u, we are also plotting a norm of a difference of the solution for the problem (3.23) and it's stationary version, i.e.

$$\begin{cases} (-\Delta)^{0.95} \tilde{u}(x,y) = \sqrt{|\tilde{u}|} + 1 & \text{in } B_1(0), \\ \tilde{u}(x,y) = 0 & \text{in } \mathbb{R}^2 \setminus B_1(0). \end{cases} \tag{3.24}$$

The norm can be seen in Figure 3.19.

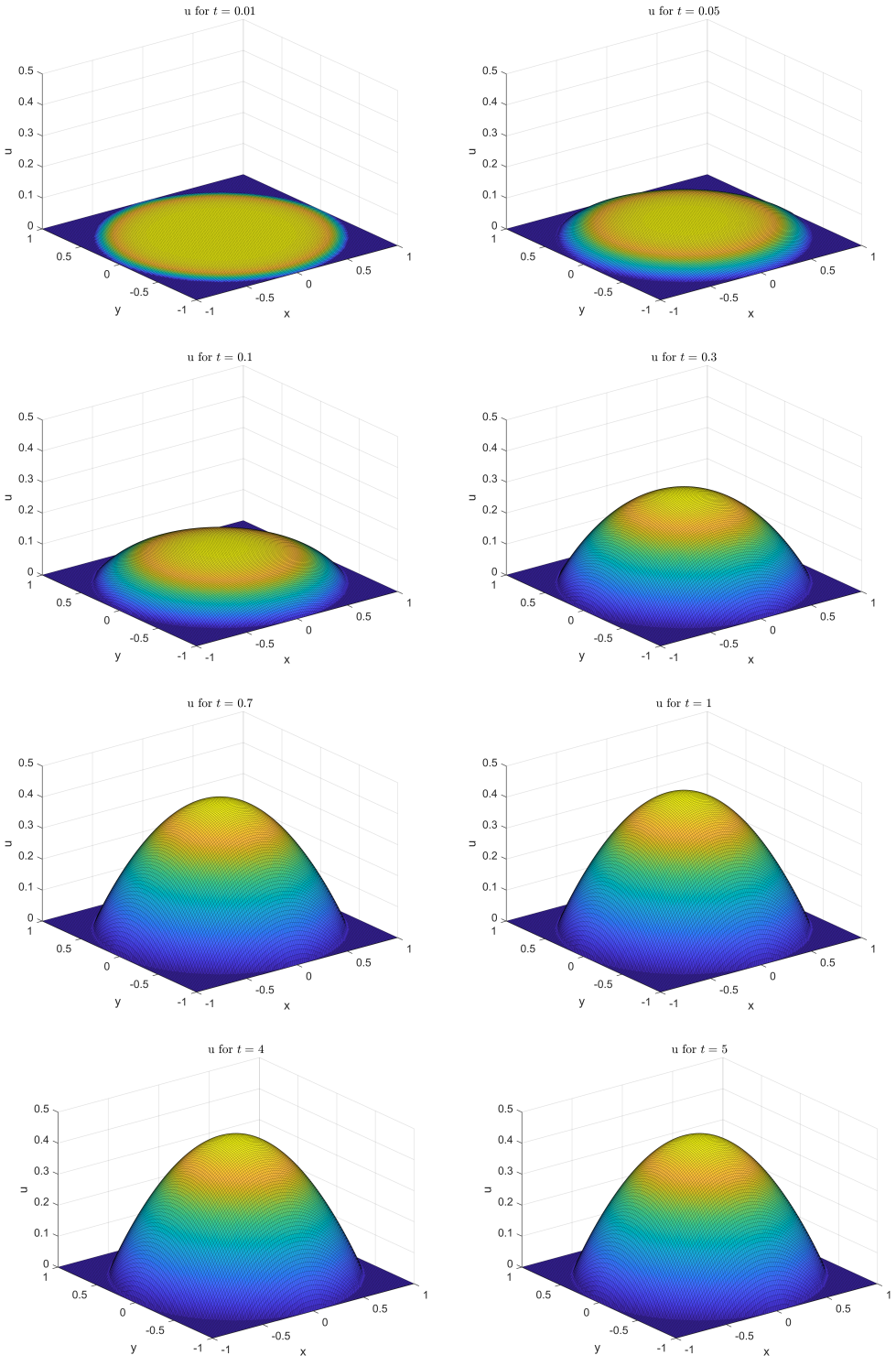

Figure 3.20: Solutions of (3.23) at different time steps.

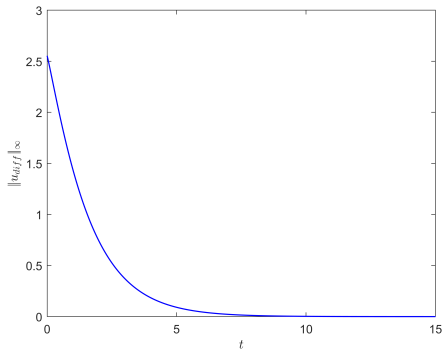

Figure 3.21: Norm of the difference $u_{diff} = u - \tilde{u}$, where u solves (3.25) and $\tilde{u}$ solves (3.26).

Example 3.12. For this example, we consider the same scenario as for the previous example with a different values of α, T, for which we set $\alpha = 0.1$ and $T = 15$. The problem we are then solving has the following form

$$\begin{cases} \dfrac{\partial u(t,x,y)}{\partial t} + (-\Delta)^{0.05} u(t,x,y) = \sqrt{|u|} + 1 & \text{in } (0,15) \times B_1(0), \\ u(t,x,y) = 0 & \text{in } (0,15) \times (\mathbb{R}^2 \setminus B_1(0)), \\ u(0,x,y) = u_{init}(x,y) := 0 & \text{in } B_1(0), \end{cases} \tag{3.25}$$

together with the subsolution $\underline{u}(t,x,y) = 0$ and supersolution $\overline{u}(t,x,y) = \tilde{u}(x,y)$, where $\tilde{u}$ is the solution of the stationary problem (3.26). Together with the problem (3.25) we are solving it's stationary version

$$\begin{cases} (-\Delta)^{0.05} \tilde{u}(x,y) = \sqrt{|\tilde{u}|} + 1 & \text{in } B_1(0), \\ \tilde{u}(x,y) = 0 & \text{in } \mathbb{R}^2 \setminus B_1(0). \end{cases} \tag{3.26}$$

Solution of the problem (3.25) for several time steps is plotted in Figure 3.22. Norm of the difference of $\tilde{u}$, which solves (3.26), and u, which solves (3.25), is plotted in Figure 3.21.

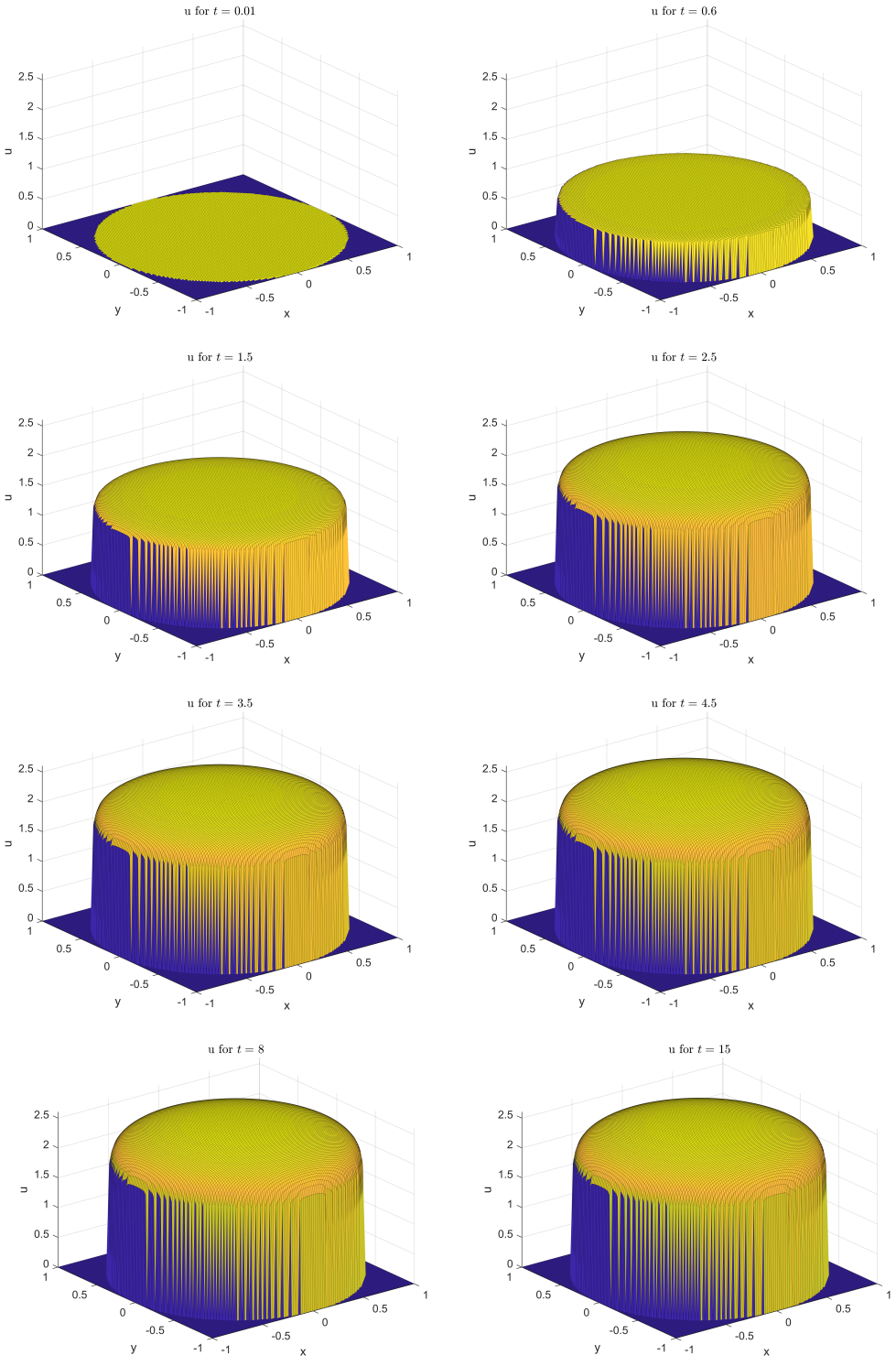

Figure 3.22: Solutions of (3.25) at different time steps.

Conclusion 4

In this work, we have implemented numerical algorithms for solving problems involving fractional Laplacian with a zero Dirichlet boundary condition, that is

$$\begin{cases} \dfrac{\partial u(t,x,y)}{\partial t} + (-\Delta)^{\alpha/2} u(t,x,y) = f(t,x,y,u) & \text{in } (T_0,T)\times\Omega, \\ u(t,x,y) = 0 & \text{in } (T_0,T)\times(\mathbb{R}^2\setminus\Omega), \\ u(T_0,x,y) = u_{init}(x,y) & \text{in } \Omega, \end{cases}$$

in one and two dimension. At the end of each section, several examples were included. For the most cases, we considered the examples in pairs, where the one example differed from the other one in the choice of the fractional order α.

In Chapter 2, we studied one dimensional case. In Section 2.1 , we discretized the fractional Laplacian $(-\Delta)^{\alpha/2}$, obtaining a matrix $\mathbf{A}_c^{(\alpha)}$, for which we derived explicit formulas for its elements. Furthermore, during the process of discretization we also discussed the errors which were introduced by neglecting reminders of Taylor's expansion. To test our discretization procedure, we used the fact (see, e.g., [31, Proposition 5.3.]) that fractional Laplacian tends to identity operator for α tending to zero and fractional Laplacian tends to usual Laplace operator for α tending to 2. After calculating the matrix $\mathbf{A}_c^{(\alpha)}$ (for particular choice of interval and number of nodes) in Section 2.2, we observed that for the fractional order α close to zero, the matrix is approaching unitary matrix and on the other hand, for the fractional order α close to 2, the matrix is approaching the matrix corresponding to the ordinary Laplacian, which agrees with the aforementioned theoretical results from [31, Proposition 5.3.].

In Section 2.3, we study stationary problems. Firstly, in Subsection 2.3.1 we considered right-hand side independent of u, that is we solved the following problem

$$\begin{cases} (-\Delta)^{\alpha/2} u(x) = f(x) \text{ in } (L,R), \\ u(x) = 0 \text{ in } \mathbb{R}\setminus(L,R). \end{cases} \tag{4.1}$$

At first, we tested our linear solver on the problem (4.1) for $f \equiv 1$ on $\Omega := B_1(0) = (-1,1)$. The exact solution for this problem is given by [4, Eq. (5.4.)], [13, pp. 89], by the following formula

$$u^*(x) = \frac{\Gamma\left(\frac{1}{2}\right)}{2^\alpha \Gamma\left(\frac{1+\alpha}{2}\right)\Gamma\left(1+\frac{\alpha}{2}\right)} \left[1-x^2\right]_+^{\frac{\alpha}{2}}.$$

Thus, we were able to compute the absolute and relative error of our numerical solution. Based on the absolute and relative errors, we found out that our solver gives satisfactory results. Although, for values of α close to 2, the relative error was quite large near the boundary, which was to be expected.

In Subsection 2.3.2, by using our solver for linear problems above, we also studied problems with right-hand side depending on nonlinearly on u with a parameter $\lambda \in \mathbb{R}$ of the following form

$$\begin{cases} (-\Delta)^{\alpha/2} u(x) = \lambda f(x,u) \text{ in } (L,R), \\ u(x) = 0 \text{ in } \mathbb{R}\backslash(L,R). \end{cases}$$

For this type of a problems, Newton's method was used. Also, we implemented simple continuation algorithm, which provided us with a results for values of the parameter λ in the range $[\lambda_{min}, \lambda_{max}]$. Because of that, we were able to plot bifurcation diagrams, which plot the dependence of the norm of the solution on the value of the parameter λ.

In Section 2.4, we studied evolutionary problems. In Subsection 2.4.1, we focused on a problem with right-hand side independent of u. The problem we were then solving had the following form

$$\begin{cases} \dfrac{\partial u(t,x)}{\partial t} + (-\Delta)^{\alpha/2} u(t,x) = f(t,x) & \text{in } (T_0,T)\times(L,R), \\ u(t,x) = 0 & \text{in } (T_0,T)\times(\mathbb{R}\setminus(L,R)), \\ u(T_0,x) = u_{init}(x) & \text{in } (L,R). \end{cases} \tag{4.2}$$

For this type of a problem, implicit Euler's method was used. The solution for the initial value problem (4.2) is not known even for a simple case where $f \equiv 1$ with a constant initial condition. To be able to determine if our linear solver of the evolution problem works, we used the fact that the solution for the stationary version of (4.2) is known for $f \equiv 1$ together with the fact that the solution of the evolutionary problem converges to the solution of the stationary version of the problem for t approaching infinity. We then computed the solution of the evolutionary problem (4.2) together with the solution of the stationary version of the problem and computed the norm of the difference of corresponding solutions. We observed that the norm tends to zero for sufficiently large t, thus we considered our solver of the evolutionary problem sufficiently tested.

In subsection 2.4.2, we solved the original evolutionary problem involving u on the right-hand side, that is the problem

$$\begin{cases} \dfrac{\partial u(t,x)}{\partial t} + (-\Delta)^{\alpha/2} u(t,x) = f(t,x,u) & \text{in } (T_0,T)\times(L,R), \\ u(t,x) = 0 & \text{in } (T_0,T)\times(\mathbb{R}\setminus(L,R)), \\ u(T_0,x) = u_{init}(x) & \text{in } (L,R), \end{cases}$$

was solved. For solving the problem, method of monotone iterations was used. Again, several examples followed.

Following Chapter 3 of the text is devoted to the two dimension case involving fractional Laplacian with zero Dirichlet boundary condition. The structure of the chapter copies the structure for the one dimensional case. As of first, we started with discretizing the operator, obtaining matrix $\mathbf{A}_c^{(\alpha)}$. Unlike the one dimension case, we are not going through the discretization

step by step, rather we overtook the disretized form of the problem

$$\begin{cases} (-\Delta)^{\alpha/2} u(x,y) = f(x,y) \text{ in } \Omega, \\ \qquad\quad u(x,y) = 0 \text{ in } \mathbb{R}^2 \backslash \Omega, \end{cases}$$

where $\Omega \subset \mathbb{R}^2$, from the monograph [25, Chapt. 6]. Our contribution is in a description of the process of computation of the matrix for a general grid. Similarly as in the one-dimensional case, we tested the discretization for limiting values of α. We used a particular choice of square domain and number of nodes. Then we computed $\mathbf{A}_c^{(\alpha)}$, for α close to zero, and obtained almost unitary matrix. On the other hand, for α close to 2, we obtained matrix close to matrix corresponding to the ordinary Laplacian. Again in agreement with theoretical results from [31, Proposition 5.3.].

Section 3.3 of Chapter 3 concerns stationary problems. In subsection 3.3.1, we tested our 2D linear solver on two problems of the following form

$$\begin{cases} (-\Delta)^{\alpha/2} u(x,y) = f(x,y) \text{ in } \Omega, \\ \qquad\quad u(x,y) = 0 \text{ in } \mathbb{R}^2 \backslash \Omega. \end{cases} \tag{4.3}$$

on the open unit disc

$$\Omega := B_1(0) = \{(x,y) \in \mathbb{R}^2 \colon x^2 + y^2 < 1\}.$$

The first example used for testing is for the right-hand side $f \equiv 1$, for which the solution is known explicitly (see Example 1.3 on page 3) and is given by

$$u^*(x) = \frac{1}{2^\alpha \Gamma\left(\frac{2+\alpha}{2}\right) \Gamma\left(1+\frac{\alpha}{2}\right)} \left[1 - |x|^2\right]_+^{\alpha/2}.$$

The second example was studied on the same domain Ω. We considered (4.3) with sign-changing right-hand side of the form

$$f(\mathbf{x}) = -y\, \Phi_{p,\alpha}^{(d+2)}(|\mathbf{x}|^2),$$

where

$$\Phi_{p,\alpha}^{(d)}(\mathbf{x}) = \frac{\mathcal{A}_{d,-\alpha} B(-\frac{\alpha}{2}, p+1) \pi^{d/2}}{\Gamma\left(\frac{d}{2}\right)}\, {}_2F_1\left(\frac{\alpha+d}{2}, -p+\frac{\alpha}{2}; \frac{d}{2}; \mathbf{x}\right),$$

and

$$\mathcal{A}_{d,-\alpha} = \frac{2^\alpha \Gamma\left(\frac{\alpha+d}{2}\right)}{\pi^{d/2} |\Gamma\left(-\frac{\alpha}{2}\right)|}.$$

In [10, Th. 1] was shown, that the solution for the problem with this right-hand side is given by the following formula

$$u^*(\mathbf{x}) = y\,(1 - |\mathbf{x}|^2)_+^2.$$

For both cases, we evaluated and plotted the absolute and relative error of the numerical solution. We found that in both cases the numerical solutions were in good agreement with known analytical solutions. Only near the boundary, where the solution is nearly zero, the relative error was quite large. However, this phenomenon was to be expected. After the linear solver was tested in this way, we solved a problem of the type (4.3) on a geometrically more complicated region known as the dumbbell (two circular domains connected by a rectangular section).

In Subsection 3.3.2 we used the tested linear solver to solve the nonlinear problems of the form

$$\begin{cases} (-\Delta)^{\alpha/2} u(x,y) = \lambda f(x,y,u) \text{ in } \Omega, \\ u(x,y) = 0 \text{ in } \mathbb{R}^2 \backslash \Omega\,, \end{cases}$$

where $\lambda \in \mathbb{R}$ is a parameter. Analogously as in the one-dimension case, Newton's method together with the simple continuation algorithm were used to produce corresponding bifurcation diagrams.

Section 3.4 of Chapter 3 was devoted to study evolutionary problem involving fractional Laplacian in two dimension. In Subsection 3.4.1, we started with right-hand side independent of u, i.e.

$$\begin{cases} \dfrac{\partial u(t,x,y)}{\partial t} + (-\Delta)^{\alpha/2} u(t,x,y) = f(t,x,y) & \text{in } (T_0,T) \times \Omega, \\ u(t,x,y) = 0 & \text{in } (T_0,T) \times (\mathbb{R}^2 \setminus \Omega), \\ u(T_0,x,y) = u_{init}(x,y) & \text{in } \Omega, \end{cases} \tag{4.4}$$

and developed linear solver based on the implicit Euler's method. We computed several examples on the open unit disk. The solution of the initial value problem (4.4) is not known even in the case of $f = 1$ and a constant initial condition. To test the linear solver of the evolution problem, we used the fact that a steady state of 4.4 is known for $f \equiv 1$ and the fact that the solution of the initial problem converges to a stationary state for t approaching infinity. Numerically, we implemented this procedure by computing the solution of the initial problem for sufficiently large t and comparing it with the corresponding steady states. We found that in all the cases studied, the numerical solutions of the initial value problem were close enough to the corresponding steady states for sufficiently large t. Thus, we considered the linear solver of the evolution problem sufficiently tested. For the convenience of the reader, we included the graphs of the norms of the difference of the solution of the initial value problem and its stationary version.

Finally, in Subsection 3.4.2 of Chapter 3, we considered two nonlinear initial value problems and solved them using the linear solver of initial value problems combined with the method of monotone iterations.

Bibliography

[1] B. Barrios, L. Del Pezzo, J. García-Melián, and A. Quaas. A priori bounds and existence of solutions for some nonlocal elliptic problems. *Rev. Mat. Iberoam.*, 34(1):195–220, 2018.

[2] F. Bartumeus. Lévy processes in animal movement: an evolutionary hypothesis. *Fractals*, 15(02):151–162, 2007.

[3] J. Benedikt, V. Bobkov, R. N. Dhara, and P. Girg. Nonuniqueness for fractional parabolic equations with sublinear power-type nonlinearity, 2023.

[4] K. Bogdan and T. Byczkowski. Potential theory of Schrödinger operator based on fractional Laplacian. *Probab. Math. Stat.*, 20(2):293–335, 2000.

[5] K. Bogdan, S. Jarohs, and E. Kania. Semilinear Dirichlet problem for the fractional Laplacian. *Nonlinear Anal.*, 193:111512, 20, 2020.

[6] C. Bucur and E. Valdinoci. *Nonlocal diffusion and applications*, volume 20 of *Lect. Notes Unione Mat. Ital.* Cham: Springer; Bologna: UMI, 2016.

[7] M. Chhetri, P. Girg, and E. Hollifield. Existence of positive solutions for fractional Laplacian equations: theory and numerical experiments. *Electron. J. Differ. Equ.*, 2020:31, 2020. Id/No 81.

[8] B. Cushman-Roisin. Beyond eddy diffusivity: an alternative model for turbulent dispersion. *Environmental fluid mechanics*, 8(5-6):543–549, 2008.

[9] P. Drábek. *Introduction to Bifurcation Theory*. Západočeská univerzita v Plzni, 2002.

[10] B. Dyda. Fractional calculus for power functions and eigenvalues of the fractional Laplacian. *Fract. Calc. Appl. Anal.*, 15(4):536–555, 2012.

[11] B. Dyda, A. Kuznetsov, and M. Kwaśnicki. Fractional Laplace operator and Meijer G-function. *Constr. Approx.*, 45(3):427–448, 2017.

[12] B. P. Epps and B. Cushman-Roisin. Turbulence modeling via the fractional laplacian, 2018.

[13] R. K. Getoor. First passage times for symmetric stable processes in space. *Trans. Am. Math. Soc.*, 101:75–90, 1961.

[14] P. Girg. Personal communication.

[15] E. Hanert, E. Schumacher, and E. Deleersnijder. Front dynamics in fractional-order epidemic models. *J. Theor. Biol.*, 279:9–16, 2011.

[16] A. Kochubei and Y. Luchko, editors. *Volume 1 Basic Theory*. De Gruyter, Berlin, Boston, 2019.

[17] A. Kölzsch, A. Alzate, F. Bartumeus, M. De Jager, E. J. Weerman, G. M. Hengeveld, M. Naguib, B. A. Nolet, and J. Van de Koppel. Experimental evidence for inherent lévy search behaviour in foraging animals. *Proceedings of the Royal Society B: Biological Sciences*, 282(1807):20150424, 2015.

[18] M. Kwaśnicki. Ten equivalent definitions of the fractional Laplace operator. *Fract. Calc. Appl. Anal.*, 20(1):7–51, 2017.

[19] T. Leonori, I. Peral, A. Primo, and F. Soria. Basic estimates for solutions of a class of nonlocal elliptic and parabolic equations. *Discrete and Continuous Dynamical Systems*, 35(12):6031–6068, 2015.

[20] A. Lischke, G. Pang, M. Gulian, F. Song, C. Glusa, X. Zheng, Z. Mao, W. Cai, M. M. Meerschaert, M. Ainsworth, and G. E. Karniadakis. What is the fractional Laplacian? A comparative review with new results. *J. Comput. Phys.*, 404:62, 2020. Id/No 109009.

[21] M. G. McDonald and A. W. Harbaugh. A modular three-dimensional finite-difference ground-water flow model. *Techniques of water-resources investigations*, 1984.

[22] R. Metzler and J. Klafter. The random walk's guide to anomalous diffusion: A fractional dynamics approach. *Phys. Rep.*, 339(1):1–77, 2000.

[23] G. Molica Bisci, V. D. Radulescu, and R. Servadei. *Variational methods for nonlocal fractional problems*, volume 162 of *Encyclopedia of Mathematics and its Applications*. Cambridge University Press, Cambridge, 2016. With a foreword by Jean Mawhin.

[24] A. Monin. The equation of turbulent diffusion. In *Dokl. Akad. Nauk SSSR*, volume 105, pages 256–259, 1955. In Russian. Part of this paper was translated in the monograph *Fractional Kinetics in the Space*[32] and commented from a contemporary point of view.

[25] C. Pozrikidis. *The fractional Laplacian*. Boca Raton, FL: CRC Press, 2016.

[26] L. F. Richardson. Atmospheric diffusion shown on a distance-neighbour graph. *Proceedings of the Royal Society of London. Series A, Containing Papers of a Mathematical and Physical Character*, 110(756):709–737, 1926.

[27] M. Riesz. L'intégrale de Riemann-Liouville et le problème de Cauchy. *Acta Mathematica*, 81(none):1 – 222, 1949.

[28] B. Ross. *Fractional calculus and its applications: proceedings of the international conference held at the University of New Haven, June 1974*, volume 457. Springer, 2006.

[29] D. H. Sattinger. Monotone methods in nonlinear elliptic and parabolic boundary value problems. *Indiana Univ. Math. J.*, 21:979–1000, 1971/72.

[30] L. Silvestre. Regularity of the obstacle problem for a fractional power of the Laplace operator. *Comm. Pure Appl. Math.*, 60(1):67–112, 2007.

[31] P. R. Stinga and J. L. Torrea. Extension problem and Harnack's inequality for some fractional operators. *Communications in Partial Differential Equations*, 35(11):2092–2122, 2010.

[32] V. Uchaikin and R. Sibatov. *Fractional Kinetics In Space: Anomalous Transport Models*. World Scientific Publishing Company, 2017.

[33] G. M. Viswanathan, V. Afanasyev, S. V. Buldyrev, E. J. Murphy, P. A. Prince, and H. E. Stanley. Lévy flight search patterns of wandering albatrosses. *Nature*, 381(6581):413–415, 1996.

[34] V. A. Volpert, Y. Nec, and A. A. Nepomnyashchy. Fronts in anomalous diffusion-reaction systems. *Philos. Trans. R. Soc. Lond., Ser. A, Math. Phys. Eng. Sci.*, 371(1982):18, 2013. Id/No 20120179.